



Chapters 1 – 5: Overview

- Photogrammetry: introduction, applications, and tools
- GNSS/INS-assisted photogrammetric and LiDAR mapping
- LiDAR mapping: principles, applications, mathematical model, and error sources and their impact.
- QA/QC of LiDAR mapping
- Quaternions & rotation in space

- This chapter will be focusing on the different alternatives for the registration of laser scans.
 - Point-based registration,
 - Feature-based registration, and
 - Image-based registration



Chapter 6

REGISTRATION OF LASER SCANNING POINT CLOUDS



Outline

- **Introduction:** Terrestrial Laser Scanners (TLS) and applications
- **Prior work:** Registration paradigm, point-based registration, feature-based registration
- **Methodology:** Linear features extraction, parameter estimation alternatives, matching process, and parameter refinement
- **Experimental results:** Segmentation and registration results
- **Conclusions and future work**

Terrestrial Laser Scanners



FARO Focus3D X 330
976,000 points/second
330 m range
 ± 2 mm range error
[*http://faro.com](http://faro.com)

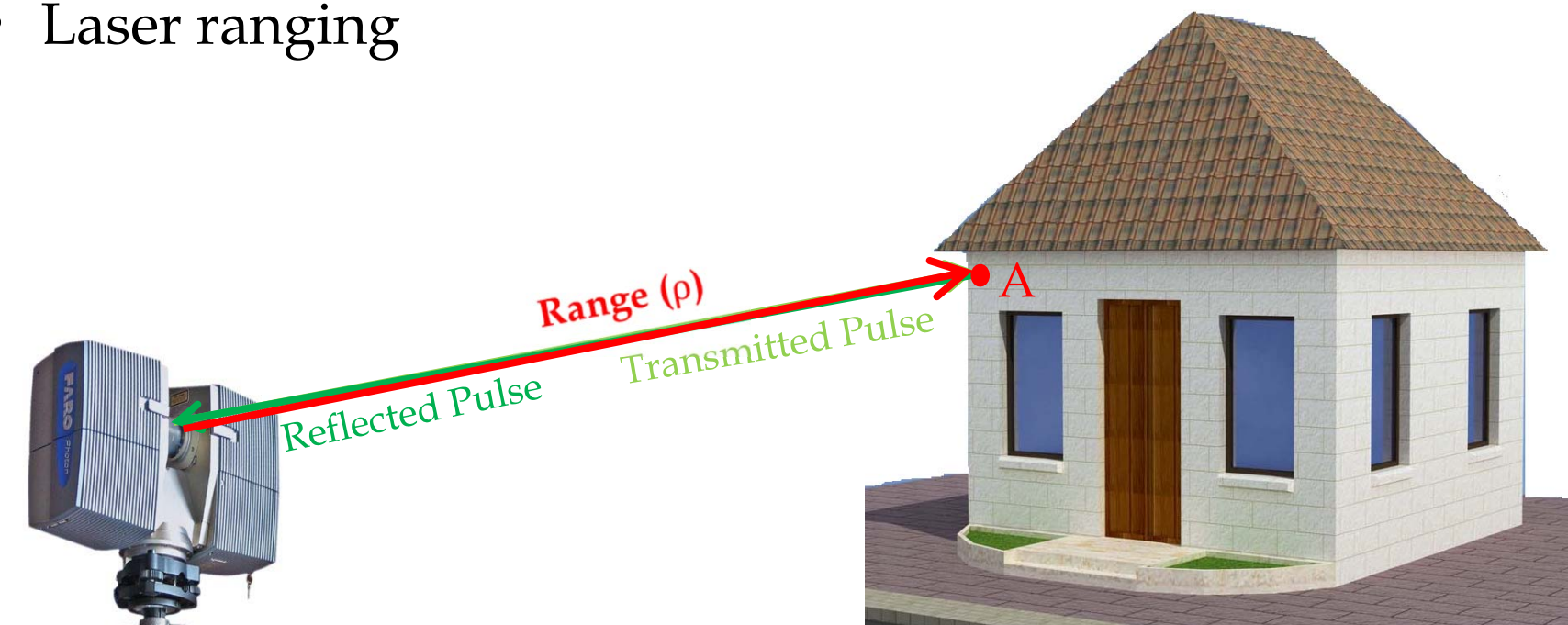


Leica Scanner P20
1 million points/second
120 m range
 ± 6 mm at 100 M position error
[*http://leica-geosystems.com](http://leica-geosystems.com)

Terrestrial Laser Scanner (TLS) refers to LiDAR equipment that is mounted on a tripod.

Terrestrial Laser Scanners

- Laser ranging



Object

$$\text{Range } (\rho) = \frac{t \cdot c}{2}$$

Terrestrial Laser Scanner*

[*http://faro.com](http://faro.com)

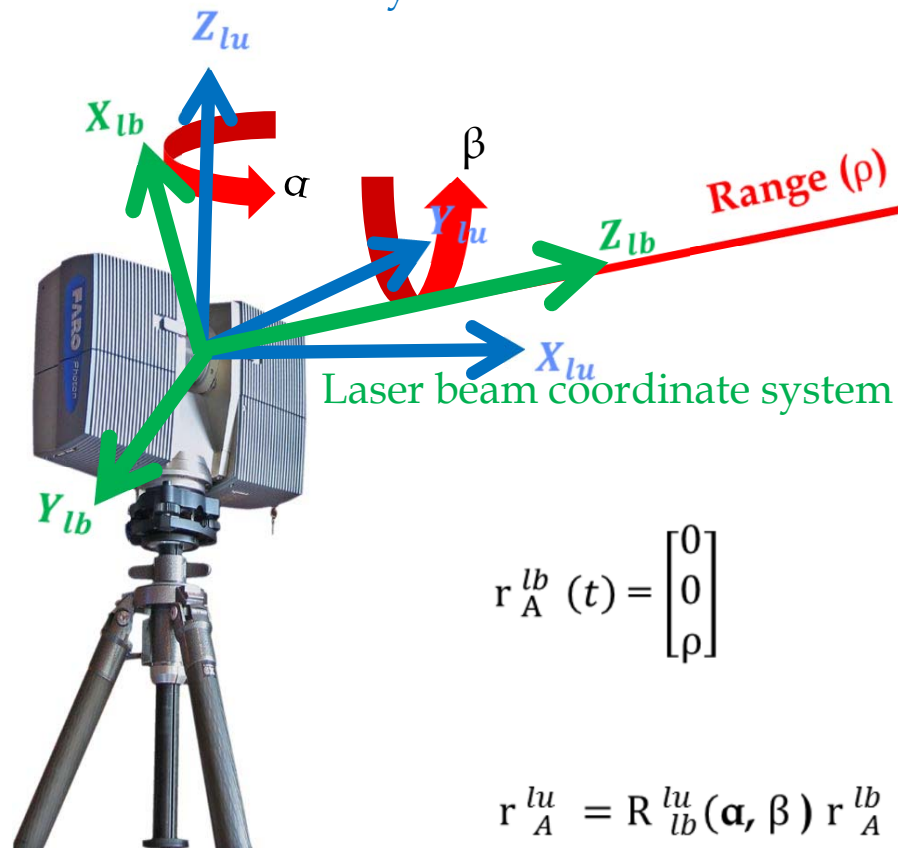
t : Time between transmitted and received pulses

c : Speed of laser light

Terrestrial Laser Scanners

- Laser ranging

Laser unit coordinate system



Object

$$r_A^{lb}(t) = \begin{bmatrix} 0 \\ 0 \\ \rho \end{bmatrix}$$

$$r_A^{lu} = R_{lb}^{lu}(\alpha, \beta) r_A^{lb}$$

r: range vector
lb: laser beam C.S.
lu: Laser unit C.S.
β: rotation around Y_{lu}
α: rotation around Z_{lu}

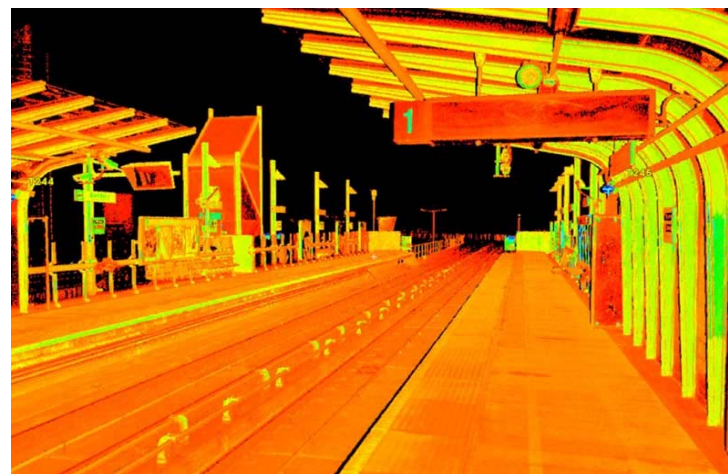
Terrestrial Laser Scanner*

[*http://faro.com](http://faro.com)

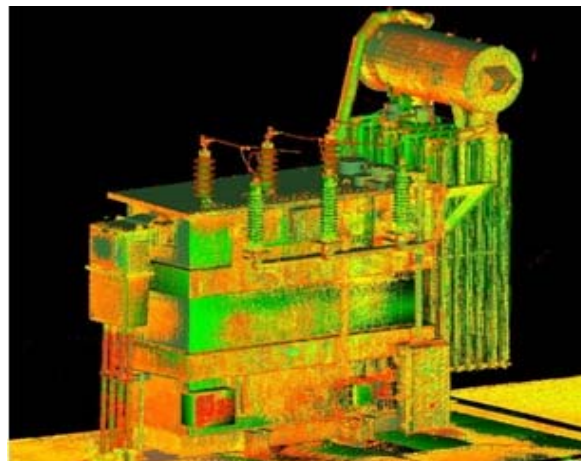
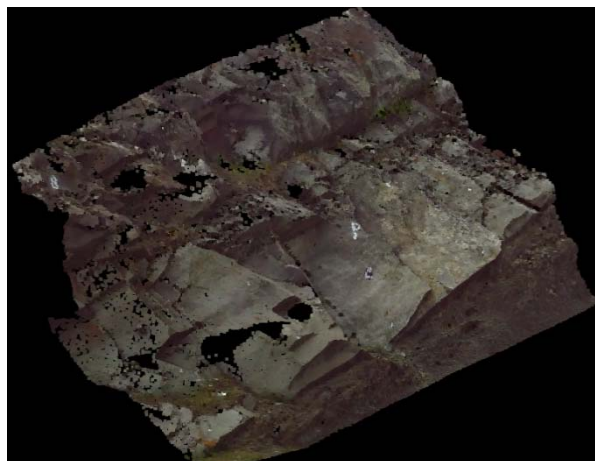
The delivered point cloud will be relative to the laser unit coordinate system.

Introduction: TLS Applications

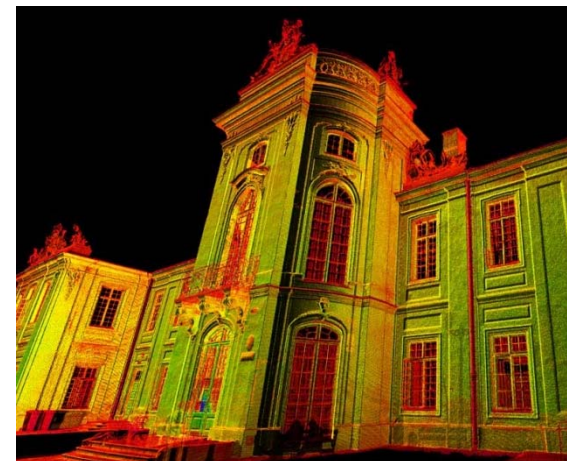
- Digital Building Model generation,
- Cultural heritage documentation,
- Industrial site modeling,
- Landslide hazard analysis, and
- Many other civilian and military applications



<http://lidarusa.com>

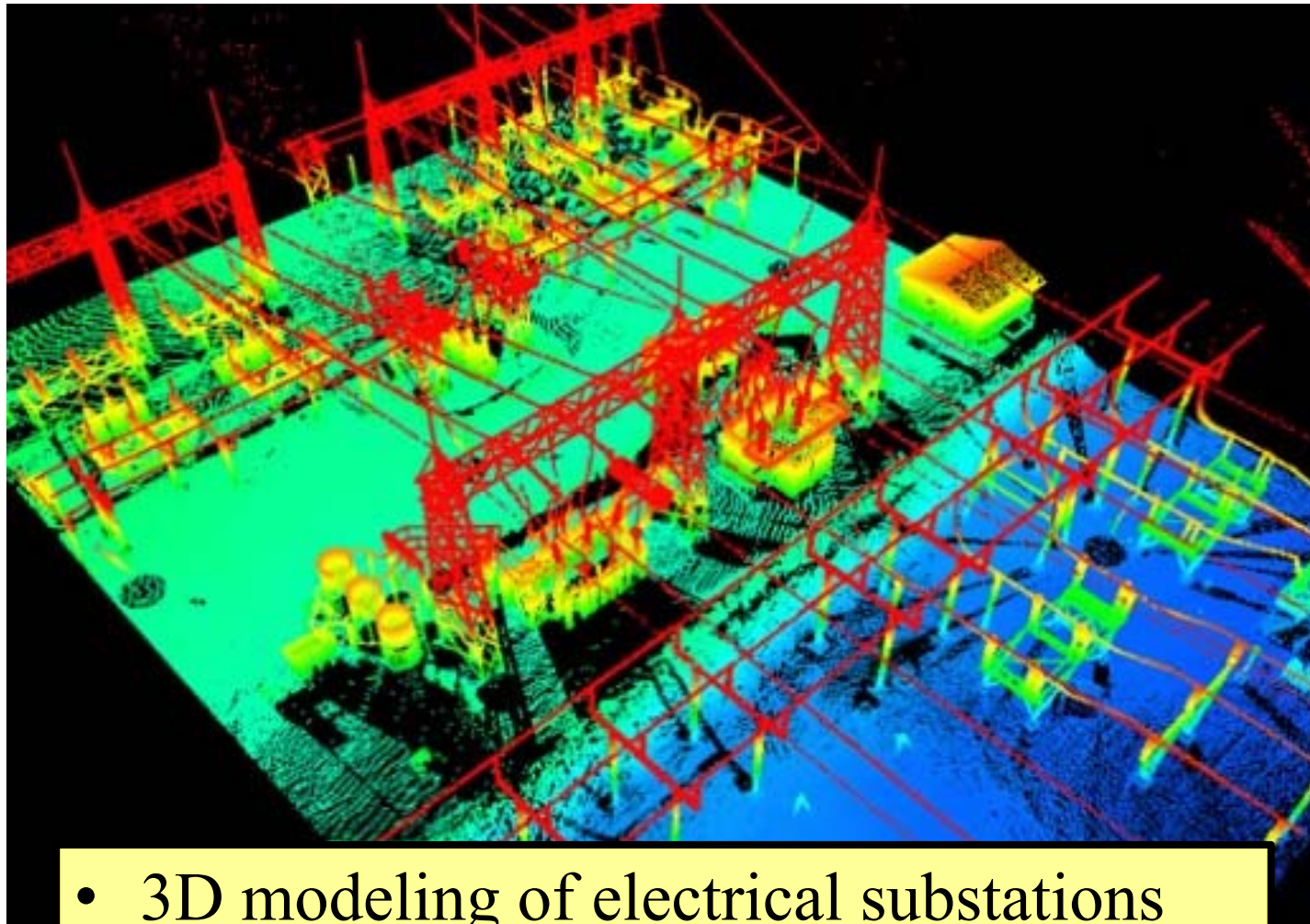


<http://lidarusa.com>



<http://www.3deling.com>

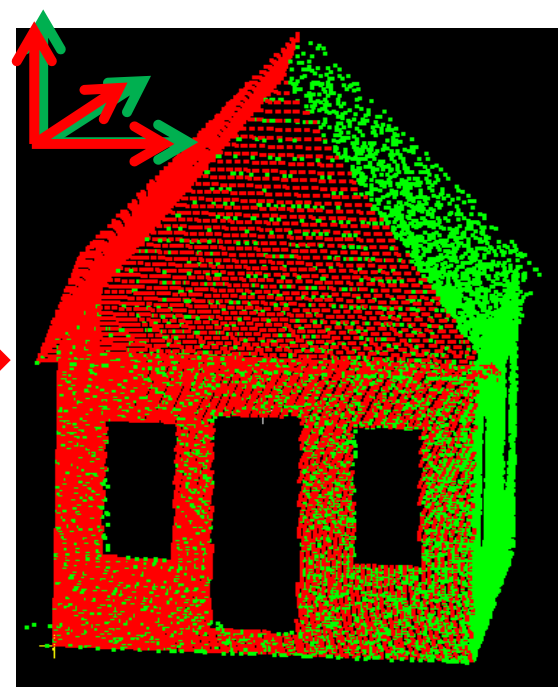
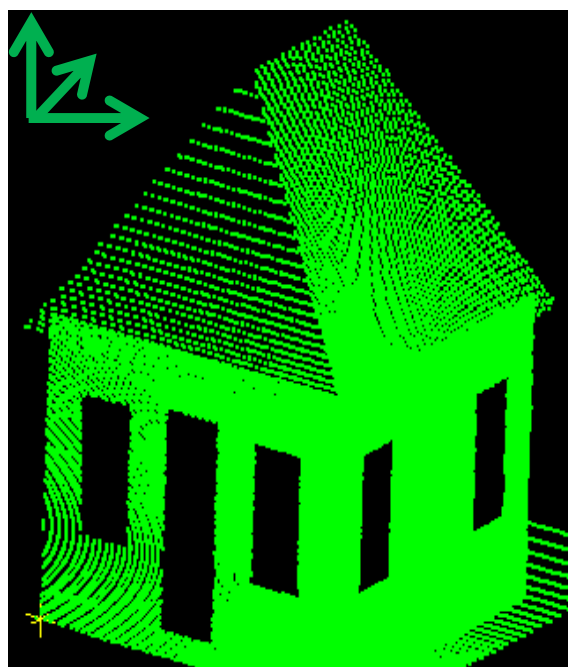
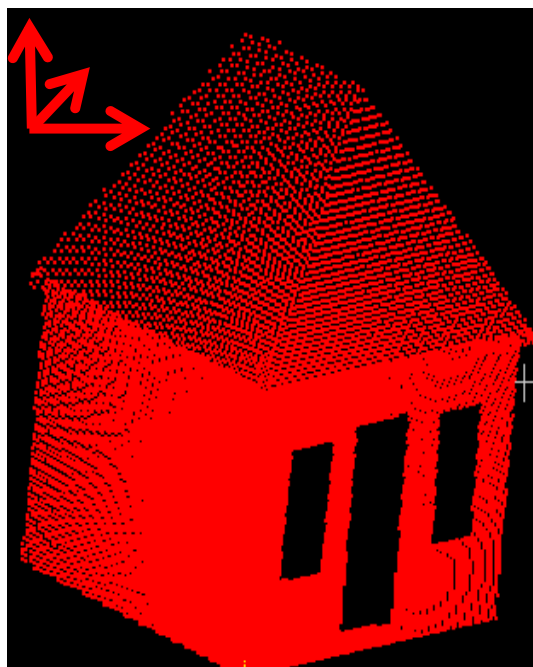
Introduction: TLS Applications



- 3D modeling of electrical substations

Introduction: TLS Registration

- Complex surfaces (or objects) require multiple scans with overlap for a full 3D model:
 - The separate point clouds must be registered to a common reference frame.



Original Scans

Registered Scans

Introduction: TLS Registration

- Complex surfaces (or objects) require multiple scans with overlap for a full 3D model:
 - The separate point clouds must be registered to a common reference frame.

$$X_n = ?$$

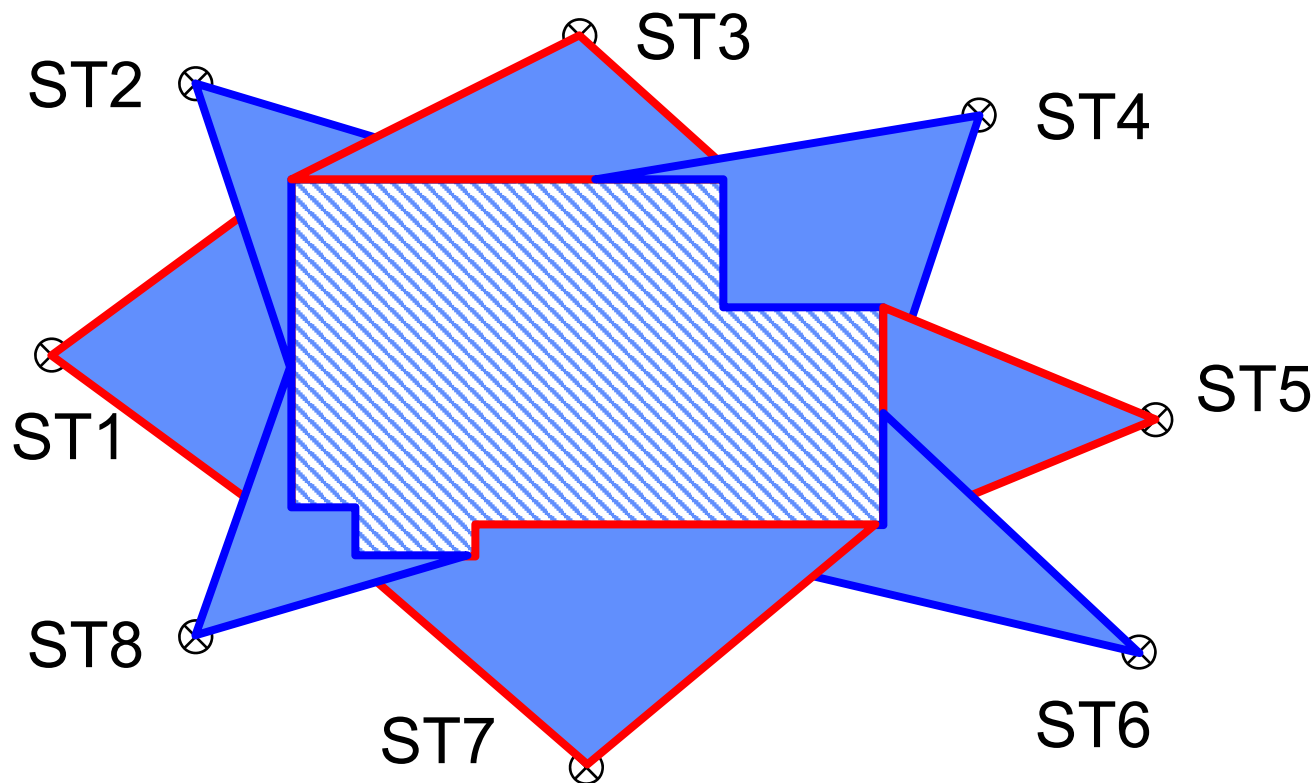
$$Y_n = ?$$

$$Z_n = ?$$

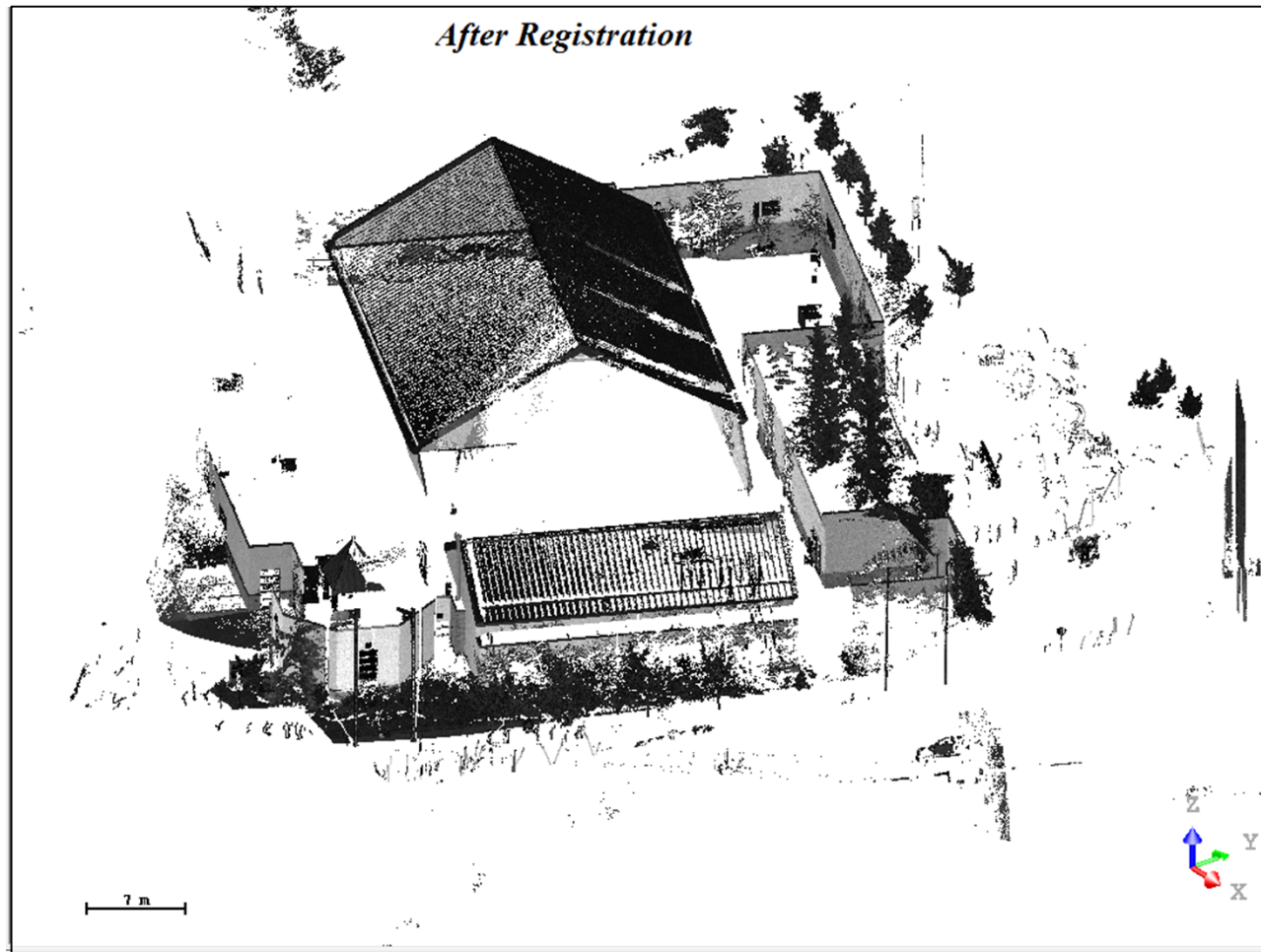
$$\omega_n = ?$$

$$\phi_n = ?$$

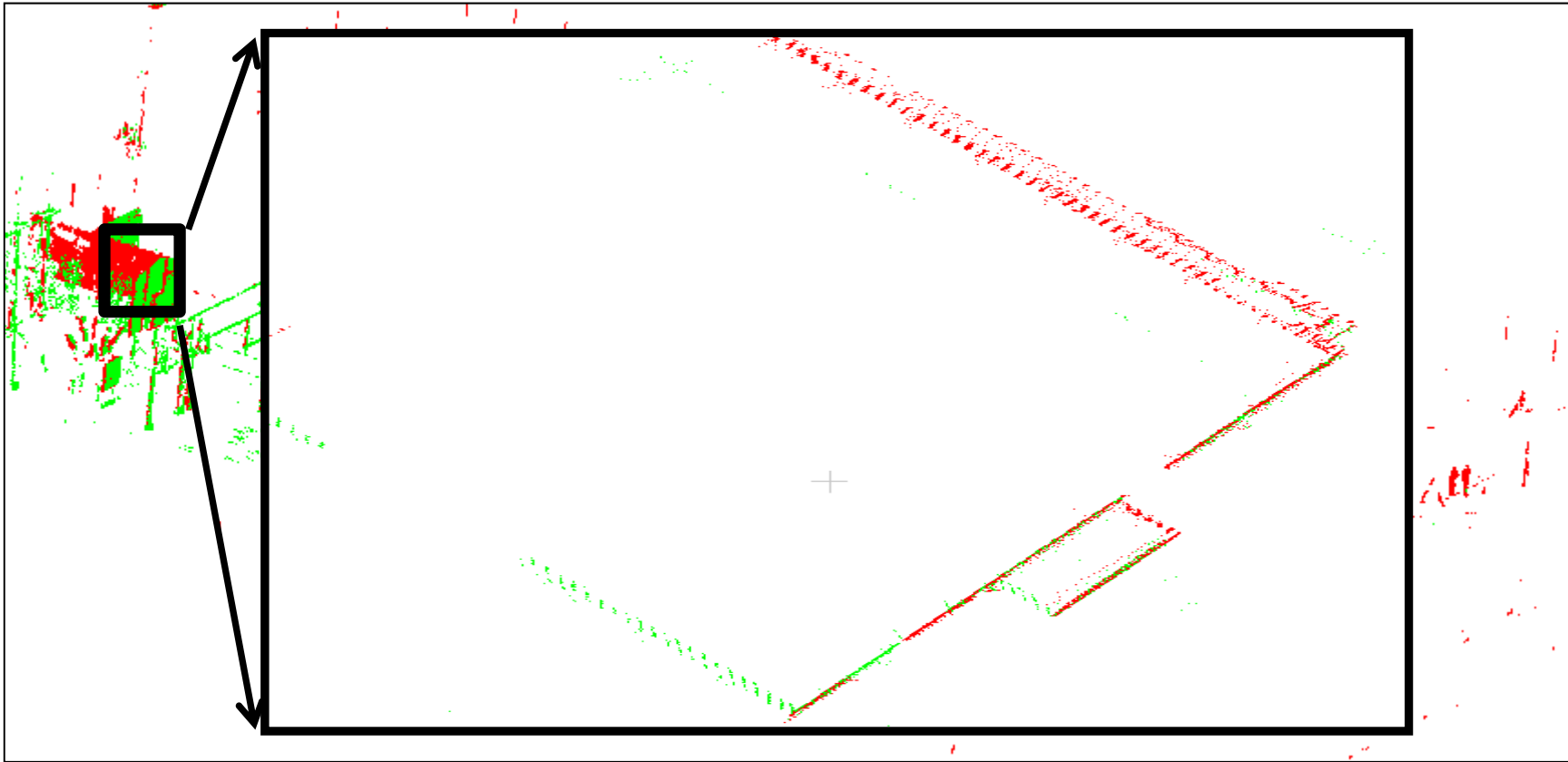
$$\kappa_n = ?$$



Introduction: TLS Registration

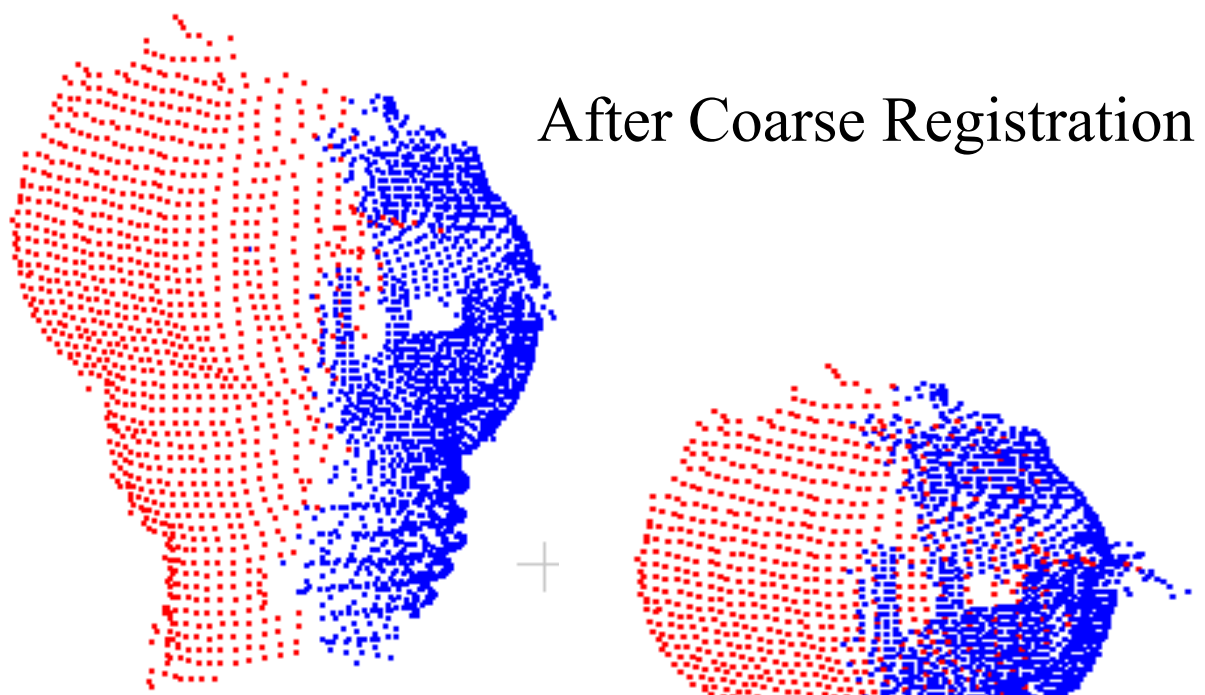


Introduction: Coarse Vs. Fine Registration



Coarse Registration

Introduction: Coarse Vs. Fine Registration



After Coarse Registration

After Fine Registration

Registration and Mobile LiDAR Data



- For LiDAR data, which has been captured by a mobile system – whether terrestrial or airborne, the point cloud will be given relative to a unified coordinate system.
 - Defined by the onboard GNSS/INS unit
- Registration is not necessary for this type of data.
- However, in some situations, systematic errors in the data acquisition system will lead to discrepancies among overlapping point clouds.
- Therefore, we might need to register overlapping mobile LiDAR data.
 - To ensure the alignment of the different datasets, and
 - To evaluate the quality of the system performance (QC).

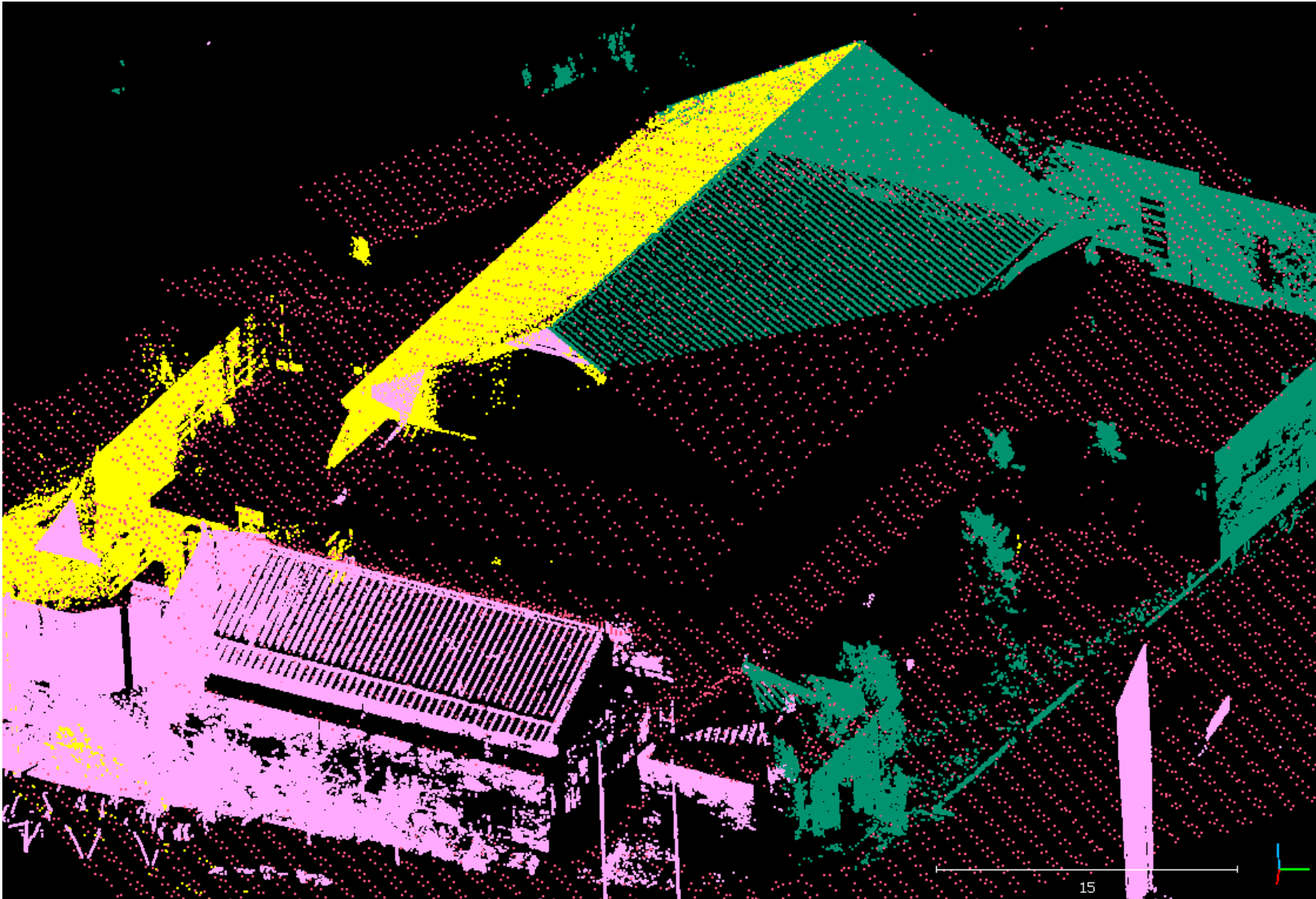
Registration and Mobile LiDAR Data



- For LiDAR data, which has been captured by a mobile system – whether terrestrial or airborne, the point cloud will be given relative to a unified coordinate system.
 - Defined by the onboard GNSS/INS unit
- Registration is not necessary for this type of data.
- However, in some situations, systematic errors in the data acquisition system will lead to discrepancies among overlapping point clouds.
- Therefore, we might need to register overlapping mobile LiDAR data.

The impact of the systematic errors will lead to **coarsely registered datasets**. Thus we need to only worry about the **fine registration** of such data.

Introduction: TLS & ALS Registration





Registration Paradigm Elements

Registration Primitives

- Features that will be identified in the individual scans, e.g. Points, Lines, and Planar features

Transformation Parameters

- Transformation parameters that describe the relationship between the reference frames of the different scans

Similarity Measure

- Describes the coincidence of conjugate primitives after registering different scans to a common reference frame

Matching Strategy

- Controlling framework which is used for manipulating primitives, transformation parameters, and similarity measure

(Habib A. & Al-Ruzouq R. , 2004)



Registration using Exact Point Correspondence

Fine Registration

Registration: Prior Work

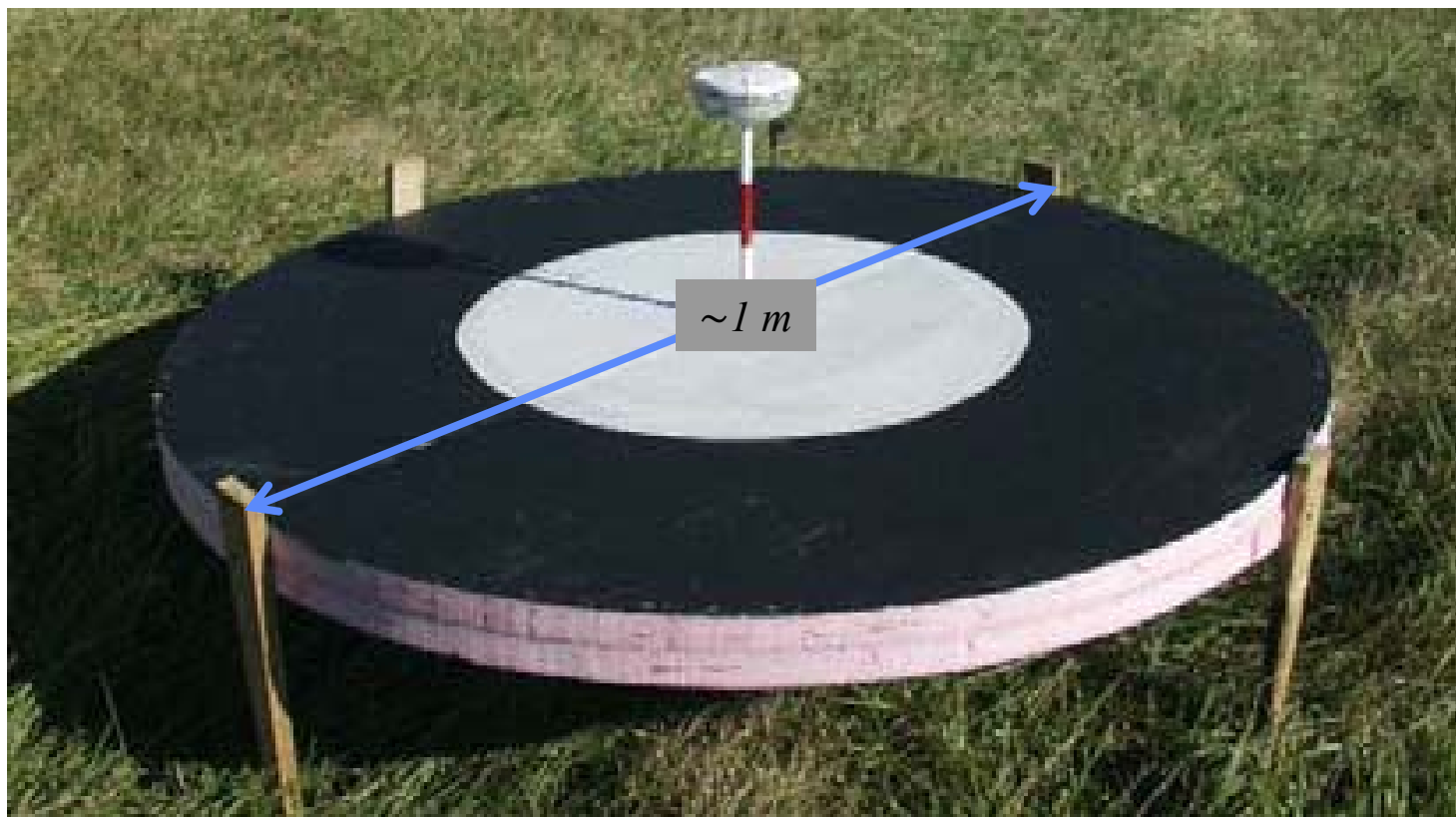
- Registration is performed using corresponding points, which could be signalized targets).



Example of targets used in the registration of terrestrial laser scans (photos courtesy of leica-geosystems)

Registration: Prior Work

- Targets for ALS registration



Example of targets used in the registration of airborne laser scans under special circumstance (photo courtesy of Csanyi & Toth, 2007)



Registration: Point-Based Mathematical Model

$$r_{a_2}^{S_2} = r_{S_1}^{S_2} + SR_{S_1}^{S_2} r_{a_1}^{S_1}$$

- a_1 and a_2 are corresponding points in scans S_1 and S_2 , respectively;
- $r_{a_2}^{S_2}$ is the coordinate of a_2 relative to the reference frame of scan S_2 ;
- $r_{a_1}^{S_1}$ is the coordinate of a_1 relative to the reference frame of scan S_1 ;
- $r_{S_1}^{S_2}$ is the shift between the reference frames of the two scans (relative to the reference frame of scan S_2);
- $R_{S_1}^{S_2}$ is the rotation matrix between the reference frames of the two scans; and
- S is the scale factor. For LiDAR data, the scale **might not** be necessary.

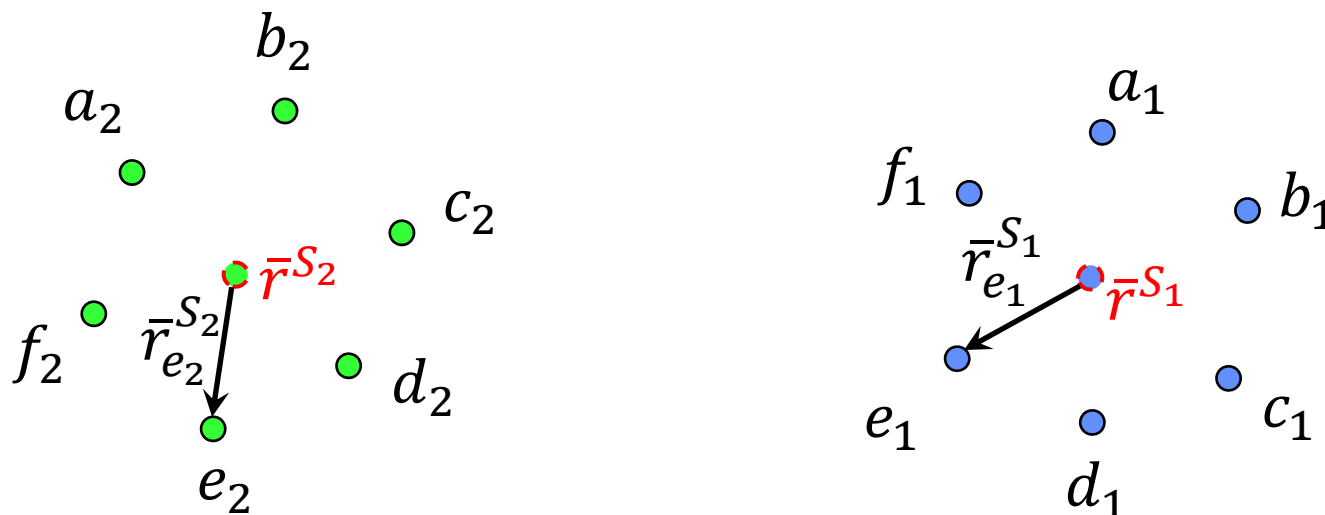


Registration: Horn's Approach

- Closed form solution, which is based on least-squares adjustment, for estimating the transformation parameters relating two 3D coordinate systems using corresponding points (Horn, 1987)
- Procedure:
 - Estimate the rotation matrix,
 - Estimate the scale factor, and
 - Estimate the shifts.

Registration: Horn's Approach

- Rotation Estimation:



$$\hat{r}_{e_2}^{S_2} = \bar{r}_{e_2}^{S_2} / \|\bar{r}_{e_2}^{S_2}\| \quad \& \quad \hat{r}_{e_1}^{S_1} = \bar{r}_{e_1}^{S_1} / \|\bar{r}_{e_1}^{S_1}\|$$

$$\hat{r}_{e_2}^{S_2} = R_{S_1}^{S_2} \hat{r}_{e_1}^{S_1}$$



Registration: Horn's Approach

- **Rotation Estimation:**

- The first step is evaluating the centroid of the points in each dataset: $\bar{r}^{S_1} = 1/n \sum_{i=1}^n r_{a_{1i}}^{S_1}$ & $\bar{r}^{S_2} = 1/n \sum_{i=1}^n r_{a_{2i}}^{S_2}$
- Subtract the centroid from each of the coordinates of the different points in both datasets & derive the corresponding unit vector:

$$\hat{r}_{a_{1i}}^{S_1} = (r_{a_{1i}}^{S_1} - \bar{r}^{S_1}) / \left\| (r_{a_{1i}}^{S_1} - \bar{r}^{S_1}) \right\|$$

$$\hat{r}_{a_{2i}}^{S_2} = (r_{a_{2i}}^{S_2} - \bar{r}^{S_2}) / \left\| (r_{a_{2i}}^{S_2} - \bar{r}^{S_2}) \right\|$$

- Then, we can write the following constraint:

$$\hat{r}_{a_{2i}}^{S_2} = R_{S_1}^{S_2} \hat{r}_{a_{1i}}^{S_1}$$



Registration: Horn's Approach

- **Rotation Estimation:**

- Using quaternions, we can derive the rotation matrix $R_{S_1}^{S_2}$ through the following procedure.

$$\dot{r}_{a_{2i}}^{S_2} = R_{S_1}^{S_2} \dot{r}_{a_{1i}}^{S_1} + e_i$$

- We need to derive $R_{S_1}^{S_2}$ that minimizes the Sum of Squared Errors.

$$\begin{aligned} \min_{R_{S_1}^{S_2}} \sum_{i=1}^n e_i^T e_i &= \min_{R_{S_1}^{S_2}} \sum_{i=1}^n \left(\dot{r}_{a_{2i}}^{S_2} - R_{S_1}^{S_2} \dot{r}_{a_{1i}}^{S_1} \right)^T \left(\dot{r}_{a_{2i}}^{S_2} - R_{S_1}^{S_2} \dot{r}_{a_{1i}}^{S_1} \right) \\ &= \min_{R_{S_1}^{S_2}} \sum_{i=1}^n \dot{r}_{a_{2i}}^{S_2 T} \dot{r}_{a_{2i}}^{S_2} + \dot{r}_{a_{1i}}^{S_1 T} \dot{r}_{a_{1i}}^{S_1} - 2 \dot{r}_{a_{1i}}^{S_1 T} R_{S_1}^{S_2 T} \dot{r}_{a_{2i}}^{S_2} \end{aligned}$$

Quaternion-Based Derivation of $R_{S_1}^{S_2}$



- Rotation Estimation:**

$$\min_{R_{S_1}^{S_2}} \sum_{i=1}^n e_i^T e_i = \min_{R_{S_1}^{S_2}} \sum_{i=1}^n \dot{r}_{a_{2i}}^{S_2 T} \dot{r}_{a_{2i}}^{S_2} + \dot{r}_{a_{1i}}^{S_1 T} \dot{r}_{a_{1i}}^{S_1} - 2 \dot{r}_{a_{1i}}^{S_1 T} R_{S_1}^{S_2 T} \dot{r}_{a_{2i}}^{S_2}$$

- Note: $\dot{r}_{a_{2i}}^{S_2 T} \dot{r}_{a_{2i}}^{S_2}$ & $\dot{r}_{a_{1i}}^{S_1 T} \dot{r}_{a_{1i}}^{S_1}$ are always +ve.

- Thus: $\sum_{i=1}^n e_i^T e_i$ is minimized when $\sum_{i=1}^n \dot{r}_{a_{1i}}^{S_1 T} R_{S_1}^{S_2 T} \dot{r}_{a_{2i}}^{S_2}$ is maximized



$$\max_{R_{S_1}^{S_2}} \sum_{i=1}^n \dot{r}_{a_{1i}}^{S_1 T} R_{S_1}^{S_2 T} \dot{r}_{a_{2i}}^{S_2} = \max_{R_{S_1}^{S_2}} \sum_{i=1}^n R_{S_1}^{S_2} \dot{r}_{a_{1i}}^{S_1} \cdot \dot{r}_{a_{2i}}^{S_2}$$

Quaternion-Based Derivation of $R_{S_1}^{S_2}$



- Rotation Estimation:**

$$\begin{aligned}
 \max_{R_{S_1}^{S_2}} \sum_{i=1}^n \dot{r}_{a_{1i}}^{S_1 T} R_{S_1}^{S_2 T} \dot{r}_{a_{2i}}^{S_2} &= \max_{R_{S_1}^{S_2}} \sum_{i=1}^n R_{S_1}^{S_2} \dot{r}_{a_{1i}}^{S_1} \cdot \dot{r}_{a_{2i}}^{S_2} \\
 \max_{\dot{q}} \sum_{i=1}^n \left(\dot{q} \dot{r}_{a_{1i}}^{S_1} \dot{q}^* \right) \cdot \dot{r}_{a_{2i}}^{S_2} &= \max_{\dot{q}} \sum_{i=1}^n \left(\dot{q} \dot{r}_{a_{1i}}^{S_1} \right) \cdot \left(\dot{r}_{a_{2i}}^{S_2} \dot{q} \right) \\
 &= \max_{\dot{q}} \sum_{i=1}^n \left(\bar{C}(\dot{r}_{a_{1i}}^{S_1}) \dot{q} \right) \cdot \left(C(\dot{r}_{a_{2i}}^{S_2}) \dot{q} \right) \\
 &= \max_{\dot{q}} \sum_{i=1}^n \dot{q}^T \bar{C}(\dot{r}_{a_{1i}}^{S_1})^T C(\dot{r}_{a_{2i}}^{S_2}) \dot{q} \\
 &= \max_{\dot{q}} \dot{q}^T \left(\sum_{i=1}^n \bar{C}(\dot{r}_{a_{1i}}^{S_1})^T C(\dot{r}_{a_{2i}}^{S_2}) \right) \dot{q} = \max_{\dot{q}} \dot{q}^T \mathbf{S} \dot{q}
 \end{aligned}$$

Quaternion-Based Derivation of $R_{S_1}^{S_2}$



- Rotation Estimation:**

$$S_i = \bar{C} \left(\dot{r}_{a_{1i}}^{S_1} \right)^T C \left(\dot{r}_{a_{2i}}^{S_2} \right)$$

$$S_i = \begin{bmatrix} \dot{r}_{a_{1i}0}^{S_1} & -\dot{r}_{a_{1i}x}^{S_1} & -\dot{r}_{a_{1i}y}^{S_1} & -\dot{r}_{a_{1i}z}^{S_1} \\ \dot{r}_{a_{1i}x}^{S_1} & \dot{r}_{a_{1i}0}^{S_1} & \dot{r}_{a_{1i}z}^{S_1} & -\dot{r}_{a_{1i}y}^{S_1} \\ \dot{r}_{a_{1i}y}^{S_1} & -\dot{r}_{a_{1i}z}^{S_1} & \dot{r}_{a_{1i}0}^{S_1} & \dot{r}_{a_{1i}x}^{S_1} \\ \dot{r}_{a_{1i}z}^{S_1} & \dot{r}_{a_{1i}y}^{S_1} & -\dot{r}_{a_{1i}x}^{S_1} & \dot{r}_{a_{1i}0}^{S_1} \end{bmatrix}^T \begin{bmatrix} \dot{r}_{a_{2i}0}^{S_2} & -\dot{r}_{a_{2i}x}^{S_2} & -\dot{r}_{a_{2i}y}^{S_2} & -\dot{r}_{a_{2i}z}^{S_2} \\ \dot{r}_{a_{2i}x}^{S_2} & \dot{r}_{a_{2i}0}^{S_2} & -\dot{r}_{a_{2i}z}^{S_2} & \dot{r}_{a_{2i}y}^{S_2} \\ \dot{r}_{a_{2i}y}^{S_2} & \dot{r}_{a_{2i}z}^{S_2} & \dot{r}_{a_{2i}0}^{S_2} & -\dot{r}_{a_{2i}x}^{S_2} \\ \dot{r}_{a_{2i}z}^{S_2} & -\dot{r}_{a_{2i}y}^{S_2} & \dot{r}_{a_{2i}x}^{S_2} & \dot{r}_{a_{2i}0}^{S_2} \end{bmatrix}$$

Quaternion-Based Derivation of $R_{S_1}^{S_2}$



- Rotation Estimation:**

$$S_i = \bar{C} \left(\dot{r}_{a_{1i}}^{S_1} \right)^T C \left(\dot{r}_{a_{2i}}^{S_2} \right)$$

$$S_i(1, 1) = \dot{r}_{a_{1i_0}}^{S_1} \dot{r}_{a_{2i_0}}^{S_2} + \dot{r}_{a_{1i_x}}^{S_1} \dot{r}_{a_{2i_x}}^{S_2} + \dot{r}_{a_{1i_y}}^{S_1} \dot{r}_{a_{2i_y}}^{S_2} + \dot{r}_{a_{1i_z}}^{S_1} \dot{r}_{a_{2i_z}}^{S_2}$$

$$S_i(2, 2) = \dot{r}_{a_{1i_x}}^{S_1} \dot{r}_{a_{2i_x}}^{S_2} + \dot{r}_{a_{1i_0}}^{S_1} \dot{r}_{a_{2i_0}}^{S_2} - \dot{r}_{a_{1i_z}}^{S_1} \dot{r}_{a_{2i_z}}^{S_2} - \dot{r}_{a_{1i_y}}^{S_1} \dot{r}_{a_{2i_y}}^{S_2}$$

$$S_i(3, 3) = \dot{r}_{a_{1i_y}}^{S_1} \dot{r}_{a_{2i_y}}^{S_2} - \dot{r}_{a_{1i_z}}^{S_1} \dot{r}_{a_{2i_z}}^{S_2} + \dot{r}_{a_{1i_0}}^{S_1} \dot{r}_{a_{2i_0}}^{S_2} - \dot{r}_{a_{1i_x}}^{S_1} \dot{r}_{a_{2i_x}}^{S_2}$$

$$S_i(4, 4) = \dot{r}_{a_{1i_z}}^{S_1} \dot{r}_{a_{2i_z}}^{S_2} - \dot{r}_{a_{1i_y}}^{S_1} \dot{r}_{a_{2i_y}}^{S_2} - \dot{r}_{a_{1i_x}}^{S_1} \dot{r}_{a_{2i_x}}^{S_2} + \dot{r}_{a_{1i_0}}^{S_1} \dot{r}_{a_{2i_0}}^{S_2}$$

Remember that $\dot{r}_{a_{1i}}^{S_1}$ & $\dot{r}_{a_{2i}}^{S_2}$ are pure quaternions.

$$\text{Trace}(S_i) = 0$$

$$\text{Trace } S = 0$$

Quaternion-Based Derivation of $R_{S_1}^{S_2}$



- **Rotation Estimation:**

$$\max_{\dot{q}} \dot{q}^T \mathbf{S} \dot{q} , \quad \|\dot{q}\| = 1$$

$$\max_{\dot{q}} \varphi(\dot{q}) = \dot{q}^T \mathbf{S} \dot{q} - 2\lambda(\dot{q}^T \dot{q} - 1)$$

$$\frac{\partial \varphi}{\partial \dot{q}} = 2\mathbf{S} \dot{q} - 2\lambda \dot{q} = 0$$

$$\mathbf{S} \dot{q} = \lambda \dot{q}$$

This is the case only when \dot{q} is the eigenvector of \mathbf{S} .

$$\dot{q}^T \mathbf{S} \dot{q} = \dot{q}^T \lambda \dot{q} = \lambda \dot{q}^T \dot{q} = \lambda$$

$\dot{q}^T \mathbf{S} \dot{q}$ will be maximum when \dot{q} is the eigenvector of \mathbf{S} that corresponds to the largest eigenvalue.

Quaternion-Based Derivation of $R_{S_1}^{S_2}$



- **Rotation Estimation:**

$$R_{S_1}^{S_2} = \begin{bmatrix} r_{11} & r_{12} & r_{13} \\ r_{21} & r_{22} & r_{23} \\ r_{31} & r_{32} & r_{33} \end{bmatrix}$$

$$r_{11} = q_x^2 + q_o^2 - q_z^2 - q_y^2$$

$$r_{12} = 2q_xq_y - 2q_oq_z$$

$$r_{13} = 2q_xq_z + 2q_oq_y$$

$$r_{21} = 2q_xq_y + 2q_oq_z$$

$$r_{22} = q_y^2 - q_z^2 + q_o^2 - q_x^2$$

$$r_{23} = 2q_yq_z - 2q_oq_x$$

$$r_{31} = 2q_xq_z - 2q_oq_y$$

$$r_{32} = 2q_yq_z + 2q_oq_x$$

$$r_{33} = q_z^2 - q_y^2 - q_x^2 + q_o^2$$



Estimation of the Scale Factor & Translation

- **Scale and Shift Estimation:**

- The scale factor can be derived according to the following formula:

$$\bar{r}_{a_{1i}}^{S_1} = (r_{a_{1i}}^{S_1} - \bar{r}^{S_1}) \quad \& \quad \bar{r}_{a_{2i}}^{S_2} = (r_{a_{2i}}^{S_2} - \bar{r}^{S_2})$$

$$S = \left(\frac{\sum_{i=1}^n \left\| \bar{r}_{a_{2i}}^{S_2} \right\|^2}{\sum_{i=1}^n \left\| \bar{r}_{a_{1i}}^{S_1} \right\|^2} \right)^{1/2}$$

- The translation component can be estimated as follows:

$$r_{S_1}^{S_2} = 1/n \sum_{i=1}^n (r_{a_{2i}}^{S_2} - SR_{S_1}^{S_2} r_{a_{1i}}^{S_1})$$



Point-Based Registration without Exact Point-to-Point Correspondence

Fine Registration

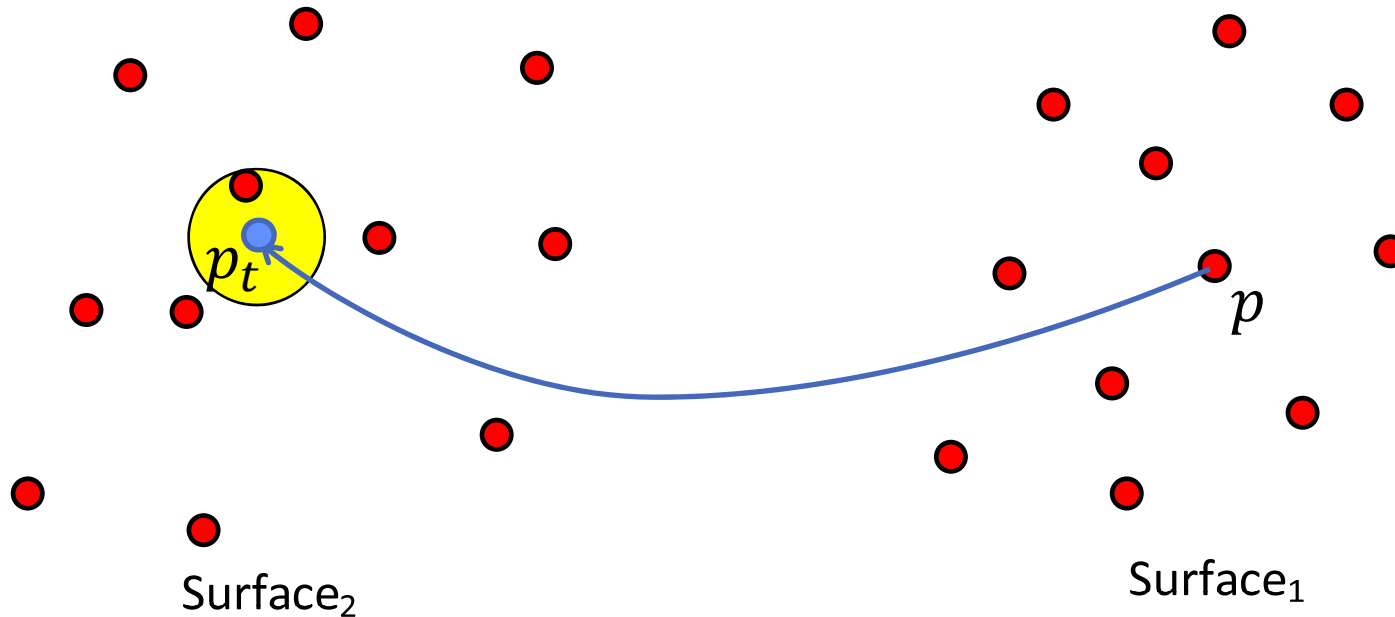


Registration: Prior Work

- **Commonly Adopted Point-Based Registration Methodologies without Exact Point-to-Point Correspondence:**
 - The Iterative Closest Point “ICP” (*Besl and Mckay, 1992*)
 - The Iterative Closest Patch “ICPatch” (*Habib et al., 2010*)
 - The Iterative Closest Projected Point “ICPP” (*Al-Durgham et al., 2011*)
- Point-based registration methodologies require good initial approximations of the transformation parameters, which could be established through **manual interaction**.

Registration: Prior Work

- Iterative Closest Point (ICP):



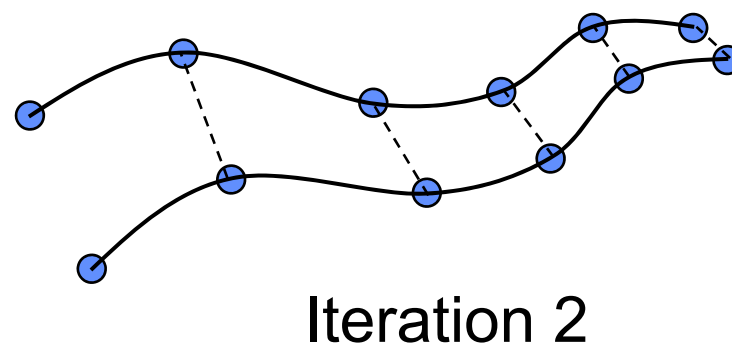
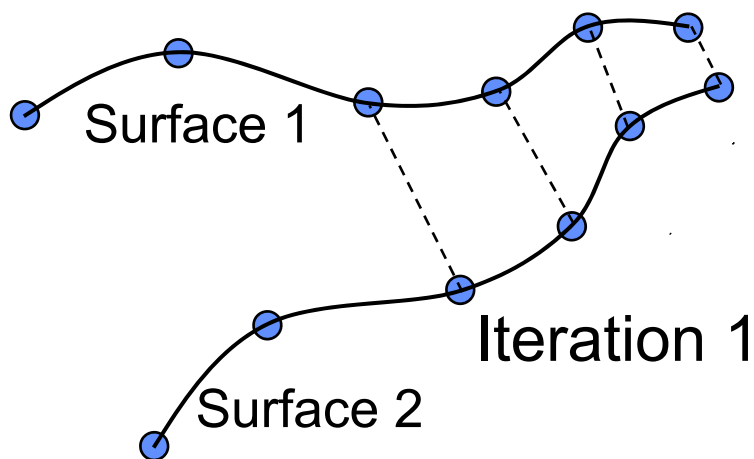
Note: ICP assumes point-to-point correspondence which is invalid among LiDAR points due to the irregular sampling nature of the points.

Registration: Prior Work

- Iterative Closest Point (ICP):
 - Besl and McKay (1992)
 - Points as primitives
 - 3D rigid body transformation
 - Minimizes Euclidian distances
 - Performed iteratively

Problem:

- Exact point correspondences cannot be guaranteed when dealing with irregular point clouds.

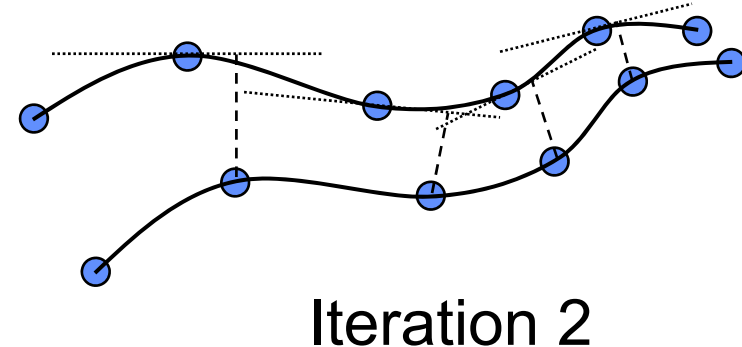
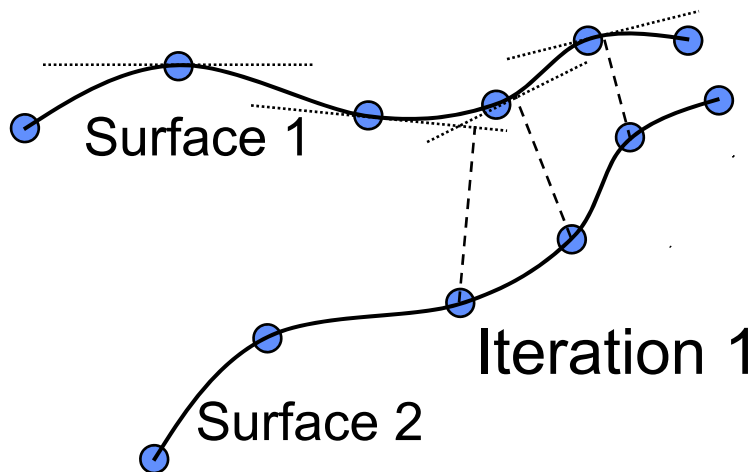


Registration: Prior Work

- Iterative Closest Point (ICP):
 - Chen and Medioni (1992)
 - Points and planes as primitives
 - Minimizes normal distances

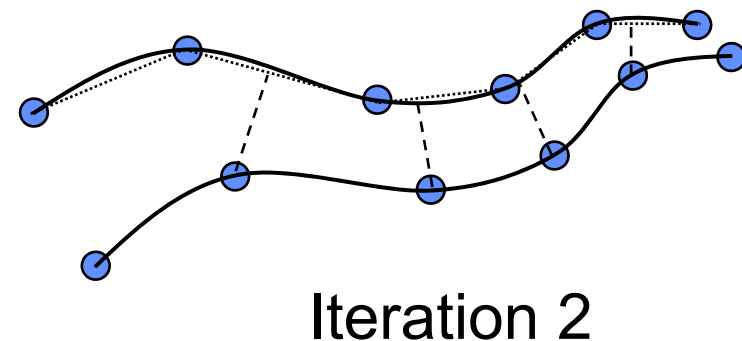
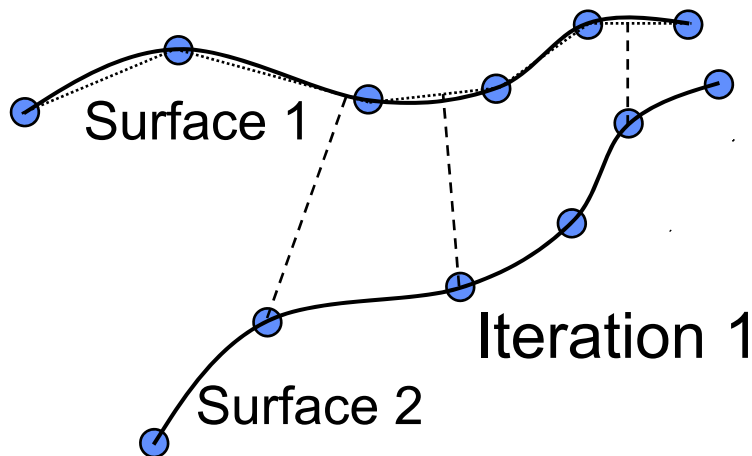
Prerequisite:

- The algorithm requires local plane fitting.



Registration: Prior Work

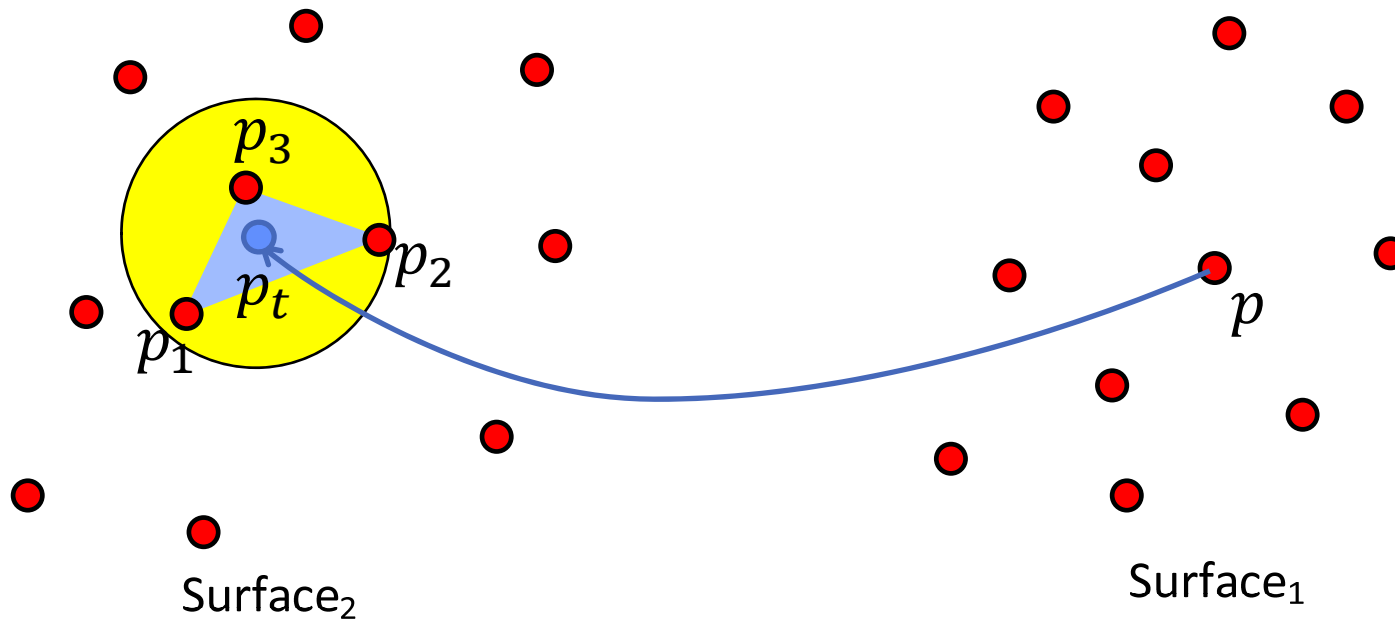
- Iterative Closest Point (ICP): Variants
 - Points and triangular irregular network (TIN) patches
 - 3D similarity transformation
 - Coplanarity constraint and modified weight matrix
 - Performed iteratively



ICPatch

Registration: Prior Work

- Iterative Closest Patch (ICPatch):

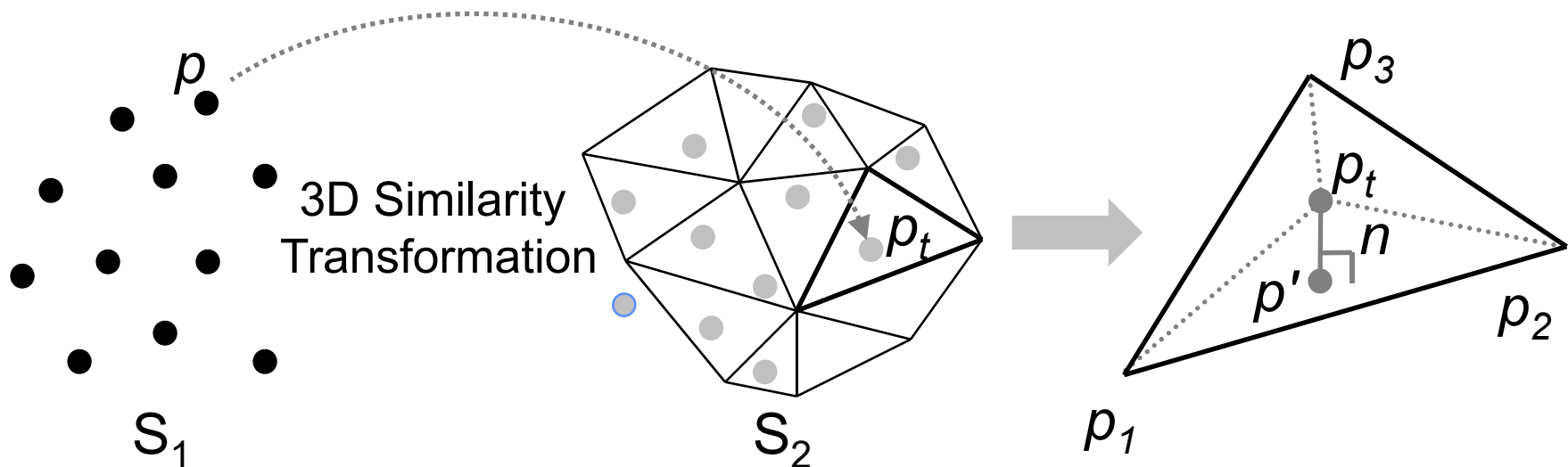


$$r_p^{S_2} = r_{S_1}^{S_2} + R_{S_1}^{S_2} r_p^{S_1}$$

$$p_t = r_{S_1}^{S_2} + R_{S_1}^{S_2} p$$

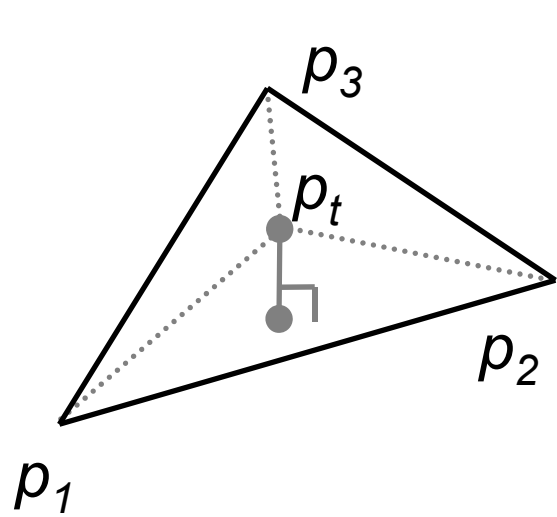
Registration: Prior Work

- Iterative Closest Patch (ICPatch):
 - Conditions for valid conjugate point-patch pairs:
 - ✓ Triangular patch $\Delta p_1 p_2 p_3$ must be the closest to the transformed point p_t , i.e. $n = \min$.
 - ✓ The normal distance, n , must be within a threshold.
 - ✓ The projection of p_t, p' , must fall within $\Delta p_1 p_2 p_3$.



Registration: Prior Work

- Iterative Closest Patch (ICPatch):
- Similarity Measure: p_1, p_2, p_3 and p_t are assumed to be coplanar, i.e. the volume of the pyramid formed by vertices p_1, p_2, p_3 and p_t should be zero.

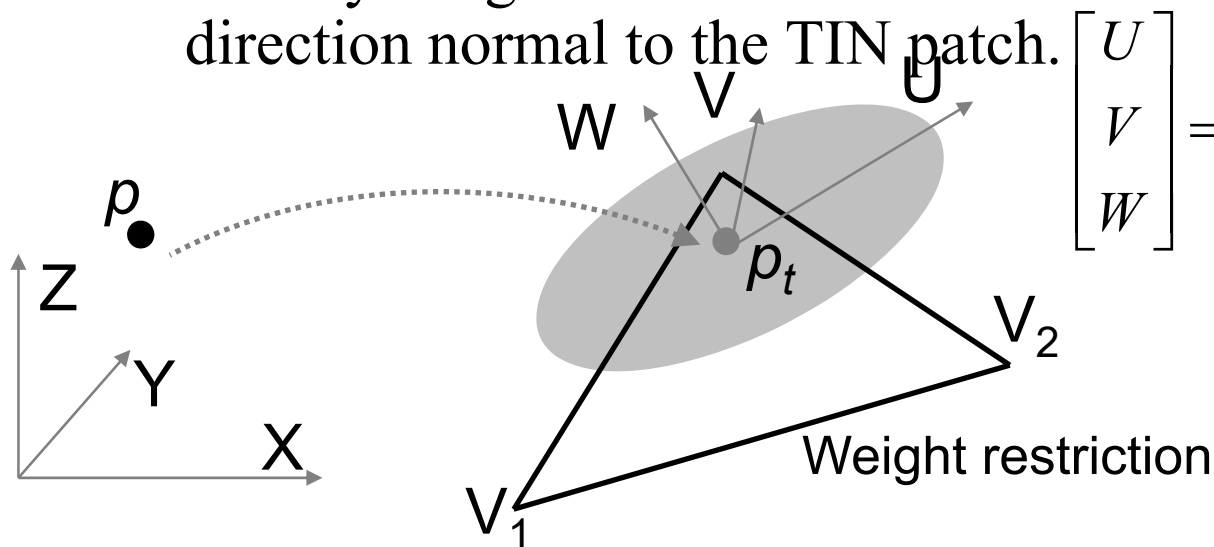


$$\det \begin{bmatrix} X_{p_t} & Y_{p_t} & Z_{p_t} & 1 \\ X_{p_1} & Y_{p_1} & Z_{p_1} & 1 \\ X_{p_2} & Y_{p_2} & Z_{p_2} & 1 \\ X_{p_3} & Y_{p_3} & Z_{p_3} & 1 \end{bmatrix} = 0$$

$$p_t = r_{s_1}^{s_2} + R_{s_1}^{s_2} p$$

Registration: Prior Work

- Iterative Closest Patch (ICPatch):
- Similarity measure: $p_3 = p_t + \text{random error} \ \& \ \text{discrepancy vector}$
 - Correspondence assumption is not true.
 - Point-based procedure, while using non-conjugate points from a valid point-patch pair
 - Modify weights so the misclosure vector is minimized in the direction normal to the TIN patch.



$$\begin{bmatrix} U \\ V \\ W \end{bmatrix} = M \cdot \begin{bmatrix} X \\ Y \\ Z \end{bmatrix}$$

$$Q_{UVW}^{-1} = M \cdot Q_{XYZ}^{-1} \cdot M^T$$

$$Q'_{UVW}^{-1} = \begin{bmatrix} 0 & 0 & 0 \\ 0 & 0 & 0 \\ 0 & 0 & q_W^{-1} \end{bmatrix}$$

$$Q'_{XYZ}^{-1} = \frac{1}{42} M^T \cdot Q'_{UVW}^{-1} \cdot M$$

Registration: Prior Work

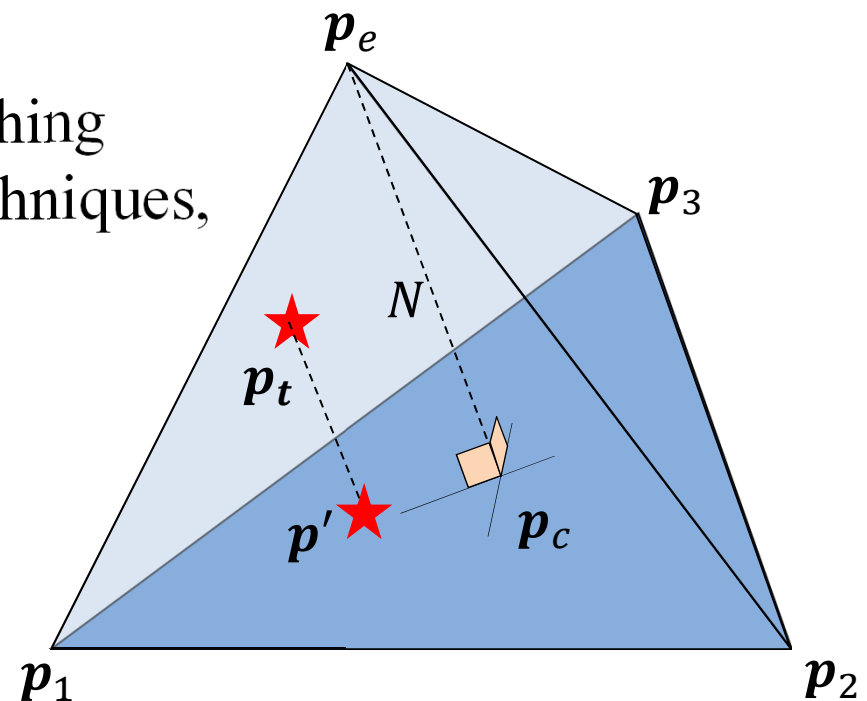
- Iterative Closest Projected Point (ICPP):
 - For a point p in S_1 , find the *closest* three points in S_2 .
 - A match is established between a point in S_1 and a triangle (p_1, p_2, p_3) in S_2 .

The pair (p_t, p') is used for matching through the conventional ICP techniques, thus named the ICPP.

$$0 = r_2^m + R_2^m p' - (r_1^m + R_1^m p)$$

Conditions:

- $p_t \in \text{Convex}(p_1, p_2, p_3, p_e)$
- Compatible surface normals





Feature-Based Registration

Coarse Registration



Registration: Prior Work

- **Registration Methodologies Based on Linear and Planar Features:**
 - Linear and planar features provide strong link between laser scans, and a good initial approximation of the transformation parameters is not required.
 - Linear and planar features can be utilized to register TLS data using different features individually and also by combining some of them (*Jaw and Chuang ,2008*).
 - Photogrammetric data can be incorporated to take advantage of additional information (*Canaz and Habib, 2013*).
 - Manual identification of conjugate features is usually required.

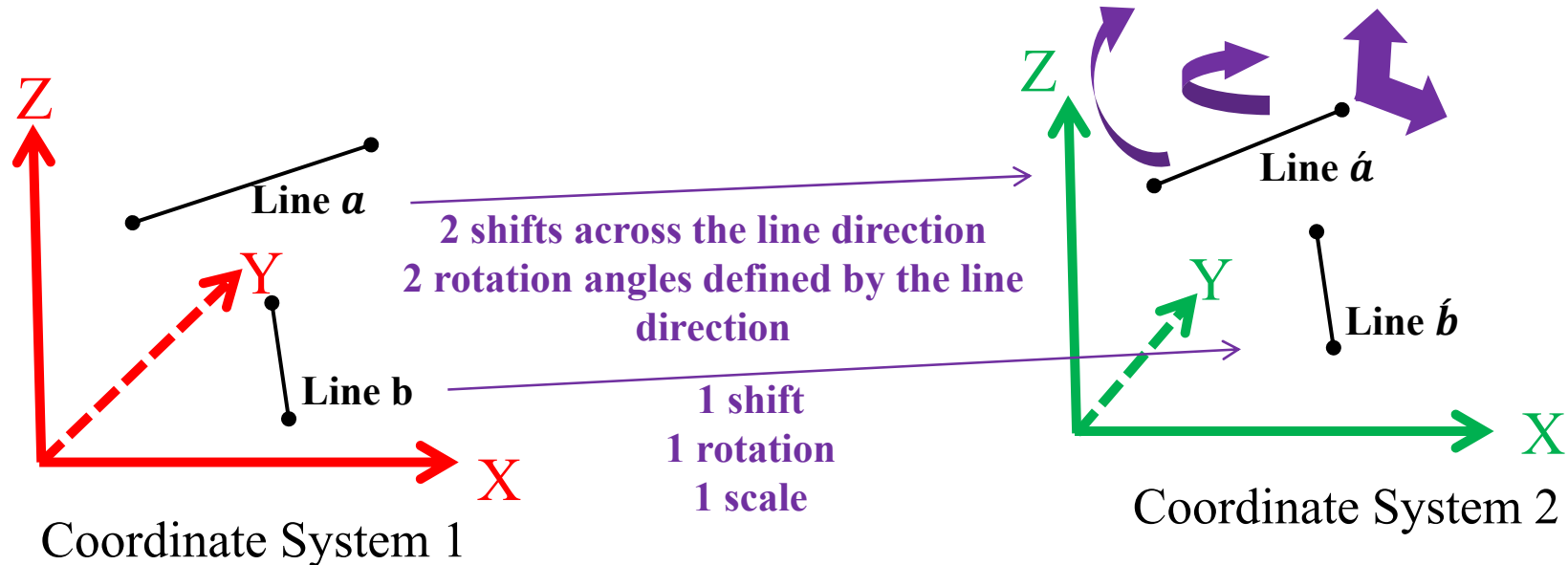


Registration: Prior Work

- **Registration Methodologies Based on Linear and Planar Features:**
 - An automatic registration method of laser scans using extracted linear and planar features is proposed by Yao et al., 2010.
 - Measures that describe the shape and distribution of groups of linear features in 3D space are proposed.
 - The line-based approach usually failed in outdoor environments.
 - Sensitive to existing symmetries present in the extracted features

Registration: Prior Work

- Registration Based on Linear Features:**



- In total, 7 transformation parameters ($X_T, Y_T, Z_T, \omega, \varphi, \kappa, S$) can be estimated using two skew lines.
- Two coplanar and non-parallel lines are enough for the estimation of the shift and rotation parameters (scale is defined by the range measurements).



Objective & Methodology

- Develop a matching strategy for the automatic registration of terrestrial laser scans in a pairwise fashion using 3D linear features:
 - Linear features extraction from TLS scans
 - Mathematical model for estimating the transformation parameters
 - Invariant characteristics of 3D linear features for the matching strategy & RANSAC approach
 - Iterative Closest Projected Point (ICPP) for identifying the most probable matches among the linear features and the refinement of the transformation parameters

Methodology: Alternative Approaches

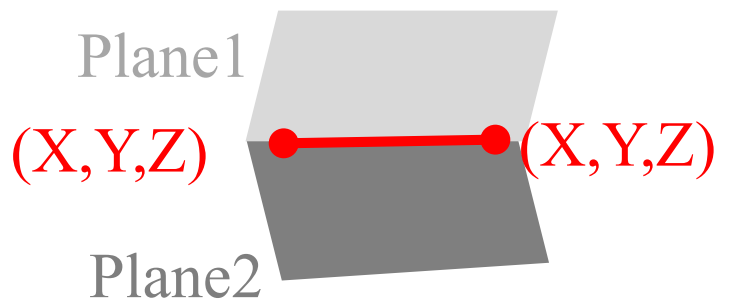


- 1 RANSAC approach
- 2 Association-based sample consensus approach
- 3 Solution frequency approach

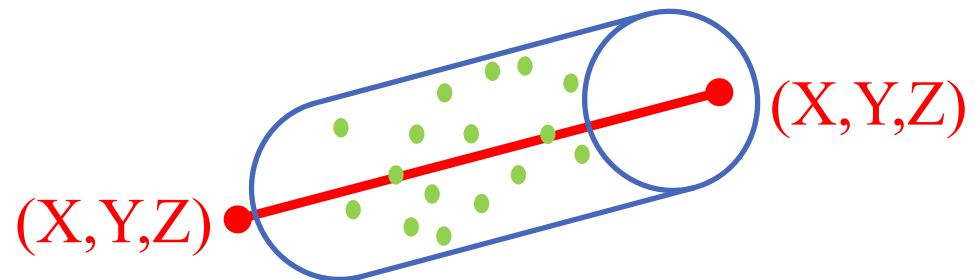
Methodology: Primitive Extraction

- **Linear Features Extraction from Terrestrial Laser Scans:**

- Planar patch segmentation and intersection for the extraction of linear features (*Lari and Habib, 2014*)
- A region growing methodology for the extraction of cylindrical/linear features from the scans



Planar patch segmentation
and intersection procedure



Region growing methodology for
the extraction of cylindrical/linear
features

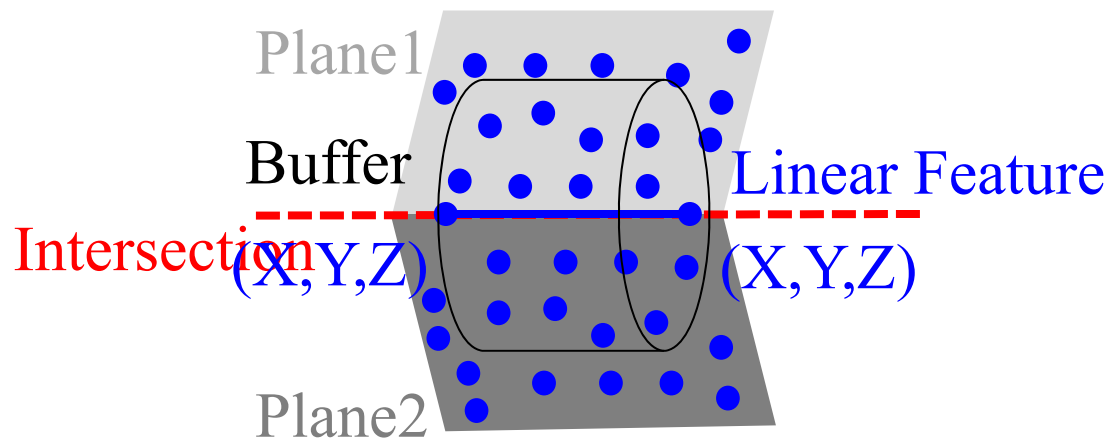
Methodology: Primitive Extraction



- **Linear Features Extraction from Terrestrial Laser Scans:**
 - **Parameter-domain segmentation for planar patch detection and intersection for the extraction of linear features**
 - Adaptive cylinder analysis for local point density estimation and attribute derivation
 - Parameter-domain segmentation
 - Intersection of neighboring planar features
 - Projection of planar points within a buffer onto the intersection line

Methodology: Primitive Extraction

- **Linear Features Extraction from Terrestrial Laser Scans:**
 - **Parameter-domain segmentation for planar patch detection and intersection for the extraction of linear features**



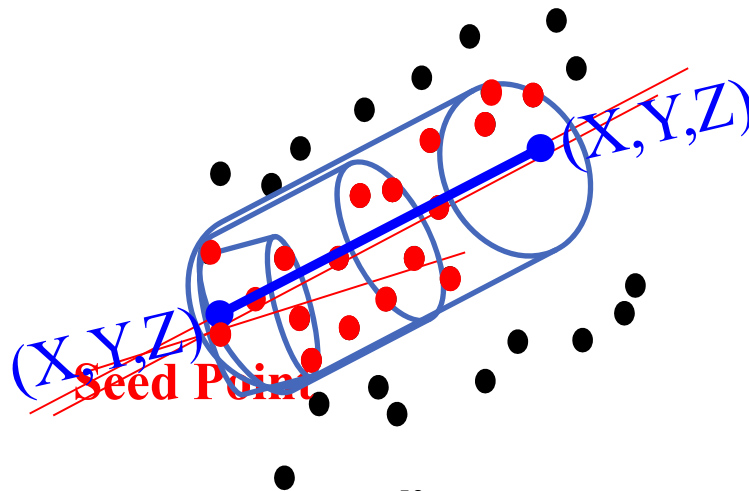
Planar patch segmentation and intersection procedure (Al-Durgham, 2007)

Methodology: Primitive Extraction

- **Linear Features Extraction from Terrestrial Laser Scans:**

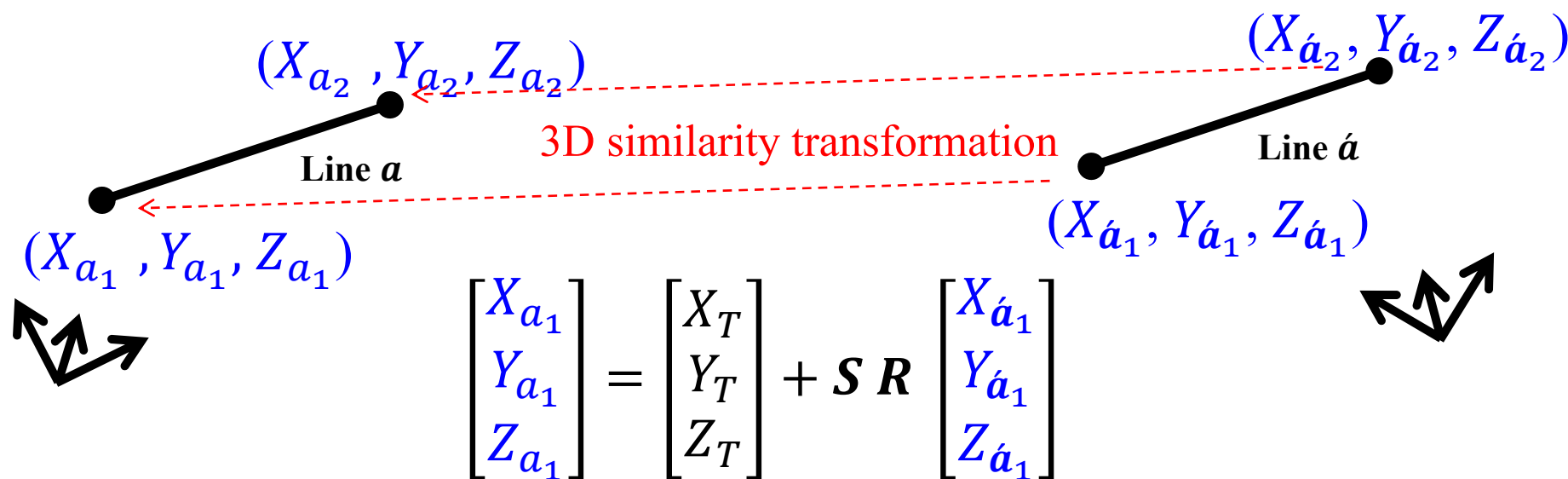
- **Region growing methodology for the extraction of cylindrical/linear features**

- PCA and adaptive cylinder analysis for local point density estimation and identification of seed points
- Minimum/non-singular parameterization of cylindrical/linear features
- Region growing segmentation
- Projection of points onto the linear feature or the axis of the cylindrical feature



Methodology: Similarity Measure

- Linear Features for the Estimation of Transformation Parameters **(Non-Linear Mathematical Model)**:



$$\begin{bmatrix} X_{a_1} \\ Y_{a_1} \\ Z_{a_1} \end{bmatrix} = \begin{bmatrix} X_T \\ Y_T \\ Z_T \end{bmatrix} + \mathbf{S} \mathbf{R} \begin{bmatrix} X_{\acute{a}_1} \\ Y_{\acute{a}_1} \\ Z_{\acute{a}_1} \end{bmatrix}$$

Mathematical relationship

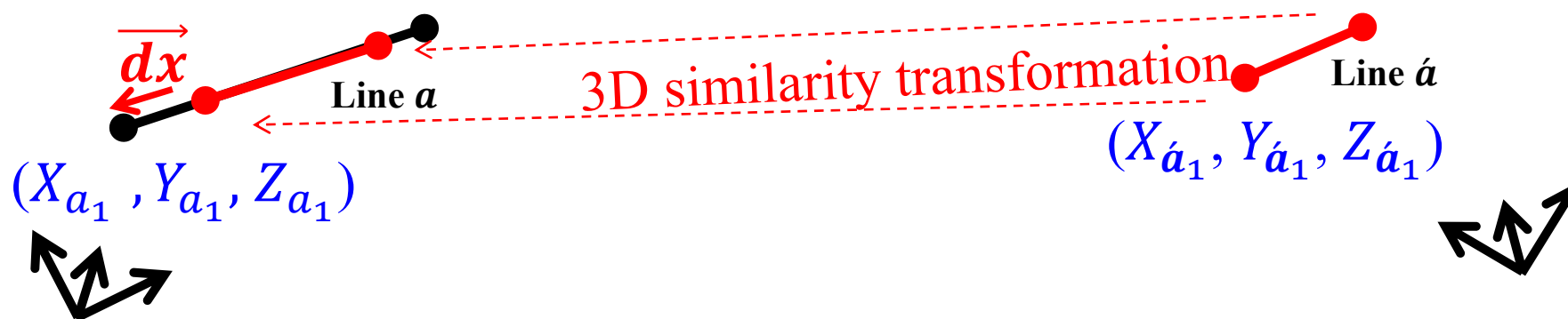
$$\vec{y}_{3 \times 1} = \mathbf{A}_{(3 \times 7)} \vec{x}_{(7 \times 1)} + \vec{e}_{(3 \times 1)}, \quad \vec{e} \sim (0, \Sigma),$$

$$\Sigma = \sigma_0 \mathbf{p}^{-1}$$

Gauss Markov representation of the mathematical model

Methodology: Similarity Measure

- **Linear Features for the Estimation of Transformation Parameters** (Non-Linear Mathematical Model):
 - Due to the nature of the linear feature extraction procedure, the definition of the line end points is quite arbitrary (non-corresponding end points).



$$\vec{y}_{(3 \times 1)} = A_{(3 \times 7)} \vec{x}_{(7 \times 1)} + \vec{dx}_{(3 \times 1)} + \vec{e}_{(3 \times 1)}, \quad \vec{e} \sim (0, \Sigma),$$

$$\Sigma = \sigma_0 P^{-1}_{(3 \times 3)}$$



Methodology: Similarity Measure

- **Linear Features for the Estimation of Transformation Parameters (Non-Linear Mathematical Model):**
 - Weight modification to account for the non-corresponding end points along conjugate linear features (Renaudin et al., 2011)

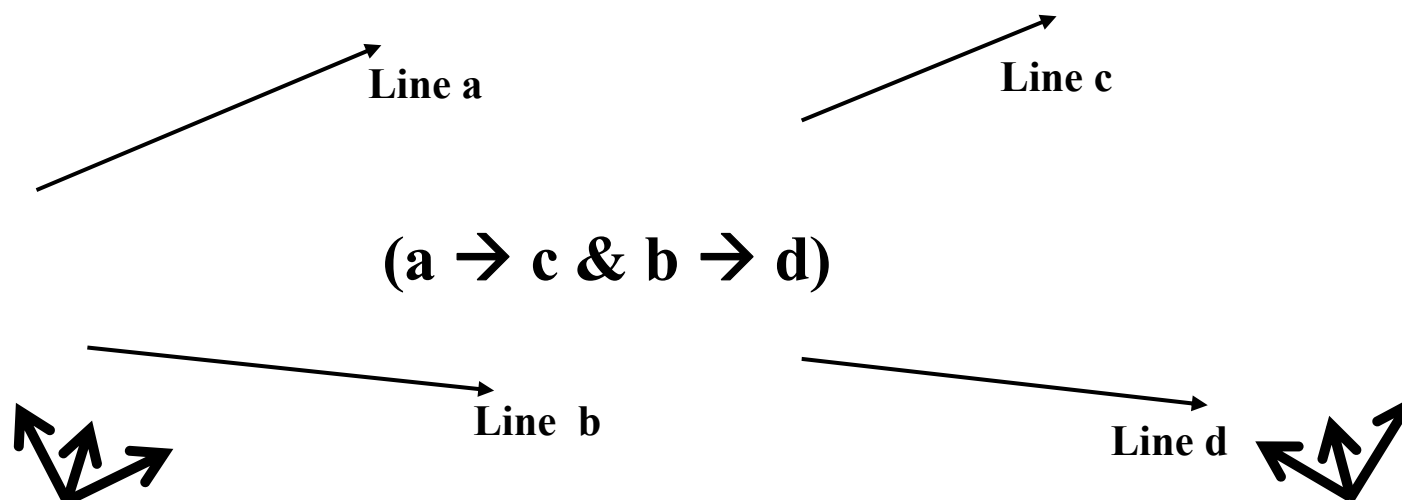
$$\vec{y}_{(3 \times 1)} = A_{(3 \times 7)} \vec{x}_{(7 \times 1)} + \overrightarrow{dx}_{(3 \times 1)} + \vec{e}_{(3 \times 1)}$$
$$\vec{e} \sim (0, \Sigma) \quad , \quad \Sigma = \sigma_0^2 P^{-1}_{(3 \times 3)}$$

- Change the stochastic properties of the random noise vector:

$$\dot{\Sigma} \{ \vec{e} \} = \sigma_0^2 \dot{P}^+_{(3 \times 3)}, \quad \dot{P} \overrightarrow{dx} = 0$$

Methodology: Similarity Measure

- **Linear Features for the Estimation of Transformation Parameters (Linear Mathematical Model):**



$$\begin{aligned}\vec{\hat{a}} &= R \vec{\hat{c}} \\ \vec{\hat{b}} &= R \vec{\hat{d}}\end{aligned}$$

\hat{a} , \hat{b} , \hat{c} , and \hat{d} are the unit vectors along the lines a, b, c, d.



Methodology: Similarity Measure

- **Linear Features for the Estimation of Transformation Parameters (Linear Mathematical Model):**

$$\vec{e} = R \vec{\hat{c}} - \vec{\hat{a}}$$

- By applying the least-squares principle:

$$\Sigma \vec{e}^T \vec{e} = \textit{minimum}$$

$$\Sigma \vec{e}^T \vec{e} = \Sigma (\vec{\hat{c}}^T \vec{\hat{c}} + \vec{\hat{a}}^T \vec{\hat{a}} - 2 \vec{\hat{a}}^T R \vec{\hat{c}})$$

$\Sigma \vec{e}^T \vec{e}$ is *minimum* when $\Sigma (\vec{\hat{a}}^T R \vec{\hat{c}})$ is *maximum*



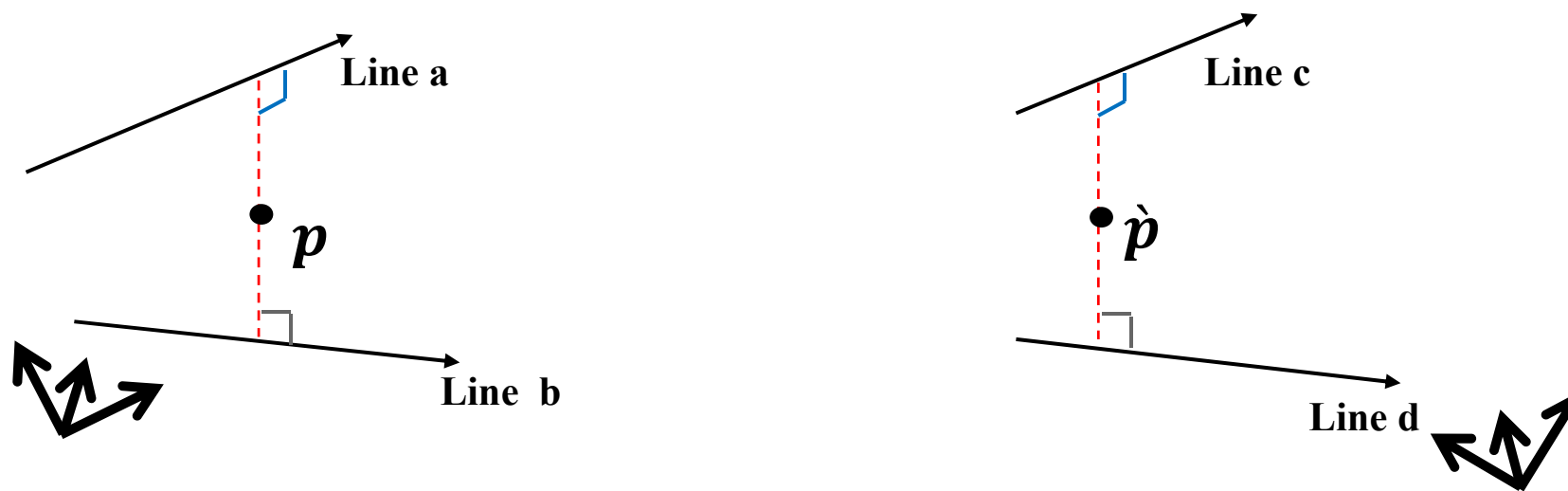
Methodology: Similarity Measure

- **Linear Features for the Estimation of Transformation Parameters (Linear Mathematical Model):**

- Using quaternion ($Q = q_0 + q_1i + q_2j + q_3k$) to represent $\vec{\hat{a}}, \vec{\hat{c}}$
 - $A = (0, \vec{\hat{a}})$, $C = (0, \vec{\hat{c}})$
 - $\sum (\vec{\hat{a}}^T R \vec{\hat{c}}) = \text{Max} \sum A^T Q C Q^* \rightarrow Q^T N_{(4 \times 4)} Q$
- The unit quaternion Q that maximizes $Q^T N_{(4 \times 4)} Q$ is the eigenvector that corresponds to the largest eigenvalue of N .
- R can be derived using this eigenvector.

Methodology: Similarity Measure

- **Linear Features for the Estimation of Transformation Parameters (Linear Mathematical Model):**



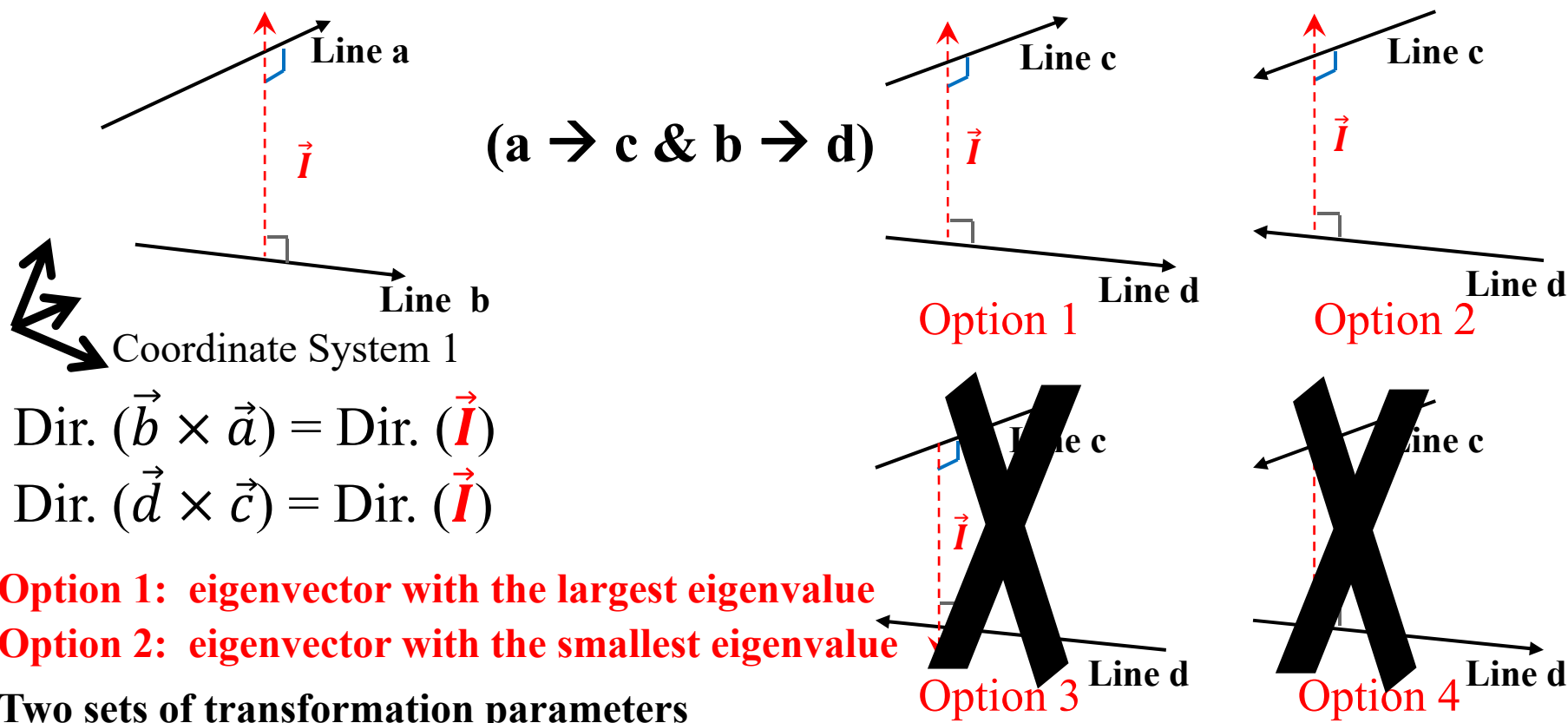
Shifts can be derived using the mid-point of the common perpendicular line.

$$\begin{bmatrix} X_T \\ Y_T \\ Z_T \end{bmatrix} = \vec{p} - R_{(3 \times 3)} \vec{\hat{p}}$$

Methodology: Matching Strategy

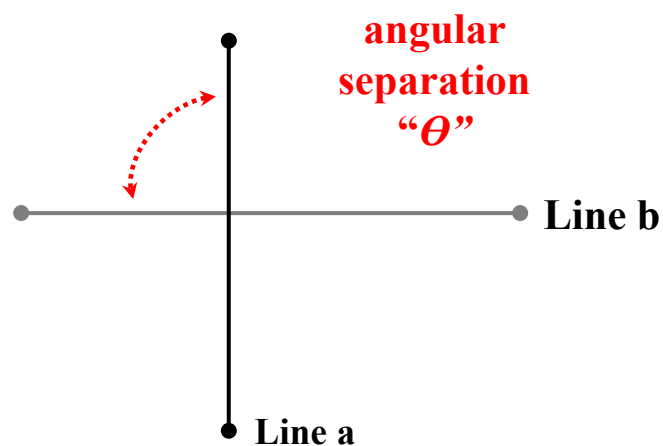
- Linear Features for the Estimation of Transformation Parameters **(Linear Mathematical Model)**:

- Directional Ambiguity (Skew Lines)

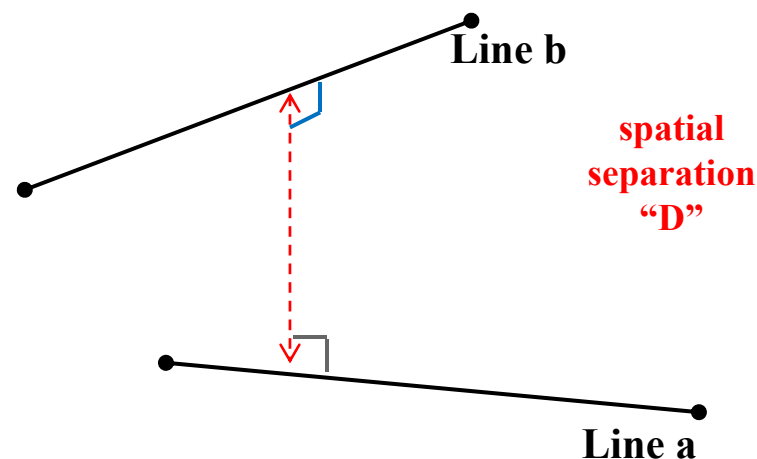


Methodology: Matching Strategy

- **Invariant Characteristics of Corresponding 3D Line-pairs:**



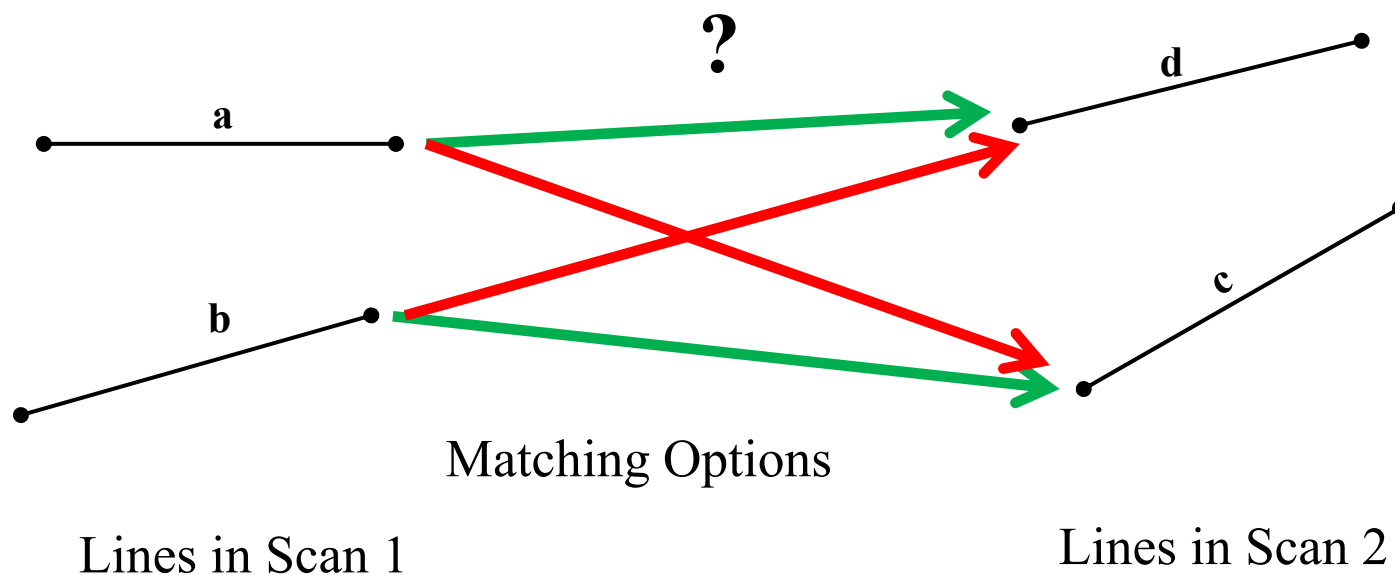
Top view of lines a and b



Side view of lines a and b

Methodology: Matching Strategy

- **Matching Ambiguity:** For line pairs whose angular and spatial separations are the same, there will be an ambiguity in the automatic matching process.



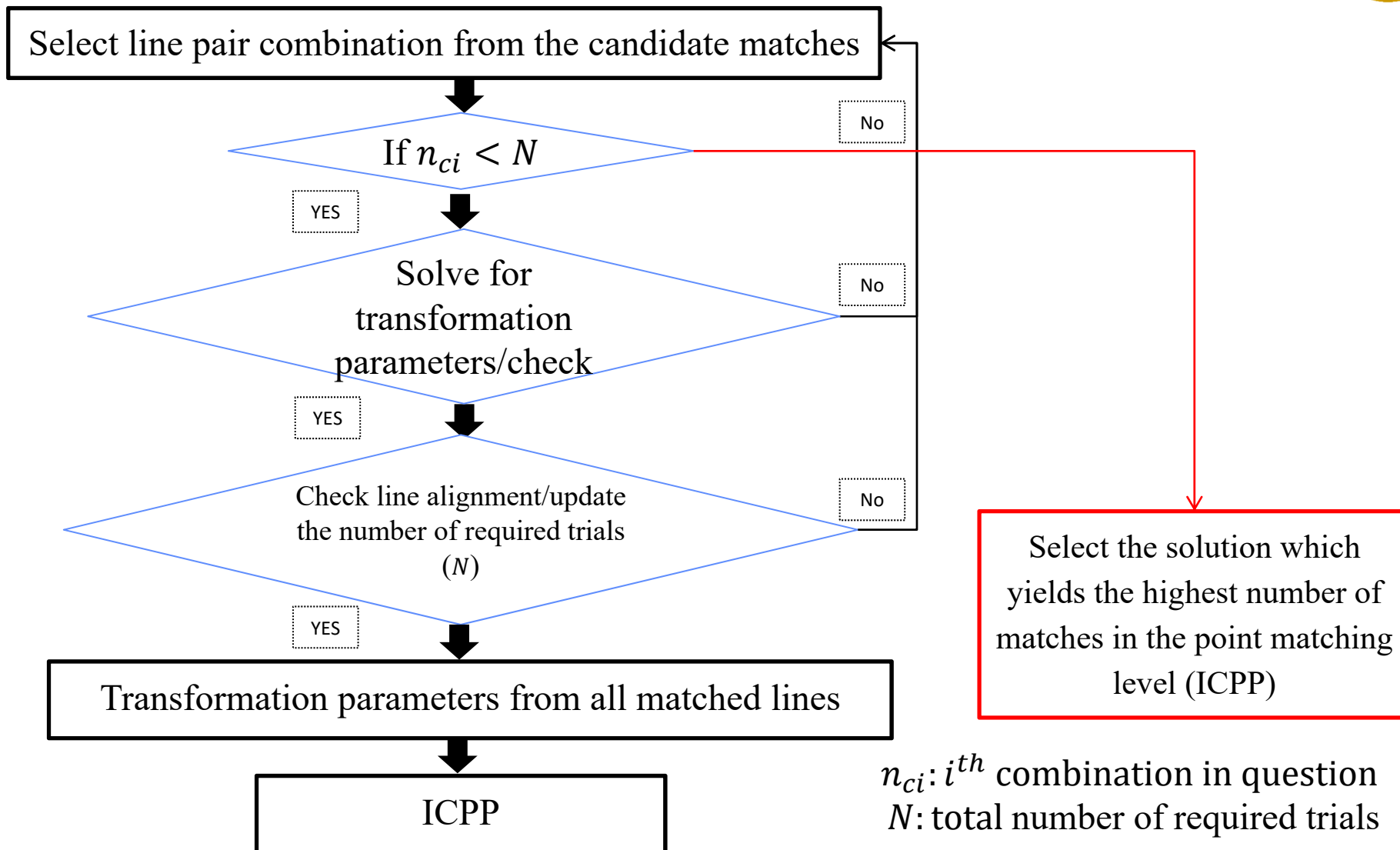
Methodology: Matching Strategy



- **Number of Possible Combinations for Laser Scans (1, 2):**
 - # line pairs in Scan 1 = $n(n - 1)/2$, “ n ” *number of lines in scan 1*
 - # line pairs in Scan 2 = $m(m - 1)$, “ m ”: *number of lines in scan 2*
 - All possible combinations of line pair = $\frac{n(n-1)}{2} \times m(m - 1)$
 - Candidate matches are line pairs which have similar angular and spatial separation values (n_{ct}).



Methodology: Matching Strategy

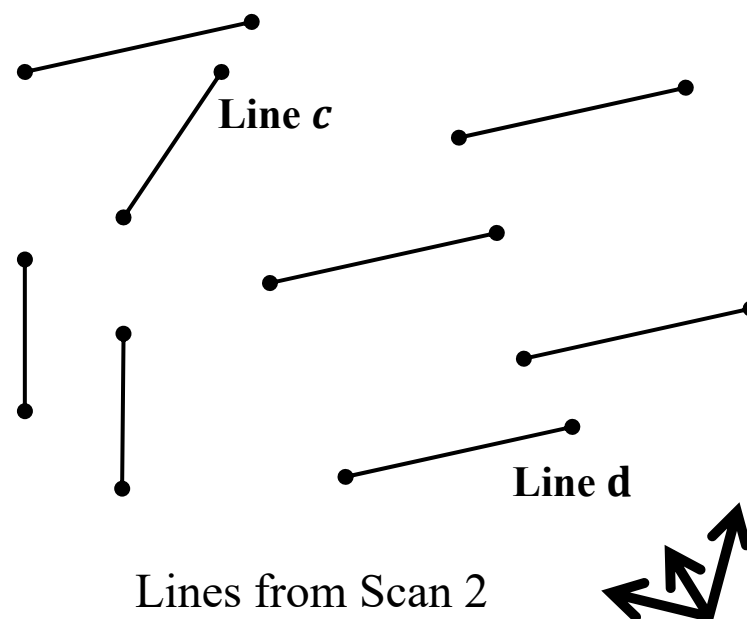
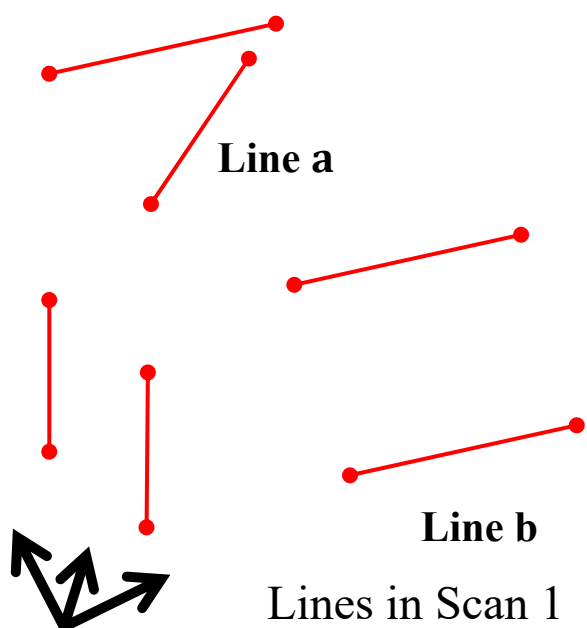


n_{ci} : i^{th} combination in question
 N : total number of required trials

RANSAC Flow Chart

Methodology: Matching Strategy

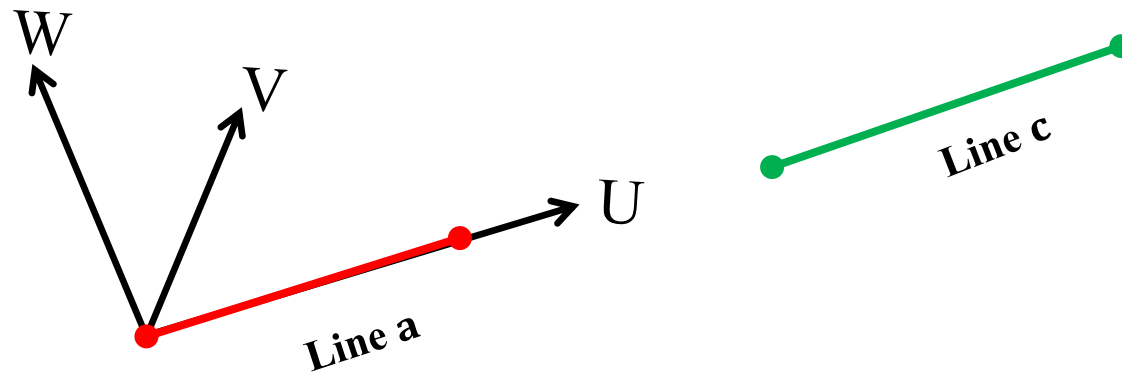
- **Lines Alignment Process (Inliers Detection):**



All the aligned lines will be used to solve for the transformation parameters again.

Methodology: Matching Strategy

- **Lines Alignment Process (Inliers Detection):**
 - Check if a linear feature “a” has a collinear mate such as line “c”



Local coordinate system (U, V, W)
definition for line “a”

If line “c” is collinear with line “a”, it will not have any components along the (V, W) axes when line “c” is transformed into the local coordinate system (U,V,W).



Methodology: Matching Strategy

- **Required RANSAC Trials (Stopping Criteria):**

- The number of the required RANSAC trials is determined as a function of the total number of hypothesized matches and the number of compatible line matches in each trial.
- Probability of having at least one correct combination of conjugate line pairs after N trials/draws = 0.99 (**pre-specified**)
- Probability of having a correct draw of conjugate line pairs:

$$= \frac{\text{number of matching pairs (**Inliers**)}}{\text{number of candidate matches (**n_{ct}**)}}$$



Methodology: Matching Strategy

- **Required RANSAC Trials (Stopping Criteria):**

- Probability of not having a correct draw of conjugate line pairs after N trials:

$$1 - 0.99 = \left(1 - \frac{\text{number of Inliers}}{\text{number of candidate matches}} \right)^N$$

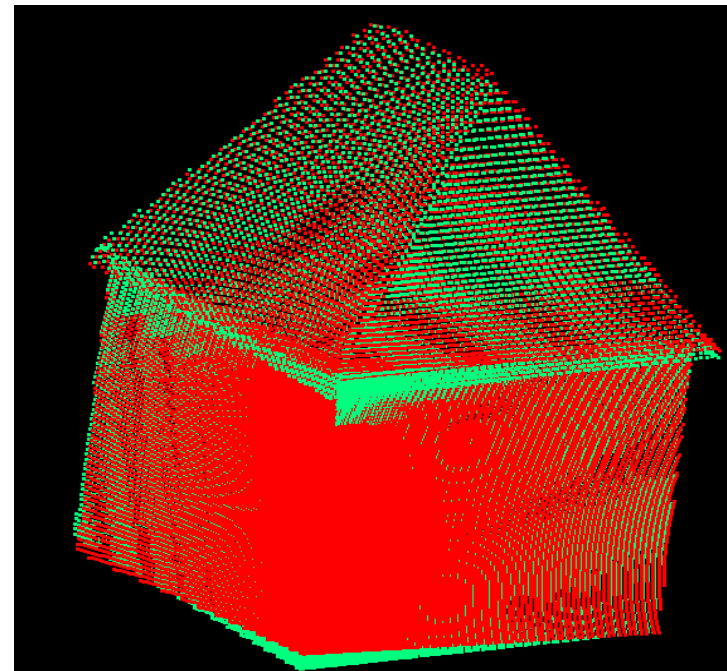
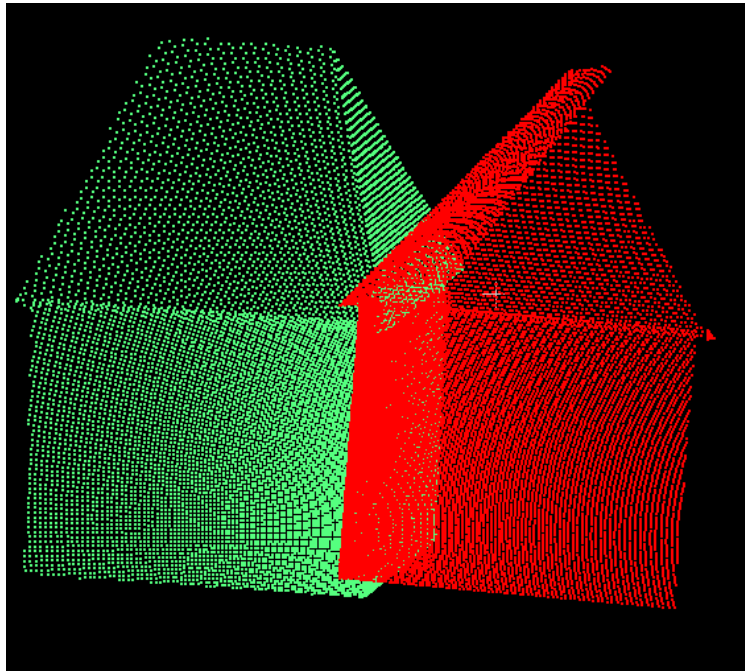
- Required trials:

$$N = \frac{\log(1 - 0.99)}{\log \left(1 - \frac{\text{number of Inliers}}{\text{number of candidate matches}} \right)}$$

- The number of inliers is determined in each RANSAC trial as $\frac{m_1(m_1-1)}{2}$, m_1 : number of matched/compatible lines

Methodology: Matching Strategy

- **ICPP Registration (Parameter Refinement):**
 - Refines the estimated transformation parameters
 - Derives the compatible matches among points in the scans





Association-Based Sample Consensus Approach for the Registration of TLS Scans using Linear Features



Association-based Sample Consensus Approach

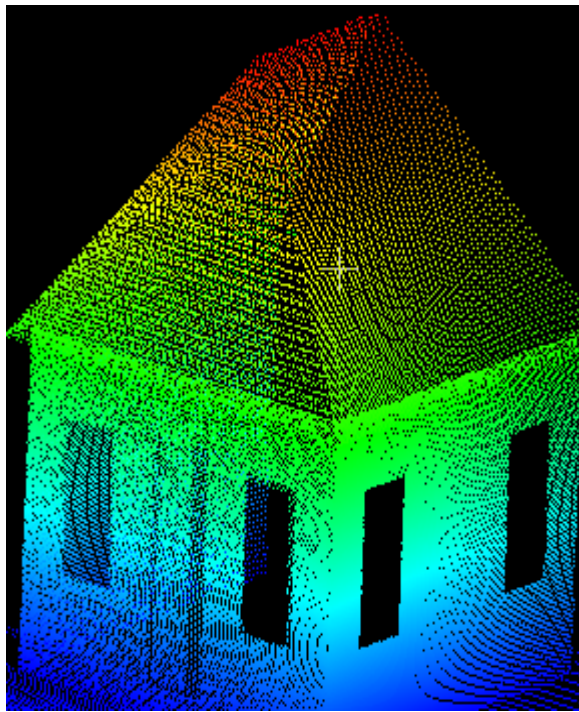
- To identify the correspondences between linear features in the overlapping scans, an $(n \times m)$ association matrix is constructed with its elements initialized to zero
 - n, m : is number of lines in the two scans
- The construction of the association matrix starts by identifying the line pairs in the overlapping scans that have similar angular and spatial separations taken two at a time.
- For any matched line pairs, increase the votes in the corresponding elements in the association matrix.
- This process is repeated until all the pairs with similar angular and spatial separations are considered.

Association-based Sample Consensus Approach

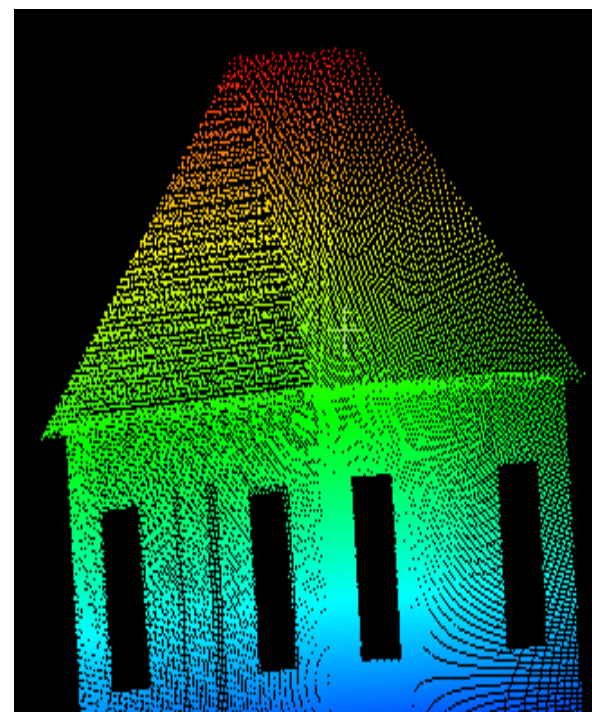
- **Example of constructing the Association Matrix:**



Building Model

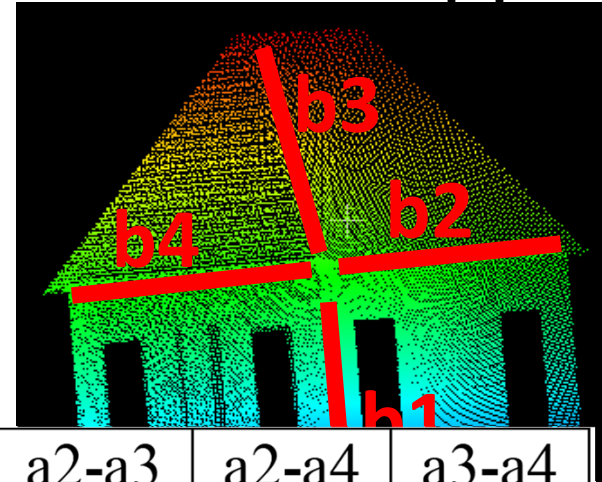
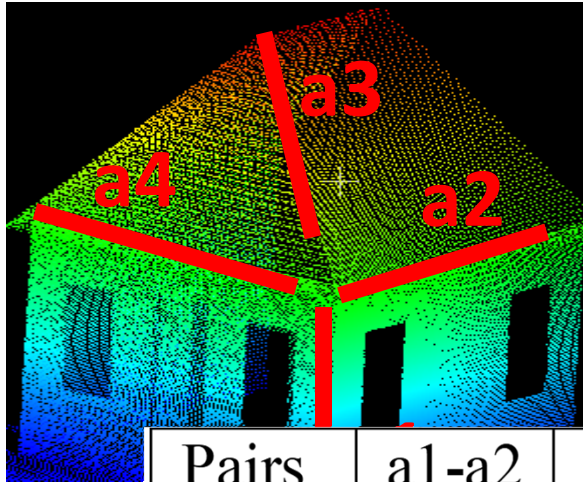


Scan 1



Scan 2

Association-based Sample Consensus Approach



Pairs | a1-a2 | a1-a3 | a1-a4 | a2-a3 | a2-a4 | a3-a4

T1
a1
p1
H1
a1
a2
a1
a2
a1
a2

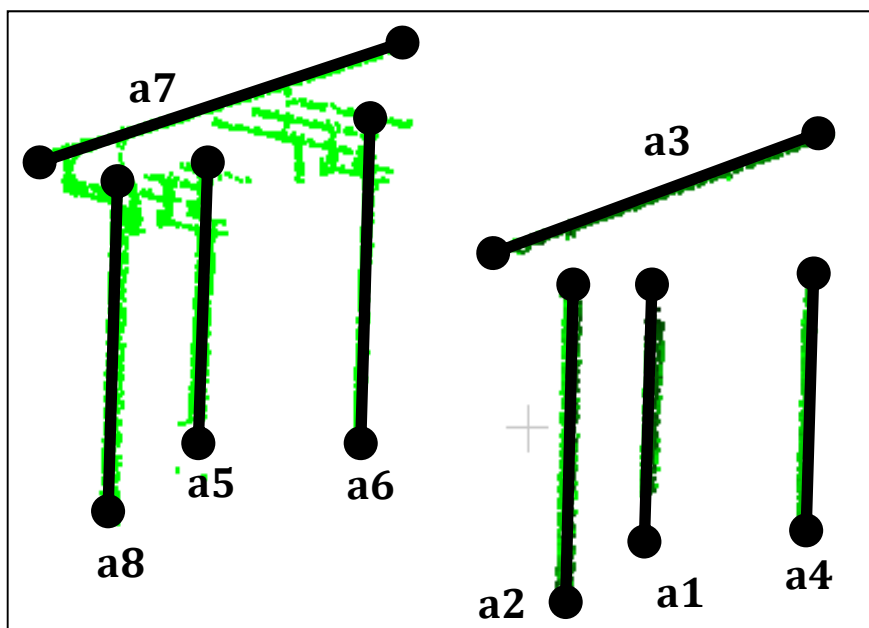
	a1	a2	a3	a4
b1				
b2				
b3				
b4				

&

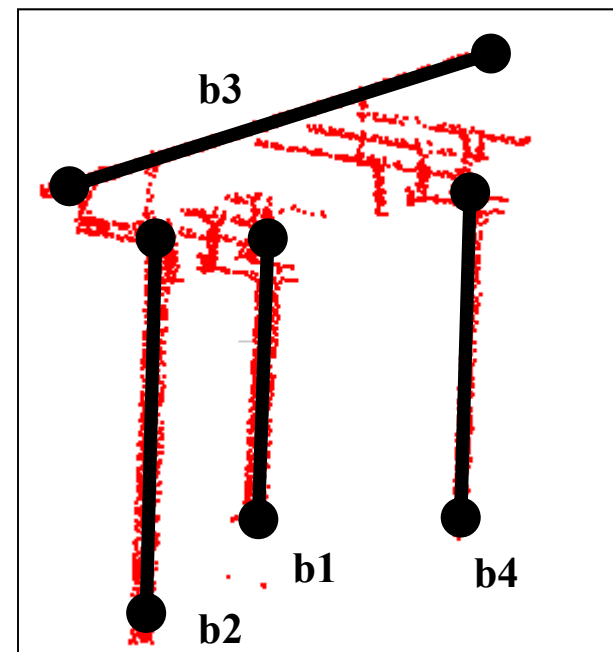
Association matrix of lines from Scans 1 and 2

Association-based Sample Consensus Approach

- Association ambiguity:



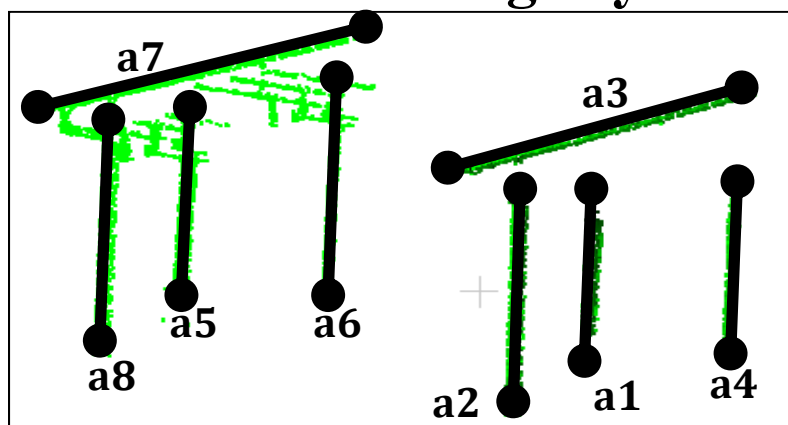
Scan 1



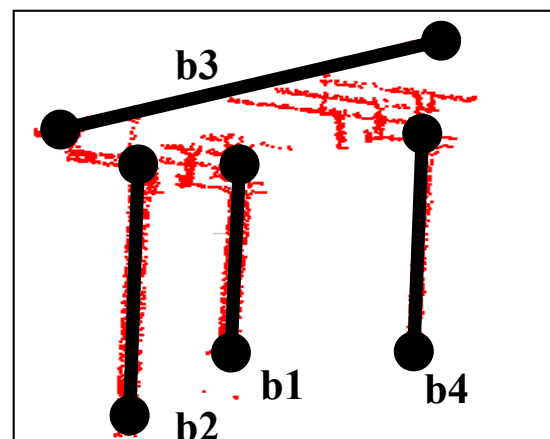
Scan 2

Association-based Sample Consensus Approach

- Association ambiguity:



Scan 1



Scan 2

ID	a1	a2	a3	a4	a5	a6	a7	a8
b1	3	2	3	2	3	2	3	2
b2	3	4	3	3	3	3	3	4
b3	3	3	9	3	3	3	9	3
b4	3	3	3	4	3	4	3	3

Final association matrix

Association-based Sample Consensus Approach

- **Association ambiguity:**

ID	a1	a2	a3	a4	a5	a6	a7	a8
b1	3	2	3	2	3	2	3	2
b2	3	4	3	2	2	2	3	4
b3	3	3	0	3	3	3	9	3
b4	3	3	3	4	3	4	3	3

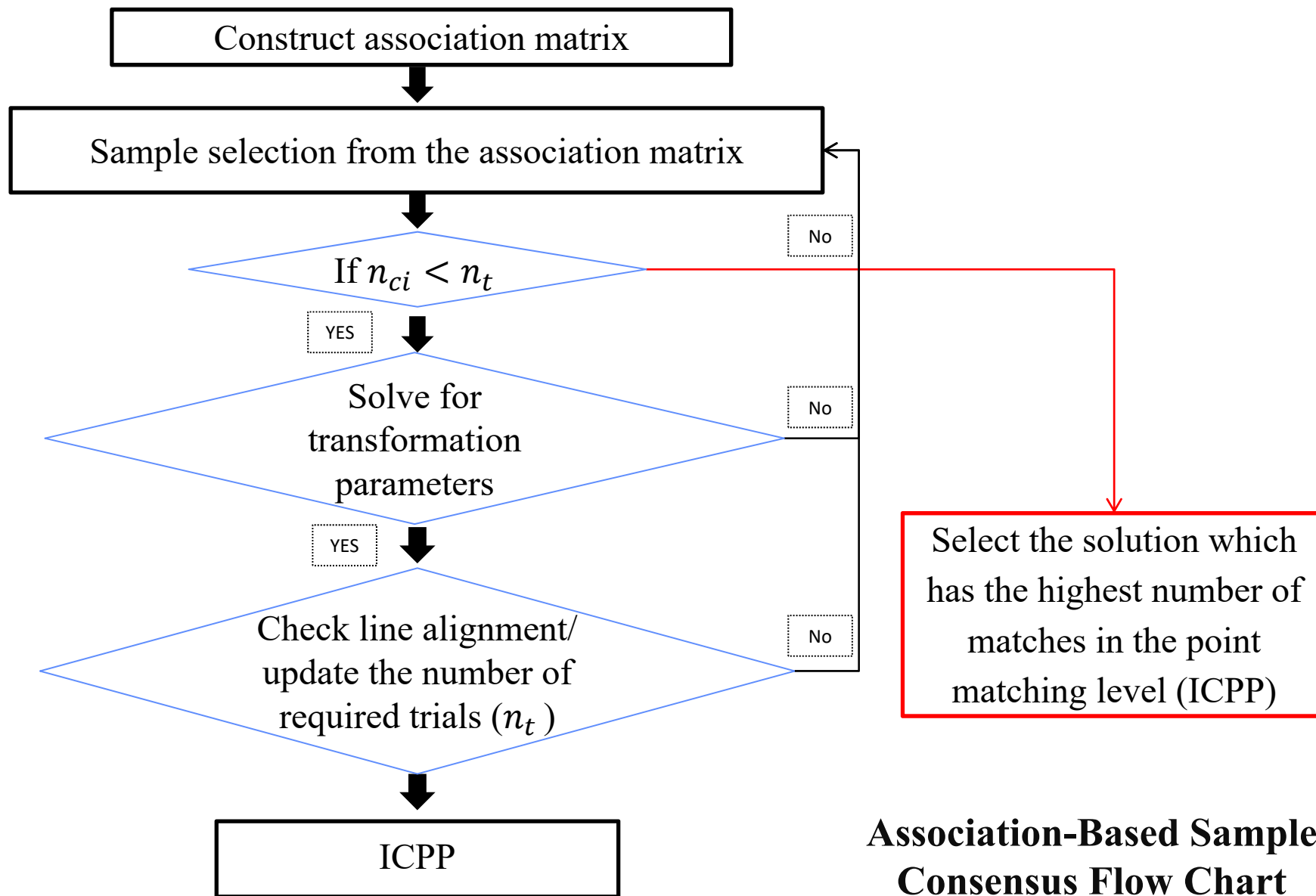
First highest vote

Second highest vote

1. The second highest vote should not pertain to the same row or column of the first highest vote in the association matrix.
2. a3 a6 & b3 b4 should have the same spatial and angular separation.



Association-based Sample Consensus Approach



Association-Based Sample Consensus Flow Chart



Solution Frequency Approach for the Registration of TLS Scans using Linear Features



Solution-Frequency Approach

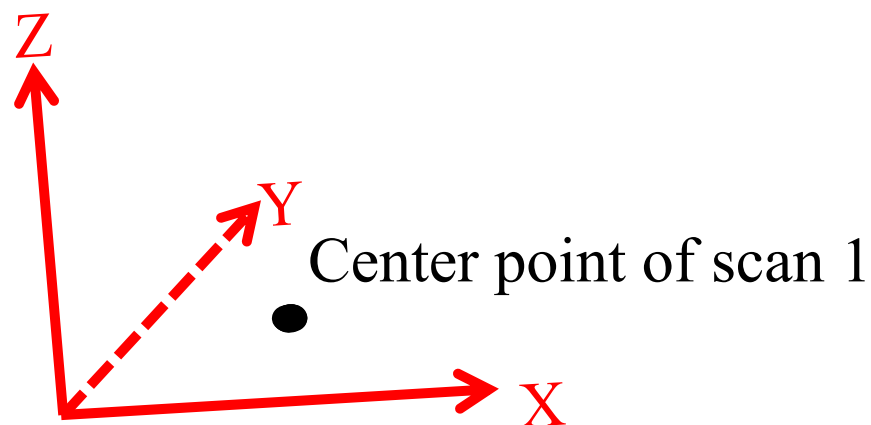
- The candidate matches of linear features are used to solve for the transformation parameters.
- Hypothesis: Among all the candidate matches, conjugate linear features will lead to similar sets of transformation parameters.
- By using each set of transformation parameters individually to transform a certain 3D point, similar transformation parameters will lead to a group of transformed points, which are spatially close to each other.



Solution-Frequency Approach

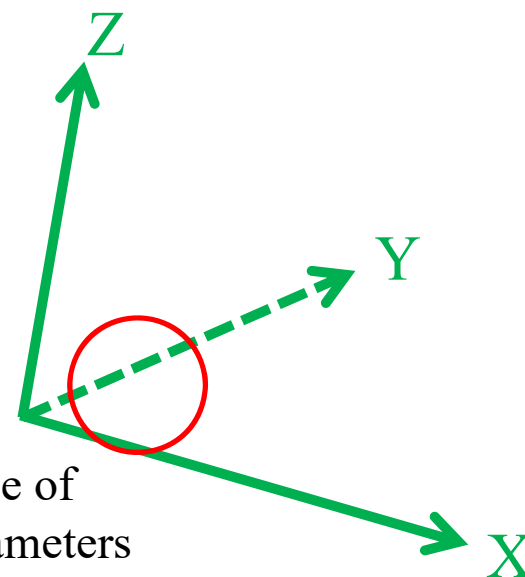
- Option to store transformation parameters
 - All the estimated transformation parameters can be stored in two separate Kd-Trees
 - (two Kd-Trees instead of one to avoid spatial deformation when using 6 dimensions):
 - Kd-Tree 1 \rightarrow (X_T, Y_T, Z_T)
 - Kd-Tree 2 \rightarrow (ω, ϕ, κ)
 - Starting from Kd-Tree 2, find the most repeated set of rotation angles (rotations peak). For this peak, find the most repeated translations associated with those rotation angles.
 - Exhaustive search that might lead to wrong peak for the translations

Solution-Frequency Approach



Coordinate system Scan 1

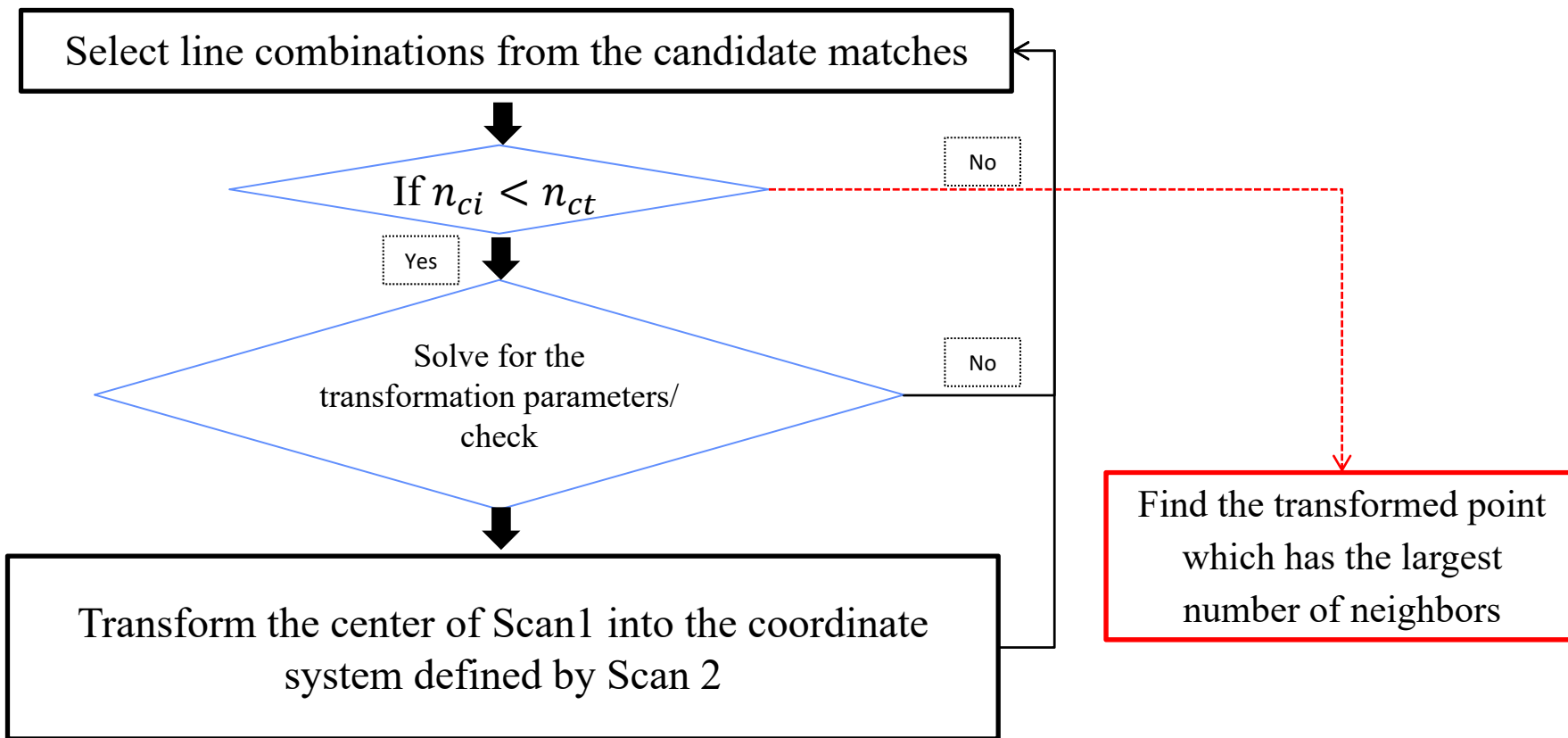
Select the average of
transformation parameters
associated with these points



Coordinate system Scan 2



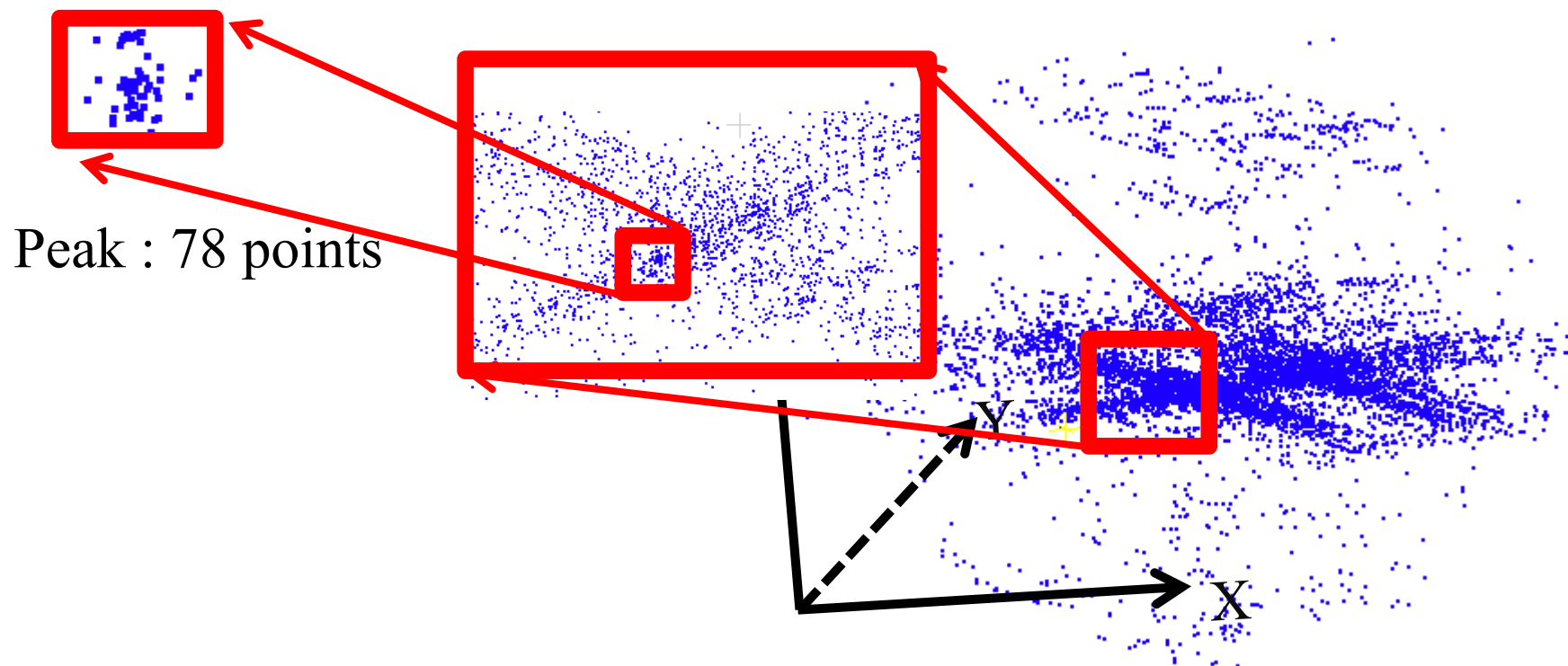
Solution-Frequency Approach



Solution Frequency Flow Chart

n_{ci} : *ith combination in question*
 n_{ct} : *total number of combinations*

Solution-Frequency Approach



Transformed center of a scan
using 14,828 candidate matches



Experimental Results

Real Datasets

Experimental Results (I)



- **Power Plant Dataset**

Scanner Specifications:

Range: 0.6m - 120m

122,000 pts/sec ~ Max

Ranging error = ± 2 mm at 25m

Scans:

Scans ID	Rough Overlap Percentage
5-0	50 %
5-1	40%
5-2	50%
5-3	35%
5-4	50%
5-6	90%

Scans are down-sampled to 400 pts/m²

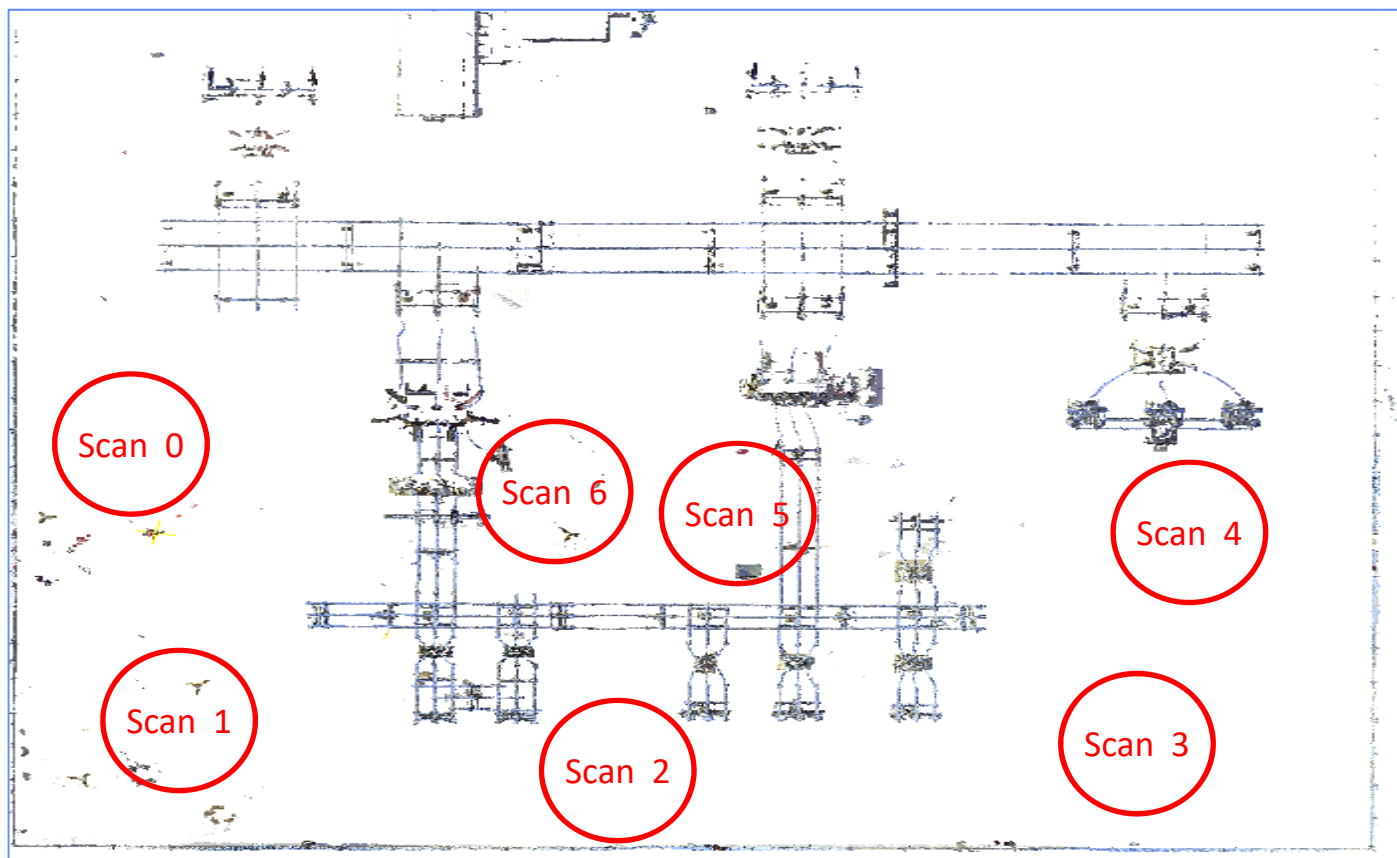


FARO Focus3D S

*FARO Laser Scanner Focus3D Manual October 2011

Experimental Results (I)

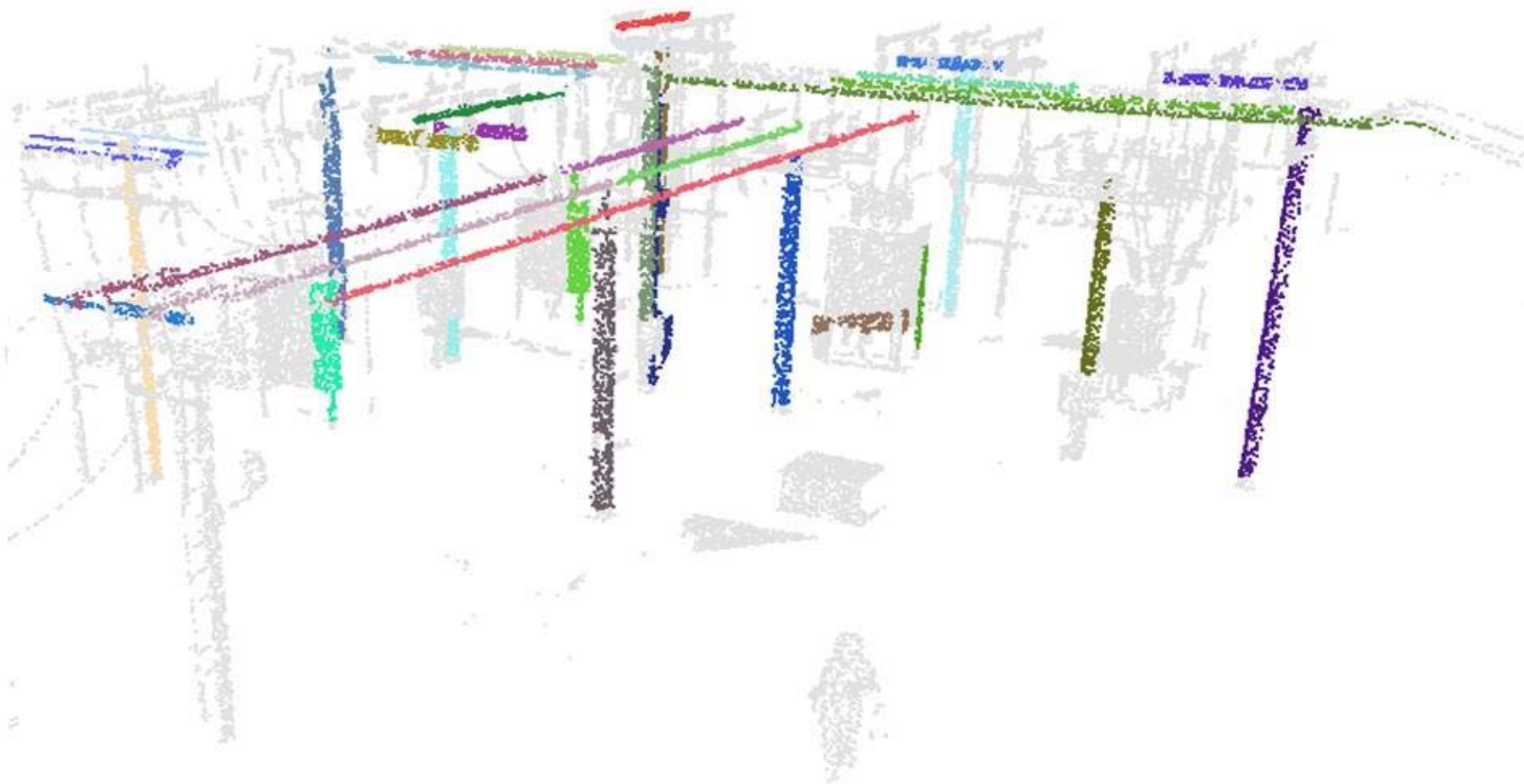
- **Power Plant Dataset:**



Scanner Positions

Experimental Results (I)

- **Power Plant Dataset: Segmentation**

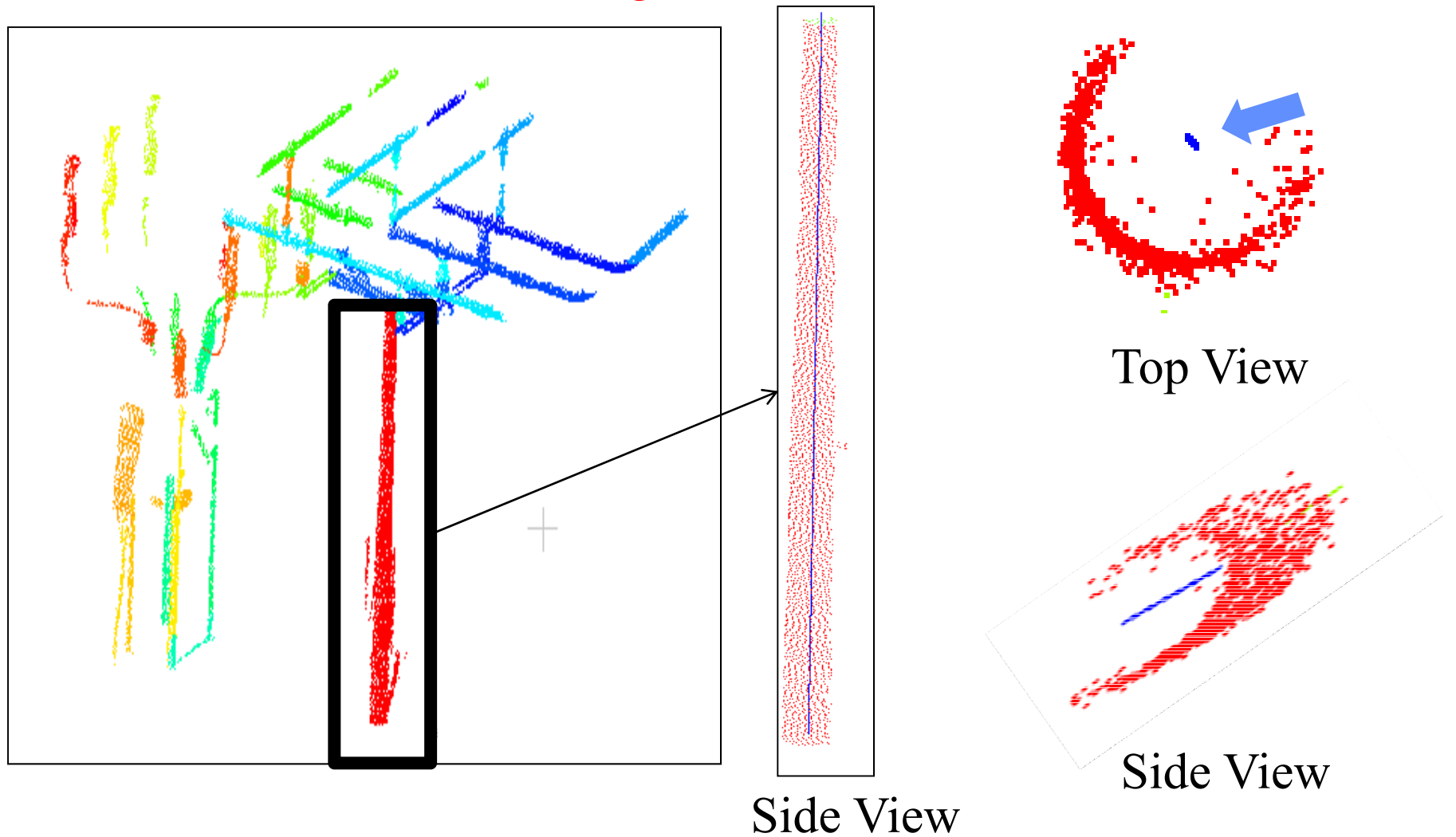


Part of the scan: only precise features

Experimental Results (I)



- **Power Plant Dataset: Segmentation**





Experimental Results (I)

- **Power Plant Dataset: Segmentation**
 - Long and precise fitting of lines:

Scan ID	Number of Linear Features
0	33
1	43
2	46
3	33
4	68
5	93
6	85

Lines > 1m, Sigma < .1m



Experimental Results (I)

- **Power Plant Dataset: Registration**
 - RANSAC approach: all combinations

Scans ID	# Combinations	Candidate matches	Solutions	Order of most probable solution (1)	Order of most probable solution (2)
5-0	4,517,568	14,828	154	148	11,320
5-1	7,726,068	26,944	130	86	7,518
5-2	8,855,460	60,446	418	62	7,246
5-3	4,517,568	13,708	120	2	364
5-4	1,949,0568	86,824	667	523	79,719
5-6	30,544,920	175,004	856	477	115,106

Combinations: total number of line pairs combinations in the scans

Candidate matches: lines with similar angular and spatial separation values

Solutions: number of times in which 3 lines aligned (7 lines for scans 5 and 6)

(1) Order among the solutions

(2) Order among the conducted trials

Experimental Results (I)



- **Power Plant Dataset: Registration**
 - Association approach: all combinations

Scans ID	Combinations	Candidate matches	Solutions	Order of most probable solution (1)	Order of most probable solution (2)
5-0	4,517,568	14,828	154	65	614
5-1	7,726,068	26,944	130	52	1,786
5-2	8,855,460	60,446	418	306	4,559
5-3	4,517,568	13,708	120	40	377
5-4	19,490,568	86,824	667	346	3,470
5-6	30,544,920	175,004	856	458	5,022

Combinations: total number of line pairs combinations in the scans

Candidate matches: lines with similar angular and spatial separation values

Solutions: number of times in which 3 lines aligned (7 lines for scans 5 and 6)

(1) Order among the solutions

(2) Order among the conducted trials



Experimental Results (I)

- **Power Plant Dataset: Registration**
 - Association and Vs. RANSAC (**probability**)

RANSAC

Scan ID	Number of Trials	Number of Solutions
5-0	2,594	36
5-1	2,725	34
5-2	2,928	40
5-3	6,010	19
5-4	12,985	26
5-6	4,399	3



Experimental Results (I)

- **Power Plant Dataset: Registration**
 - Association and Vs. RANSAC (**probability**)

Association

Scan ID	Number of Trials	Number of Solutions
5-0	1,002	75
5-1	2,725	82
5-2	2,928	241
5-3	6,010	120
5-4	3,460	344
5-6	1,964	149



Experimental Results (I)

- **Power Plant Dataset: Registration**
 - Frequency-Based Approach

Scans ID	Candidate matches	Peak Size (transformed center)
5-0	14,828	78
5-1	26,944	104
5-2	60,446	165
5-3	13,708	23
5-4	86,824	132
5-6	175,004	769



Experimental Results (I)

- **Power Plant Dataset: Registration**
 - Transformation Parameters using linear features

Scans ID	XT (M)	YT (M)	ZT (M)	ω°	ϕ°	κ°
0	5.7652	16.203	3.321	-5.492	-4.456	30.192
1	4.3278	14.506	8.243	-8.053	-1.533	19.743
2	-14.911	-7.061	8.223	2.202	0.907	-11.092
3	-4.7681	1.652	18.215	-4.181	-9.783	14.011
4	-35.187	-6.675	-5.499	1.267	-6.864	-40.798
5	0	0	0	0	0	0
6	5.974	14.266	6.345	-0.374	-1.390	9.253

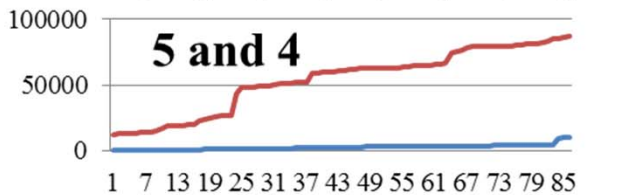
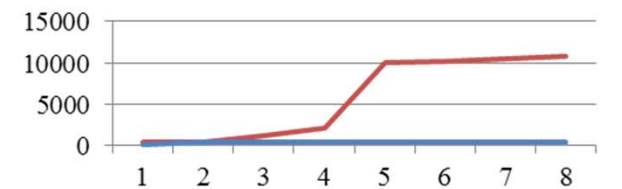
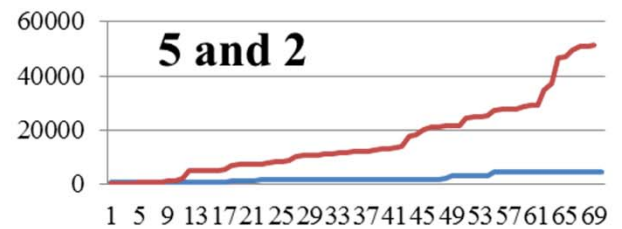
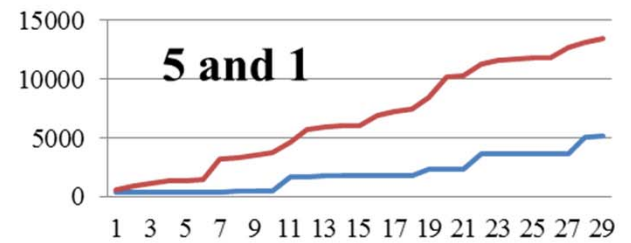
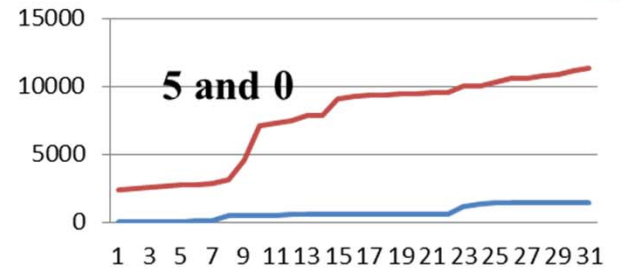
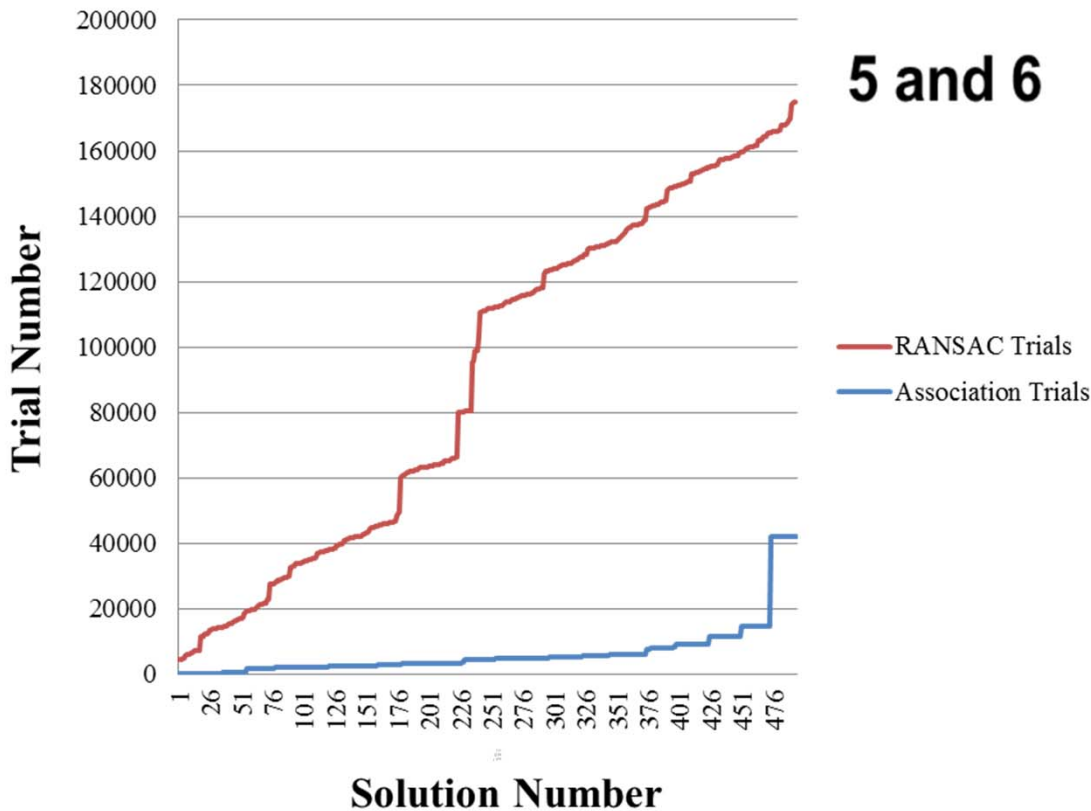
RANSAC approach

Experimental Results (I)



- **Power Plant Dataset: Registration**

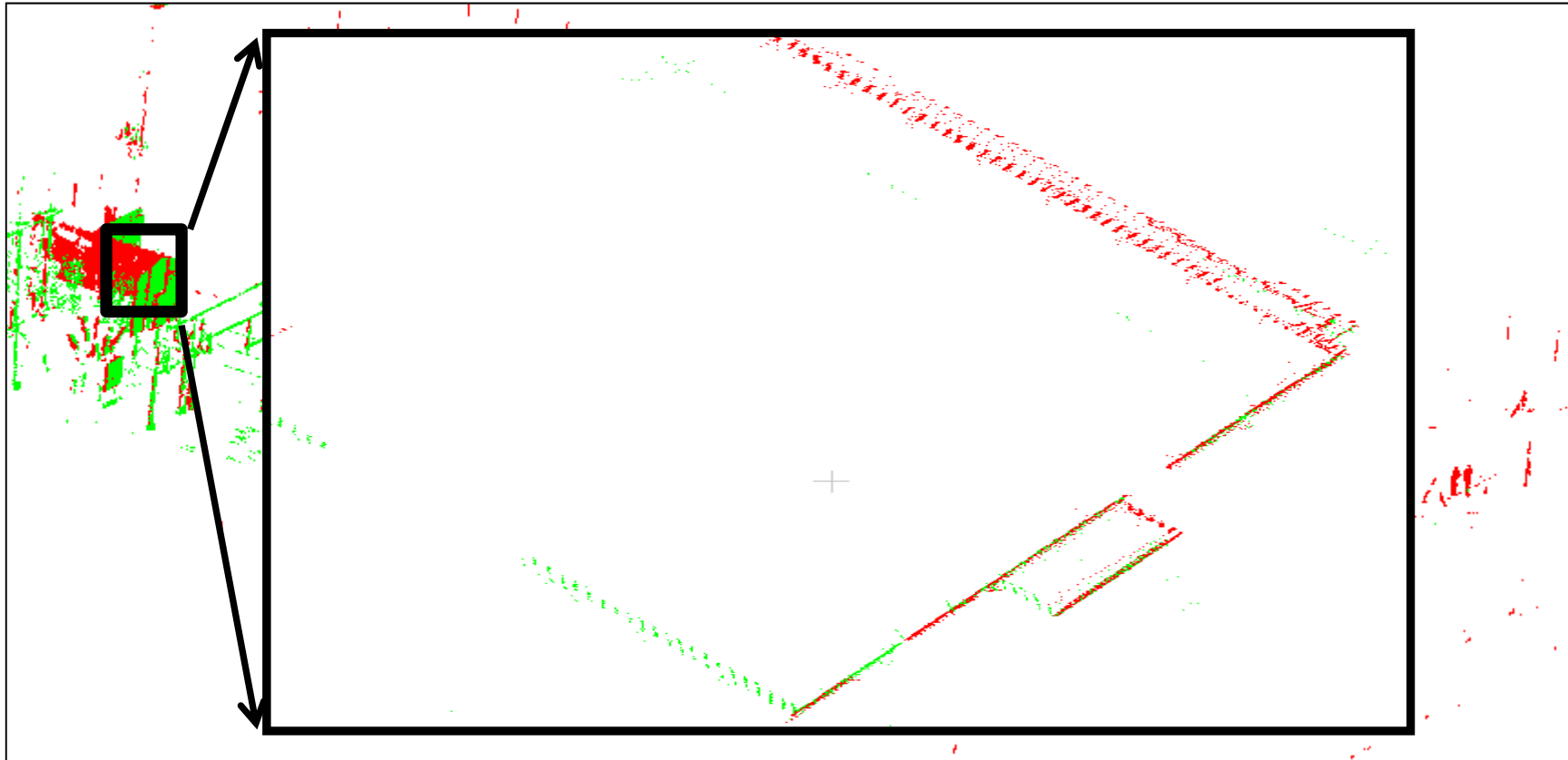
- Association and Vs. RANSAC



Experimental Results (I)



- **Power Plant Dataset: Registration**

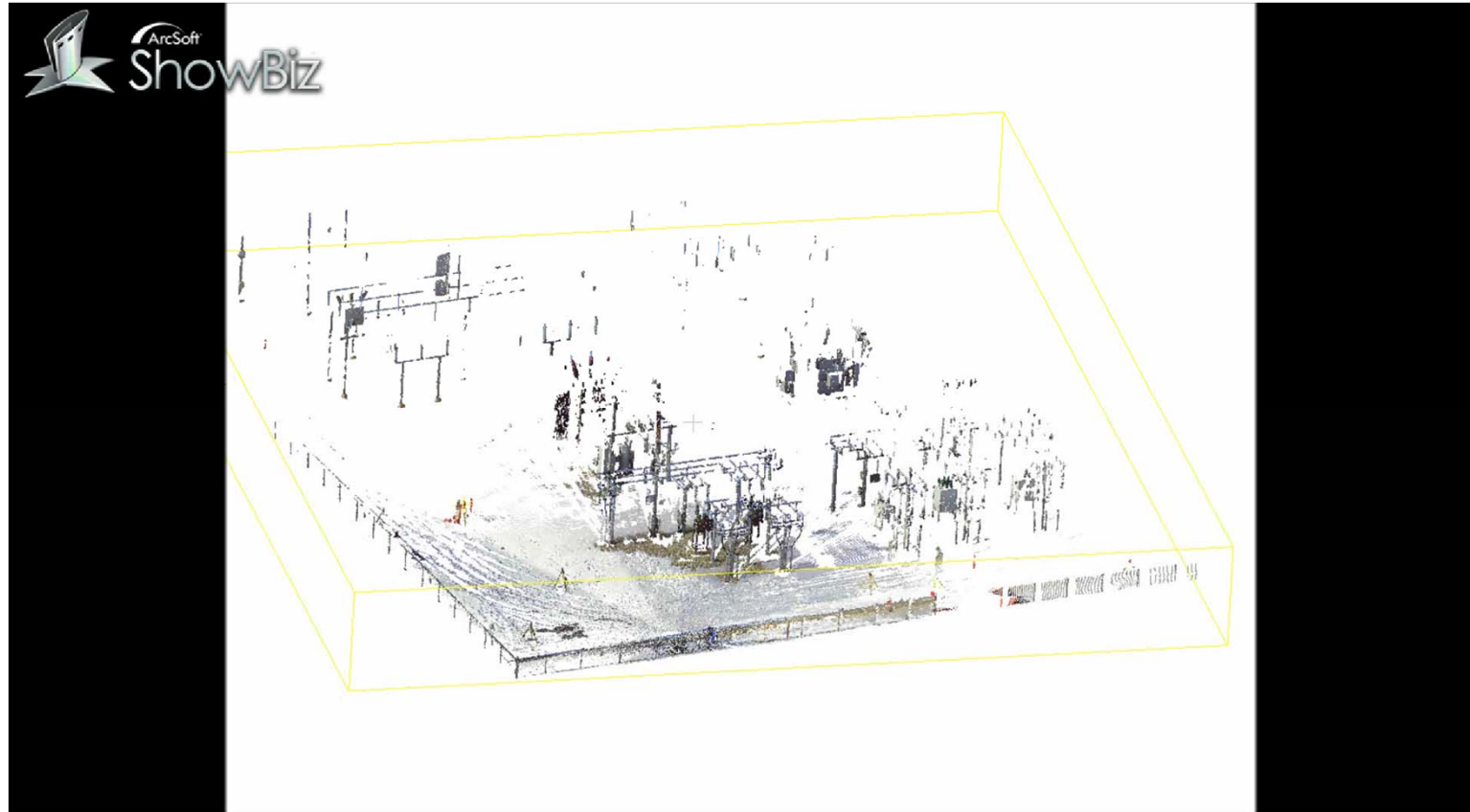


Registered Scans (5 and 0) using ICP features

Experimental Results (I)



- **Power Plant Dataset: Registration**



Experimental Results



- **Power Plant Dataset: Registration**





Experimental Results (II)

- A set of four laser scans of the Ronald McDonald House have been acquired using Leica HDS6100 laser scanner .



Ronald McDonald House



Experimental Results (II)

Scanner Positions



Scan4



Scan2



Scan3



Scan1

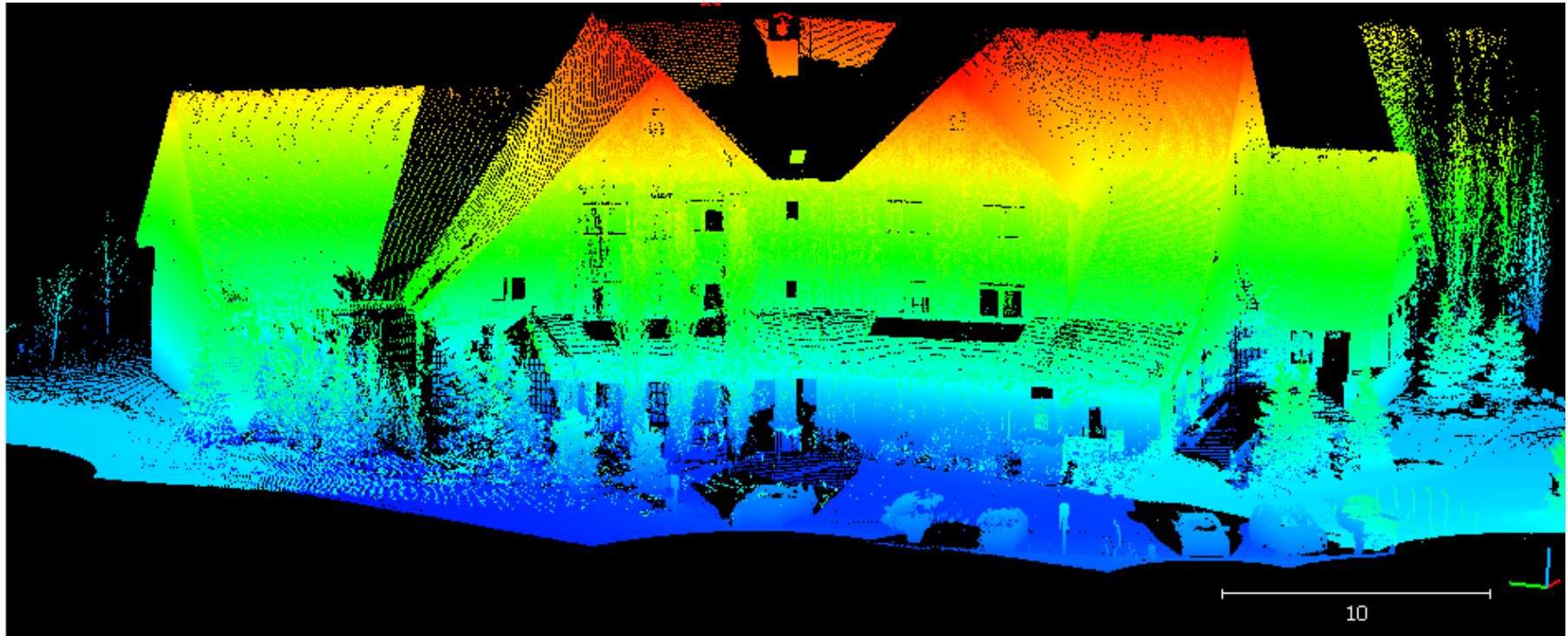


Experimental Results (II)

Line ID	a1	a2	a3	a4	a5	a6	a7	a8	a9	a11	a13	a14	a17	a19	a21	a22	a23	a24	a26
b1	4	0	4	4	2	12	12	12	0	16	0	4	18	4	22	4	4	2	4
b2	4	2	4	4	0	12	14	12	0	16	0	4	19	6	22	4	4	3	4
b3	2	3	10	10	5	18	17	18	0	25	0	5	24	5	32	6	8	0	6
b4	4	2	0	4	6	2	0	0	0	4	0	0	2	3	0	0	0	5	0
b5	4	2	0	4	7	2	0	1	0	4	0	0	2	3	0	0	0	5	0
b6	1	2	4	4	16	3	6	3	2	9	2	5	15	4	4	4	1	6	3
b7	3	1	2	5	7	9	11	8	1	14	1	5	18	4	16	5	3	1	4
b8	2	6	9	6	3	12	17	12	4	25	4	4	20	5	30	7	8	3	7
b12	1	0	6	6	2	18	19	18	0	25	0	8	24	7	21	6	2	2	7
b13	1	3	1	1	0	1	2	1	2	6	2	0	2	2	7	2	1	3	1
b14	1	0	1	3	1	0	3	0	1	3	1	0	2	0	3	3	1	1	2
b15	0	2	0	1	0	1	0	0	1	0	1	0	0	2	0	0	1	9	0
b17	0	1	1	1	0	0	3	0	3	5	2	0	3	0	2	2	1	4	2
b18	3	5	7	9	6	20	18	19	1	30	1	5	24	7	32	9	8	0	6
b19	4	1	2	1	5	3	7	3	3	11	3	5	9	6	11	3	2	2	3
b20	1	4	7	6	4	9	16	8	1	18	1	8	16	6	20	6	6	3	4
b21	3	5	8	7	2	12	17	12	6	23	5	5	21	6	31	6	7	1	5
b22	2	5	6	4	3	8	11	8	3	13	3	8	19	2	18	2	4	1	2
b23	2	3	9	10	6	19	20	17	1	26	1	9	25	7	27	5	6	0	5
b24	4	1	2	1	5	3	7	3	3	11	3	5	9	6	11	3	2	2	3
b26	0	5	11	6	5	13	17	13	1	19	1	9	24	7	26	5	6	4	4
b27	2	3	11	9	5	18	19	18	0	25	0	5	24	5	29	7	6	0	6
b28	0	2	0	1	0	1	2	1	0	3	0	1	3	5	1	0	1	5	0
b29	2	4	9	7	2	12	16	13	3	25	3	3	21	6	31	9	8	0	6

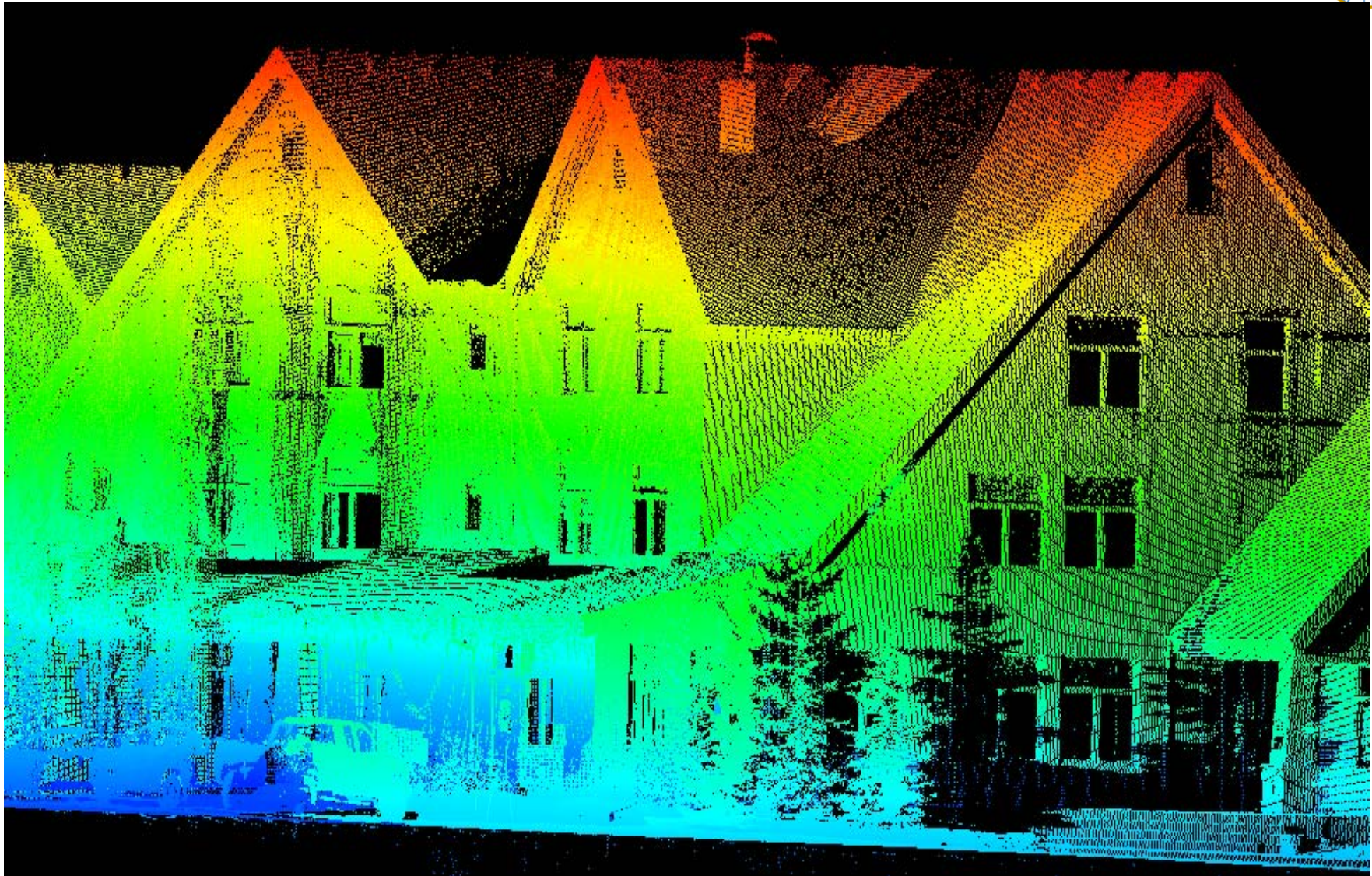
Example of an association matrix from scans 1 and 3

Experimental Results (II)



Scans 1,2,3, and 4 registered together

Experimental Results (II)



Side view of the registered scans



Conclusions

- The proposed research outlined several approaches for the automatic registration of terrestrial laser scans using linear features.
- Parameter-domain and region growing approaches for the extraction of linear features from terrestrial laser scans are introduced.
- The synergistic integration of two different registration methodologies (i.e., linear features and ICP) helps in overcoming the drawbacks of each method.
- The registration results for the electrical substation are satisfactory.



Current & Future Work

- Develop an automatic matching procedure that will be able to estimate the transformation parameters between multiple laser scans simultaneously
- Utilize non-positional point cloud characteristics such as intensity/RGB information for the automatic matching process
- Hypothesis generation using more than two lines at a time
- Recognition and modeling of objects of interest



Planar and Linear Feature-Based Registration of Terrestrial Laser Scans with Minimal Overlap Using Photogrammetric Data

CASE STUDY

3D Data Derivation

- 3D data can be obtained through either **photogrammetric** or **laser scanning** systems.



Camera

source: <http://www.dpreview.com>

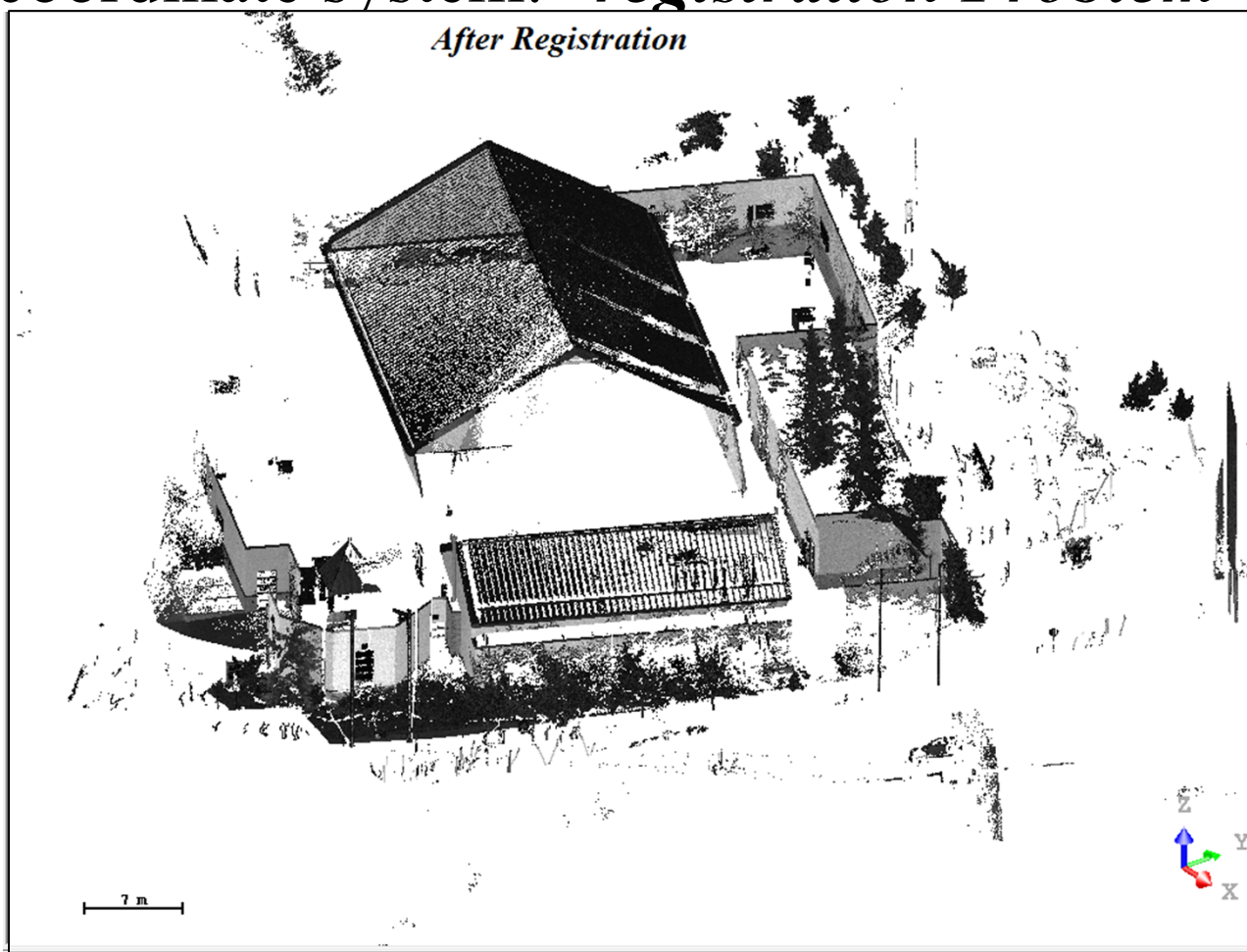


Laser Scanner

source: <http://swissmon.com/images/>

Registration: Introduction

- Relationship between the TLS scans and a reference frame has to be estimated to align the scans relative to a single coordinate system: “*registration Problem*”.





Registration: Introduction

- The most commonly used method for registering 3D data is the “Iterative Closest Point” (ICP); Besl and McKay, 1992.
 - Similar method to the ICP; Chen and Medioni 1992
- These registration methods require large overlap area among the scans.
- In this research, the large overlap area requirement among the scans is reduced using photogrammetric data, which can be acquired in a relatively short time, as additional information.



Research Objectives

- The primary objective of this research is to avoid the large overlap area requirement among the TLS scans using photogrammetric data (planar & linear features).
- The second objective is to compare and analyze the results of the planar and linear feature-based registration approaches using quality control techniques.
- A quantitative quality control is proposed by calculating the point to plane normal distance between the registered surfaces.

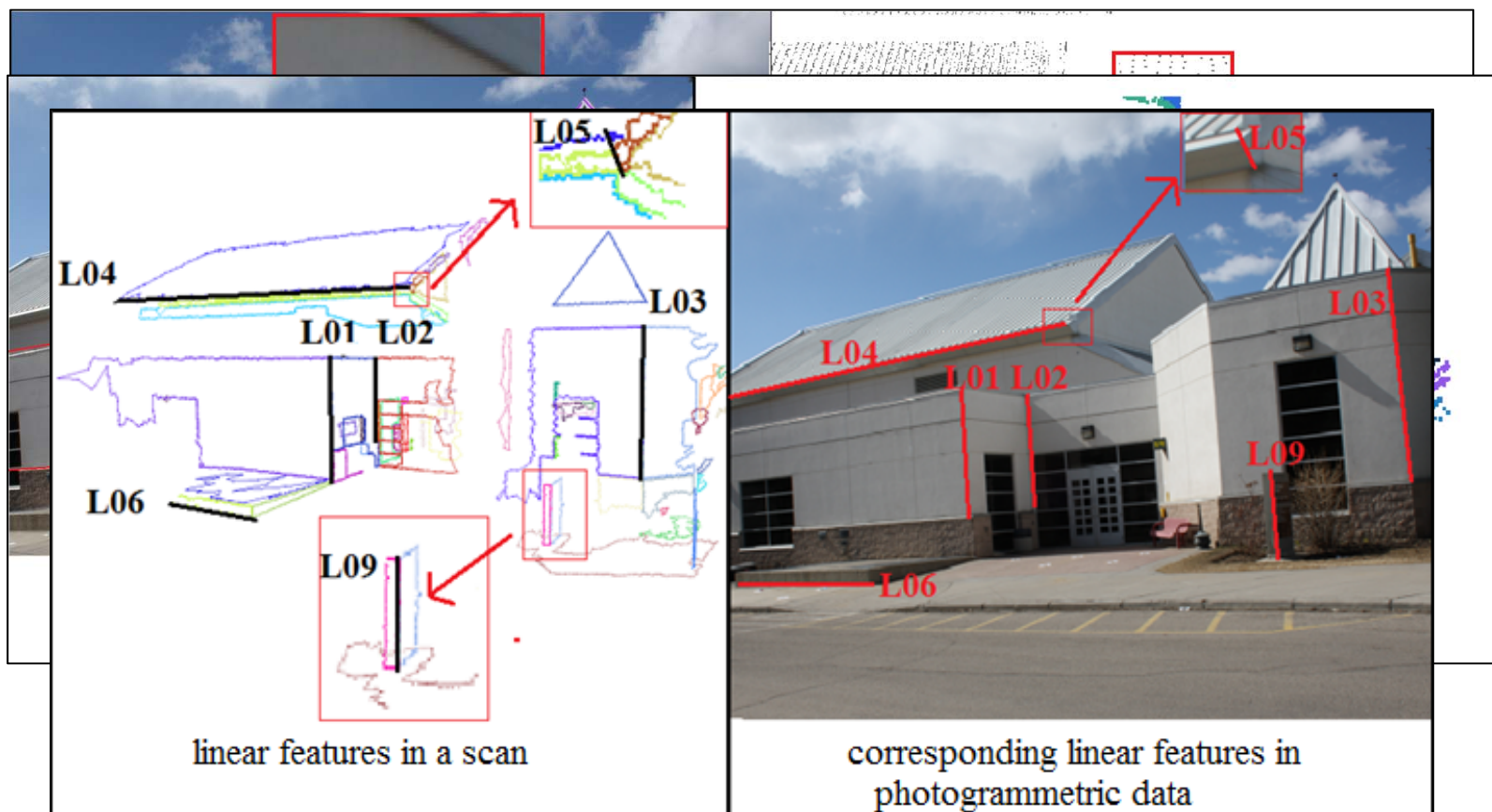
Proposed Approach: Conceptual Basis



- Capture TLS data with minimal overlap
- Capture overlapping images of the object of interest
 - Generate 3D features (planar or linear features) from the photogrammetric model, which is defined relative to an arbitrary reference frame: Photogrammetrically Reconstructed Data (PRD)
- Least-Squares Adjustment (LSA) for the registration of the TLS data using the PRD
 - Derive the corresponding TLS features to those in the PRD
 - The TLS data is aligned relative to the photogrammetric model, which is finally aligned to the global reference frame.
 - This is done through a single step procedure.

Registration Paradigm

- *Registration Primitives:* Points, planar, and linear features are possible primitives.





Registration Paradigm

- ***Transformation Parameters:*** Rigid body transformation
 - The photogrammetric model and TLS scans need to be rotated, scaled, and shifted until they fit at the global coordinate system.
- ***Similarity Measure:*** Mathematically describes the coincidence of conjugate primitives after applying the appropriate transformation parameters
- ***Matching Strategy:*** Utilizes primitives, similarity measure, and transformation parameters to automatically solve the registration problem



Features Extraction: Photogrammetric Data

Planar Features

Three or four non-collinear points are observed in multiple images and their object space coordinates are estimated through the bundle adjustment procedure.



Features Extraction: Laser Scanning Data



Planar Features

- A segmentation procedure, which is established by Lari et al. (2011), is used to derive the planar features within the building in question.

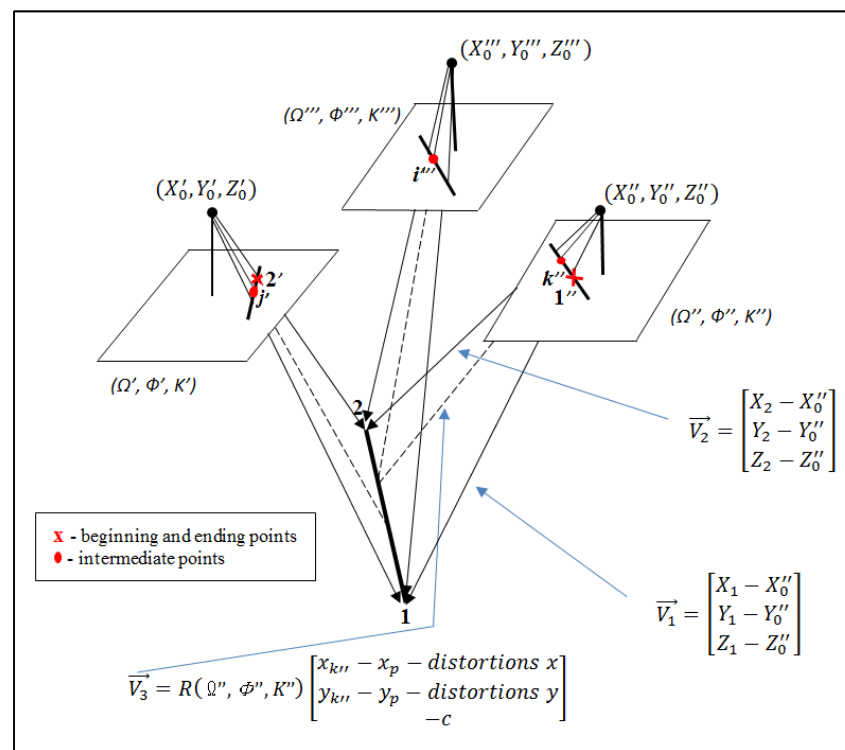


- The TLS planar feature will be represented by randomly selected points (three or more non-collinear points).
- The number of points is equivalent to the number of points defining the corresponding planar feature in the PRD (no need for conjugate points).

Features Extraction: Photogrammetric Data

Linear Features

- \vec{V}_1 : the vector connecting the perspective center to the beginning point along the line in object space;
- \vec{V}_2 : the vector connecting the perspective center to the ending point along the line in object space;
- \vec{V}_3 : the vector connecting the perspective center to the intermediate point along the



- The linear feature in the PRD will be represented by two points.

Features Extraction: Laser Scanning Data



Linear Features

- Two points, which define the linear features, are extracted automatically through the intersection of neighboring segmented planes (Al-Durgham, 2007; Lari et al, 2011).



- The TLS linear feature will be represented by two points.
- No need for conjugate points along the TLS and PRD linear features



Transformation Parameters–Similarity Measure

Point-Based 3D Similarity Transformation

$$\vec{X}_{scan_i/PRD} = \vec{X}_{T_{scan_i/PRD}} + S_{scan_i/PRD} R_{scan_i/PRD} \vec{X}_G$$

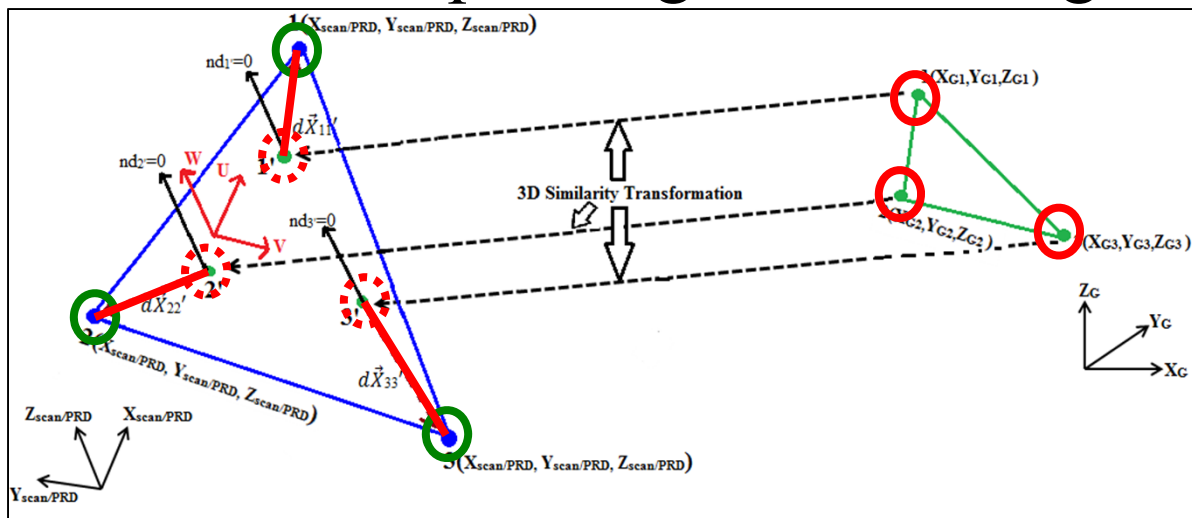
PRD = Photogrammetrically Reconstructed Data

$scan_i/PRD$ = scan or PRD

- \vec{X}_G : coordinates in the global reference frame
- $\vec{X}_{scan_i/PRD}$: the observation vector (model coordinates)
- $\vec{X}_{T_{scan_i/PRD}}$: the translation vector between $scan_i/PRD$ and global coordinate system (reference scan)
- $S_{scan_i/PRD}$: the scale factor between $scan_i/PRD$ and global coordinate system
- $R_{scan_i/PRD}$: the rotation matrix relating $scan_i/PRD$ and global coordinate system; defined by the angles: Ω , Φ , and K

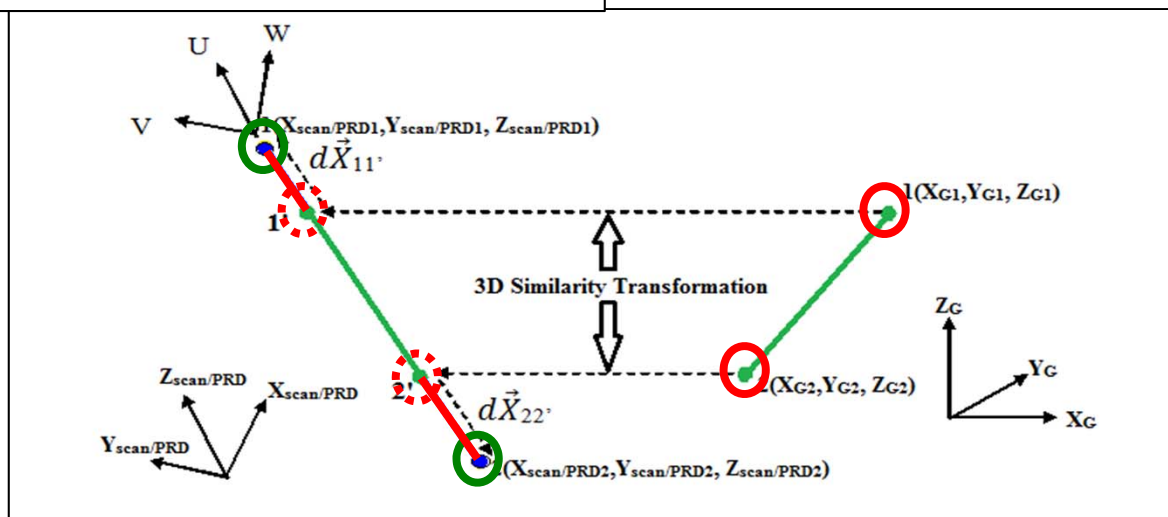
Transformation Parameters–Similarity Measure

Non-corresponding Points Along Conjugate Features



Planar Features

Linear Features



LSA Weight Modification

$$\vec{X}_{scan_i/PRD} = \vec{X}_{T_{scan_i/PRD}} + S_{scan_i/PRD} R_{scan_i/PRD} \vec{X}_G + d\vec{X} \quad P' d\vec{X} = 0$$

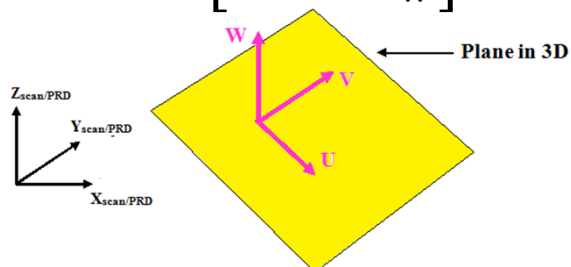
$$\begin{bmatrix} U \\ V \\ W \end{bmatrix} = M \begin{bmatrix} X \\ Y \\ Z \end{bmatrix} \quad M = \begin{bmatrix} U_x & U_y & U_z \\ V_x & V_y & V_z \\ W_x & W_y & W_z \end{bmatrix}$$

original weight matrix $P_{XYZ} = \Sigma_{XYZ}^{-1}$

$$P_{UVW} = M P_{XYZ} M^T = \begin{bmatrix} P_U & P_{UV} & P_{UW} \\ P_{VU} & P_V & P_{VW} \\ P_{WU} & P_{WV} & P_W \end{bmatrix}$$

Planar Features

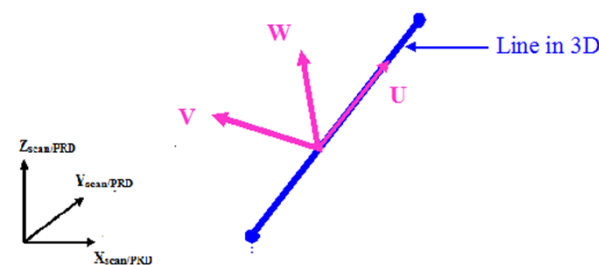
$$P'_{UVW} = \begin{bmatrix} 0 & 0 & 0 \\ 0 & 0 & 0 \\ 0 & 0 & P_W \end{bmatrix}$$



$$P'_{XYZ} = M^T P'_{UVW} M$$

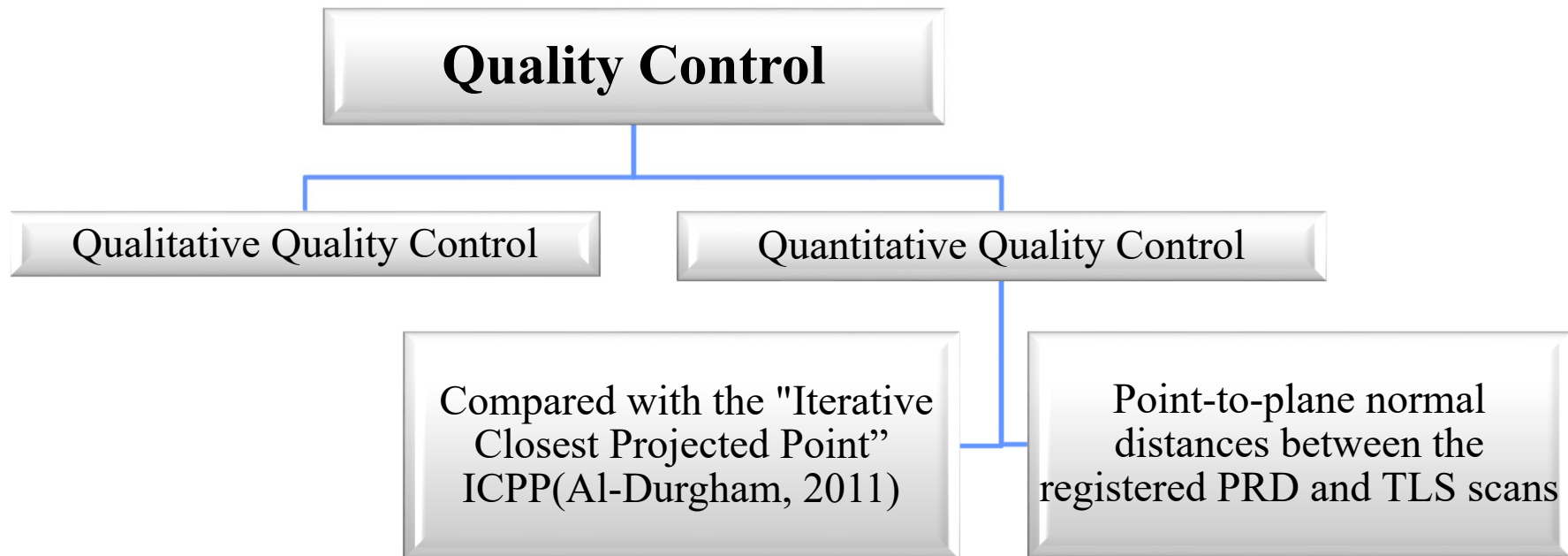
Linear Features

$$P'_{UVW} = \begin{bmatrix} 0 & 0 & 0 \\ 0 & P_V & P_{VW} \\ 0 & P_{WV} & P_W \end{bmatrix}$$





Quality Control Procedure



Dataset Description

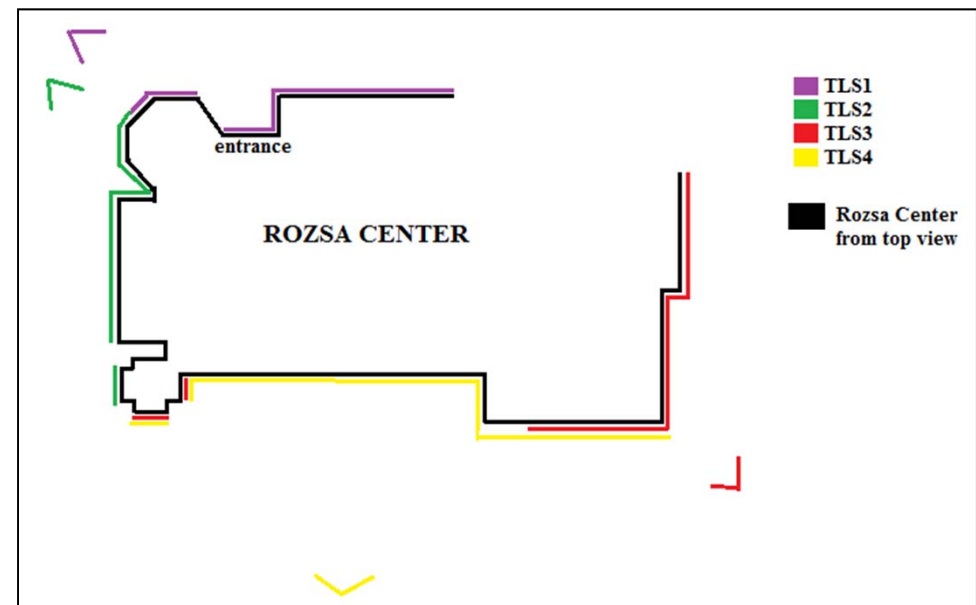
- 4 minimally overlapping TLS scans were collected using a Trimble GS200 scanner around the Rozsa Center (UofC).



Rozsa Center

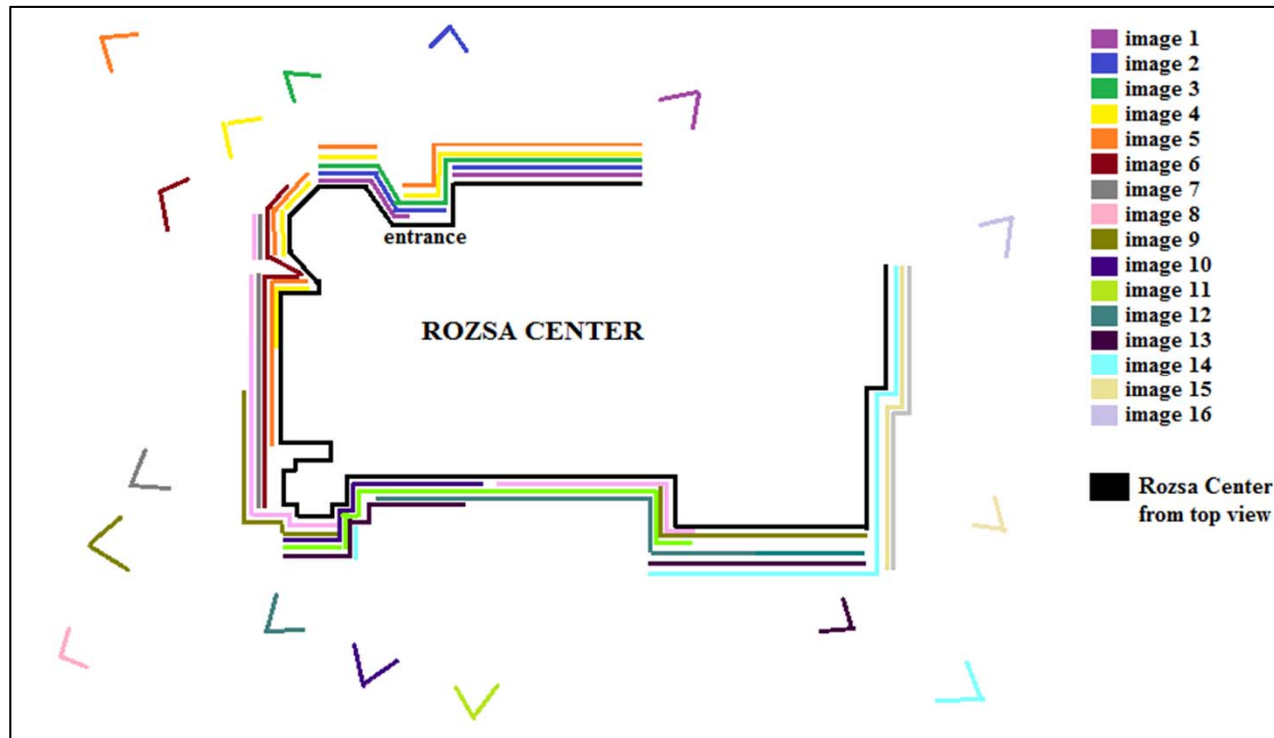
(<http://arts.ucalgary.ca/theatres/conferences/>)

	TLS scan1	TLS scan2	TLS scan3	TLS scan4
TLS scan1		%1	%0	%0
TLS scan2	%1		%0	%0
TLS scan3	%0	%0		%19
TLS scan4	%0	%0	%19	



Dataset Description

- 16 images of the Rozsa Center were collected for photogrammetric object reconstruction using a Canon EOS Rebel XS camera.

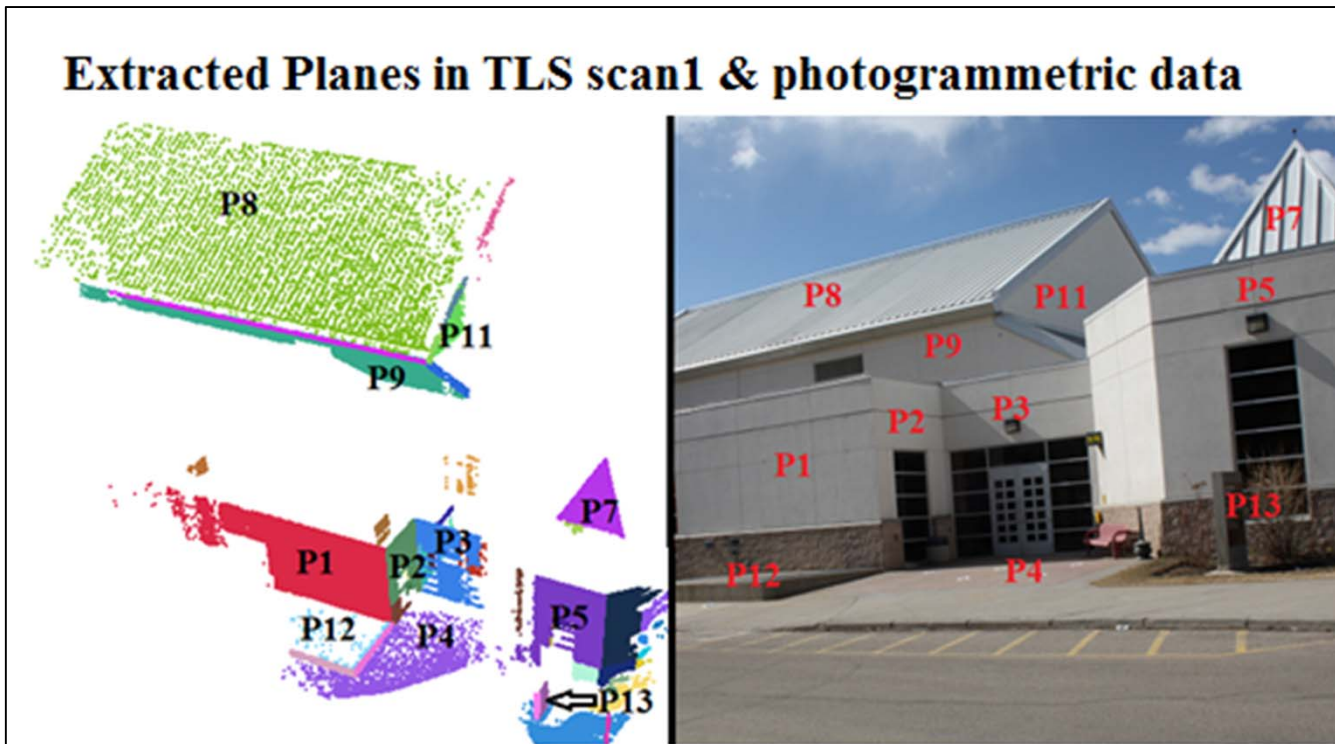


Top view of overlap area and camera positions among the 16 images covering Rozsa Center

Results: Planar Feature-Based Registration



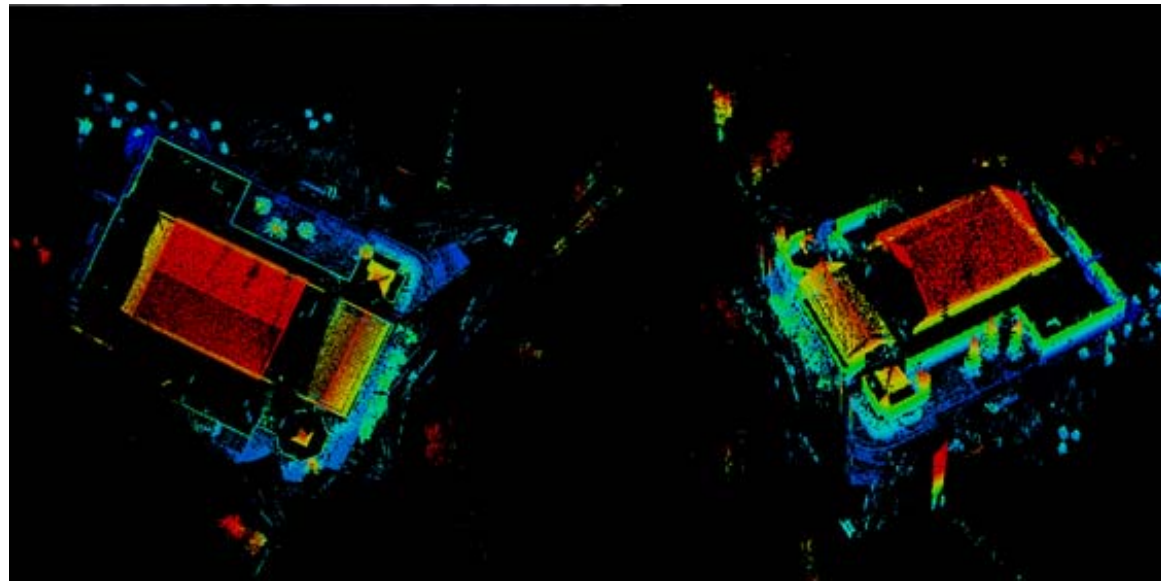
Extracted Planes in TLS scan1 & photogrammetric data



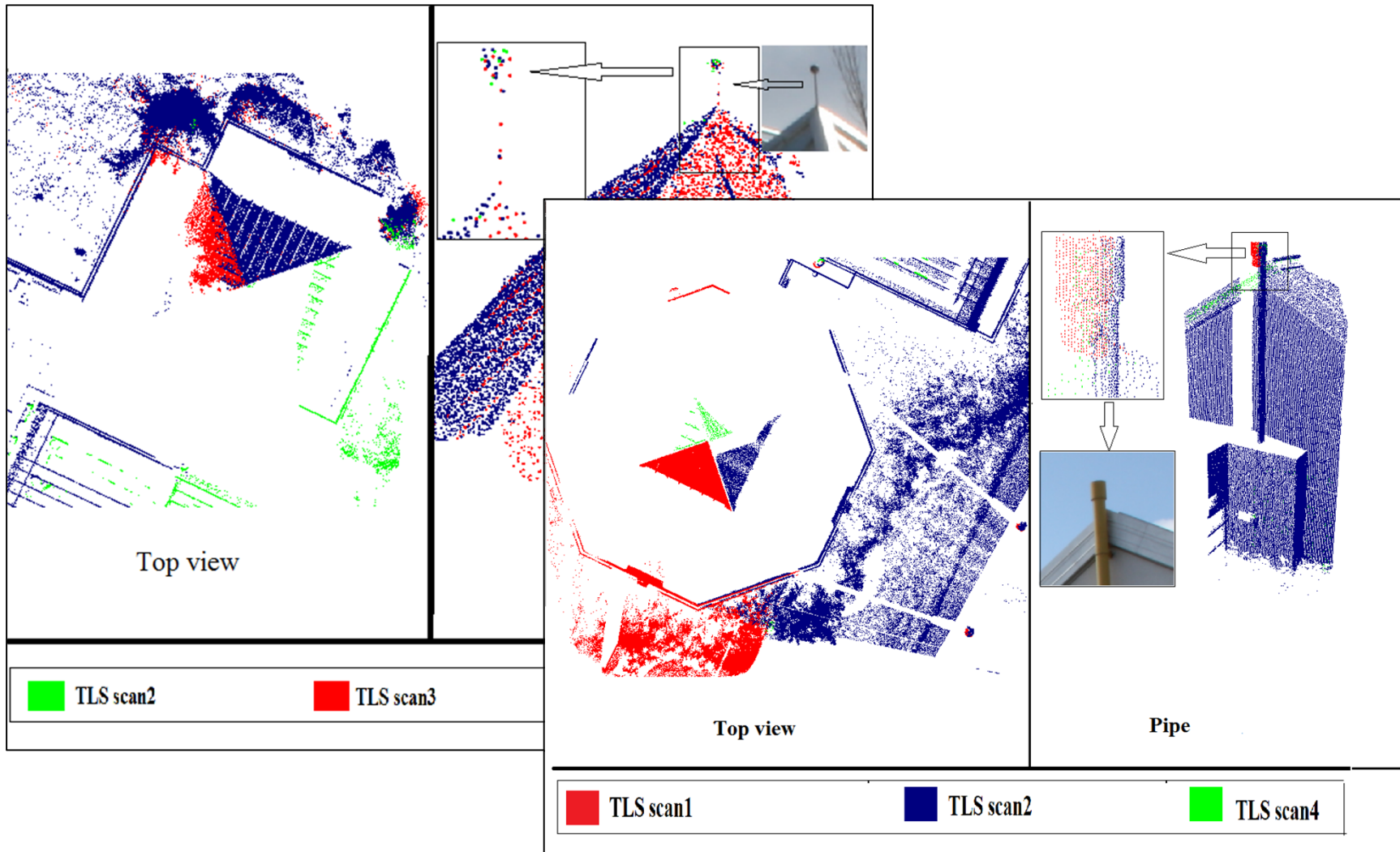
Results: Planar Feature-Based Registration



	XT (m)	YT (m)	ZT (m)	Scale	Ω (°)	Φ (°)	K (°)
TLS scan1	0	0	0	1	0	0	0
TLS scan2	-23.186 (±0.0287)	-14.801 (±0.0219)	-0.687 (±0.0805)	1	0.234 (±0.1133)	-0.429 (±0.2092)	8.373 (±0.0484)
TLS scan3	69.677 (±0.0221)	92.511 (±0.0293)	1.335 (±0.0431)	1	0.243 (±0.0624)	0.313 (±0.0781)	121.373 (±0.0441)
TLS scan4	-41.693 (±0.0298)	91.370 (±0.0234)	-0.251 (±0.0916)	1	-0.291 (±0.1273)	0.165 (±0.0769)	-145.531 (±0.0447)
PRD	5.372 (±0.0184)	1.610 (±0.0163)	37.383 (±0.0143)	0.998 (±0.0003)	30.584 (±0.2271)	-74.546 (±0.0419)	91.168 (±0.2261)



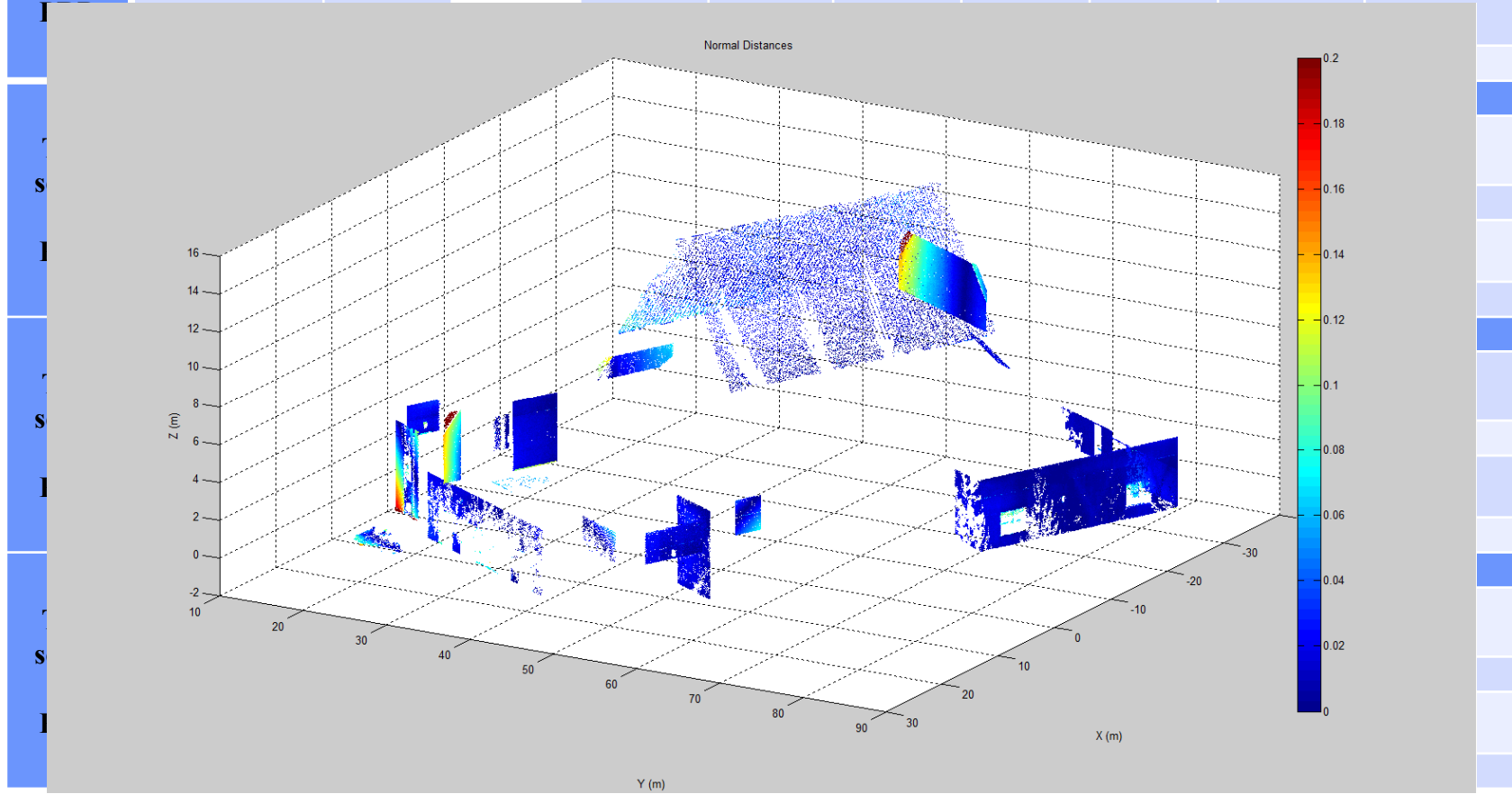
Results: Planar Feature-Based Registration



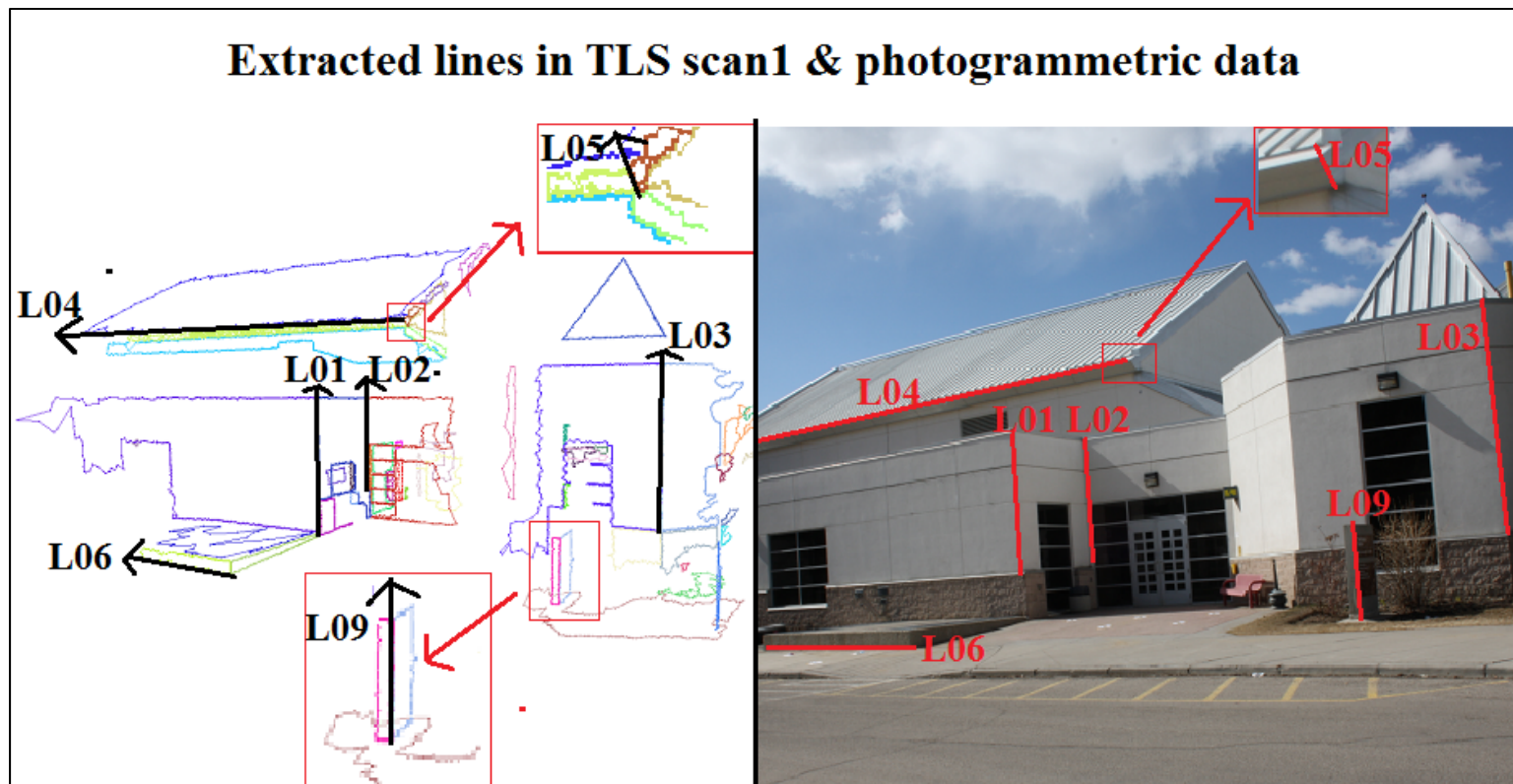
Results: Planar Feature-Based Registration



Plane ID	Plane 1	Plane 2	Plane 3	Plane 4	Plane 5	Plane 8	Plane 9	Plane 12	Plane 13
Plane Orientation	XZ-plane	YZ-plane	XZ-plane	XY-plane	XZ-plane	Slope plane	XZ-plane	XY-plane	YZ-plane
Mean (m)	0.012	0.004	0.005	0.032	0.023	0.009	-0.037	0.059	-0.024



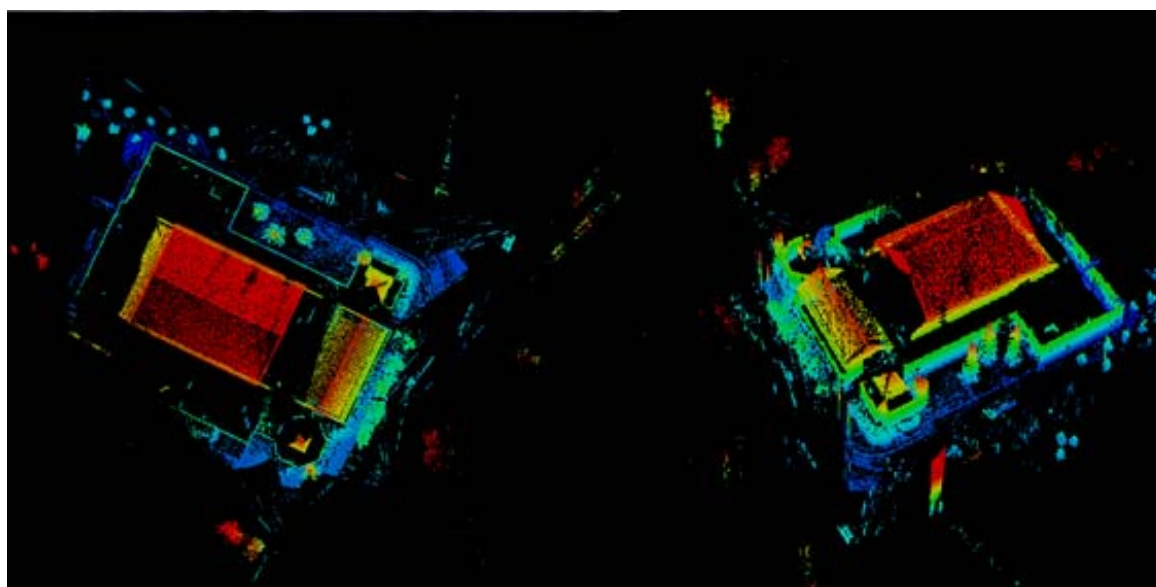
Results: Linear Feature-Based Registration



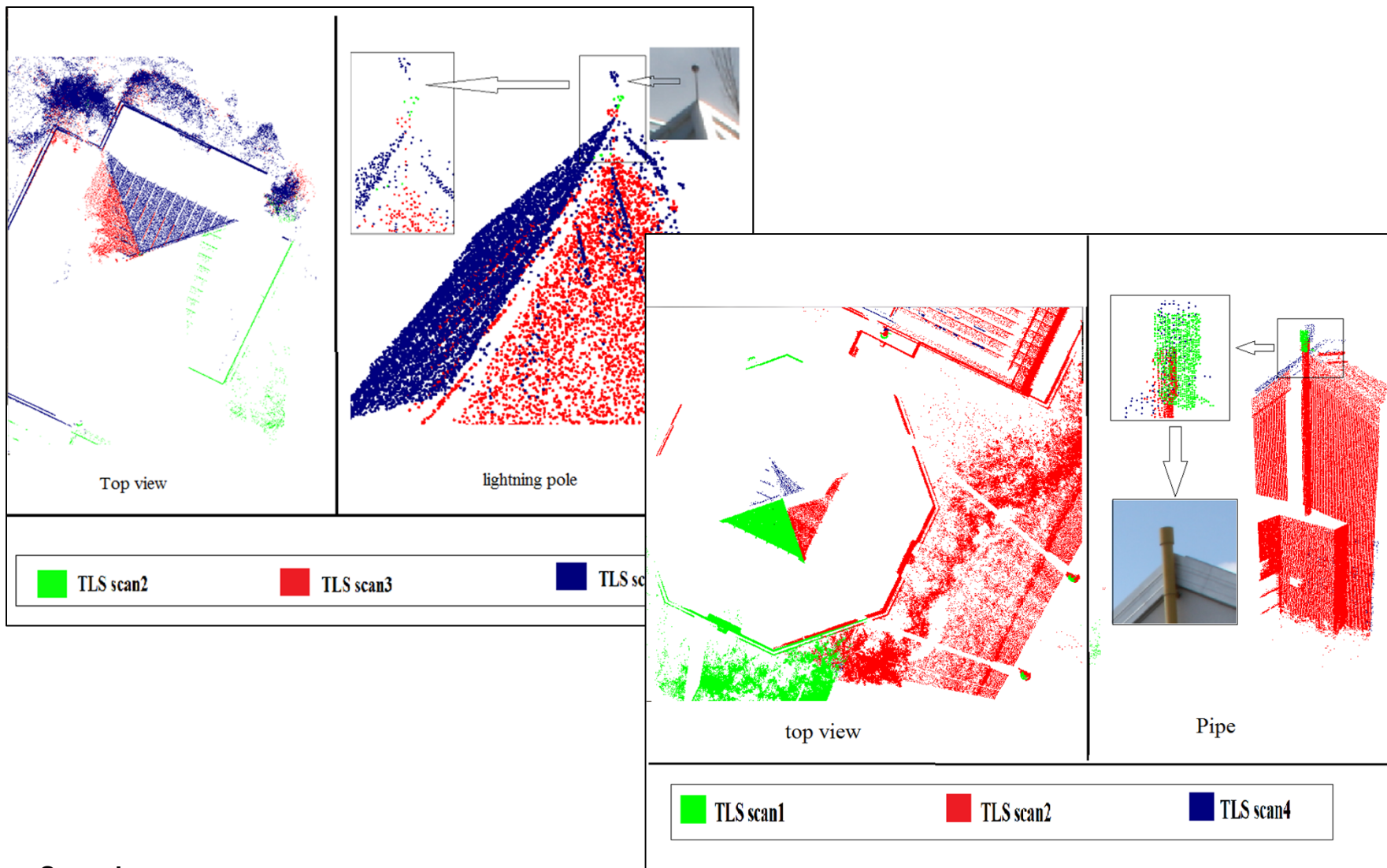


Results: Linear Feature-Based Registration

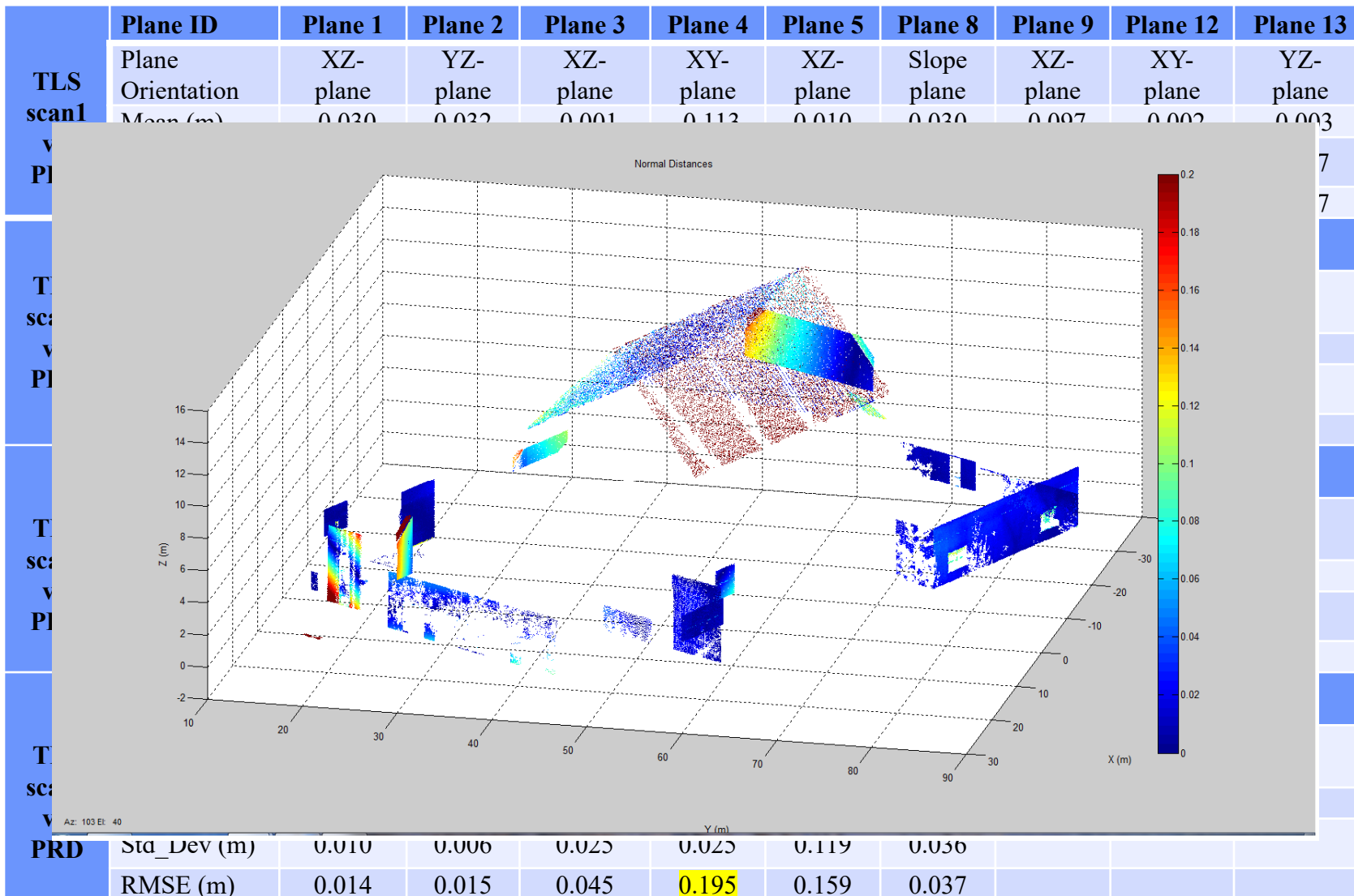
	XT (m)	YT (m)	ZT (m)	Scale	Ω (°)	Φ (°)	K (°)
TLS scan1	0	0	0	1	0	0	0
TLS scan2	-23.217 (± 0.0685)	-14.792 (± 0.0341)	-0.667 (± 0.1226)	1	0.869 (± 0.2571)	1.073 (± 0.5158)	8.421 (± 0.1569)
TLS scan3	69.639 (± 0.0661)	92.565 (± 0.0646)	1.284 (± 0.7231)	1	0.681 (± 0.4161)	0.824 (± 0.5422)	121.411 (± 0.1071)
TLS scan4	-41.787 (± 0.0983)	91.305 (± 0.0724)	-0.751 (± 0.3747)	1	-0.803 (± 0.4175)	0.009 (± 0.2541)	-145.441 (± 0.1263)
PRD	5.461 (± 0.0722)	1.635 (± 0.0393)	37.384 (± 0.0336)	0.998 (± 0.0006)	31.338 (± 0.8272)	-74.372 (± 0.1408)	91.914 (± 0.7643)



Results: Linear Feature-Based Registration

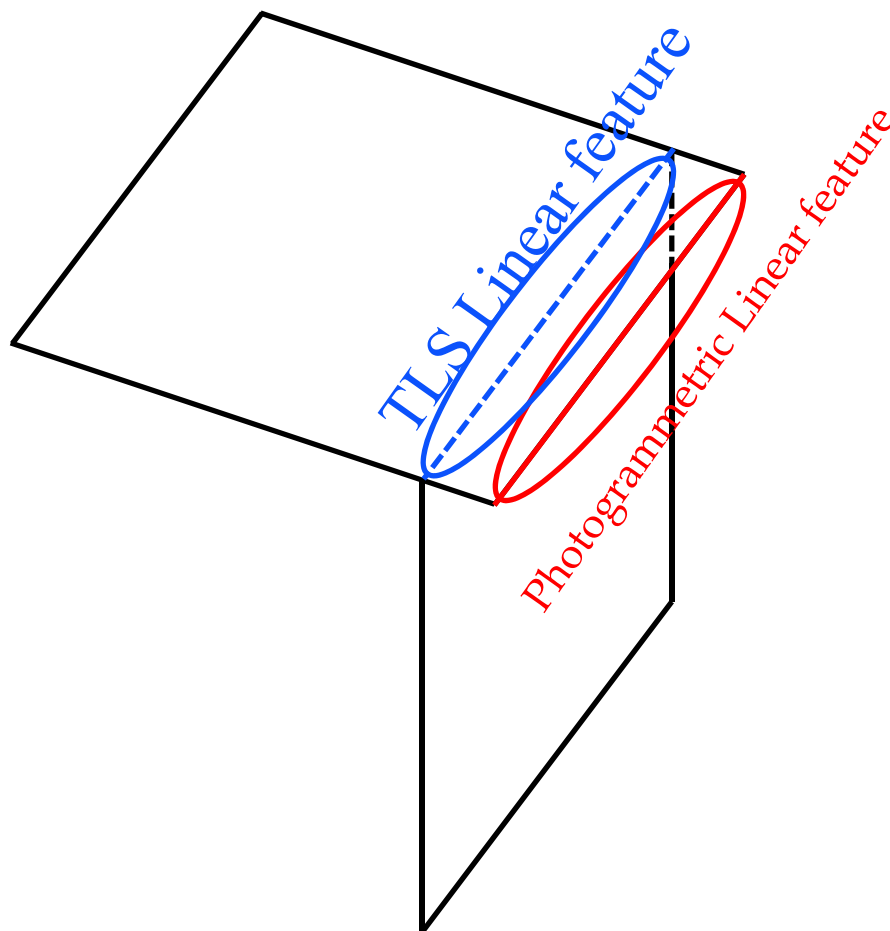


Results: Linear Feature-Based Registration



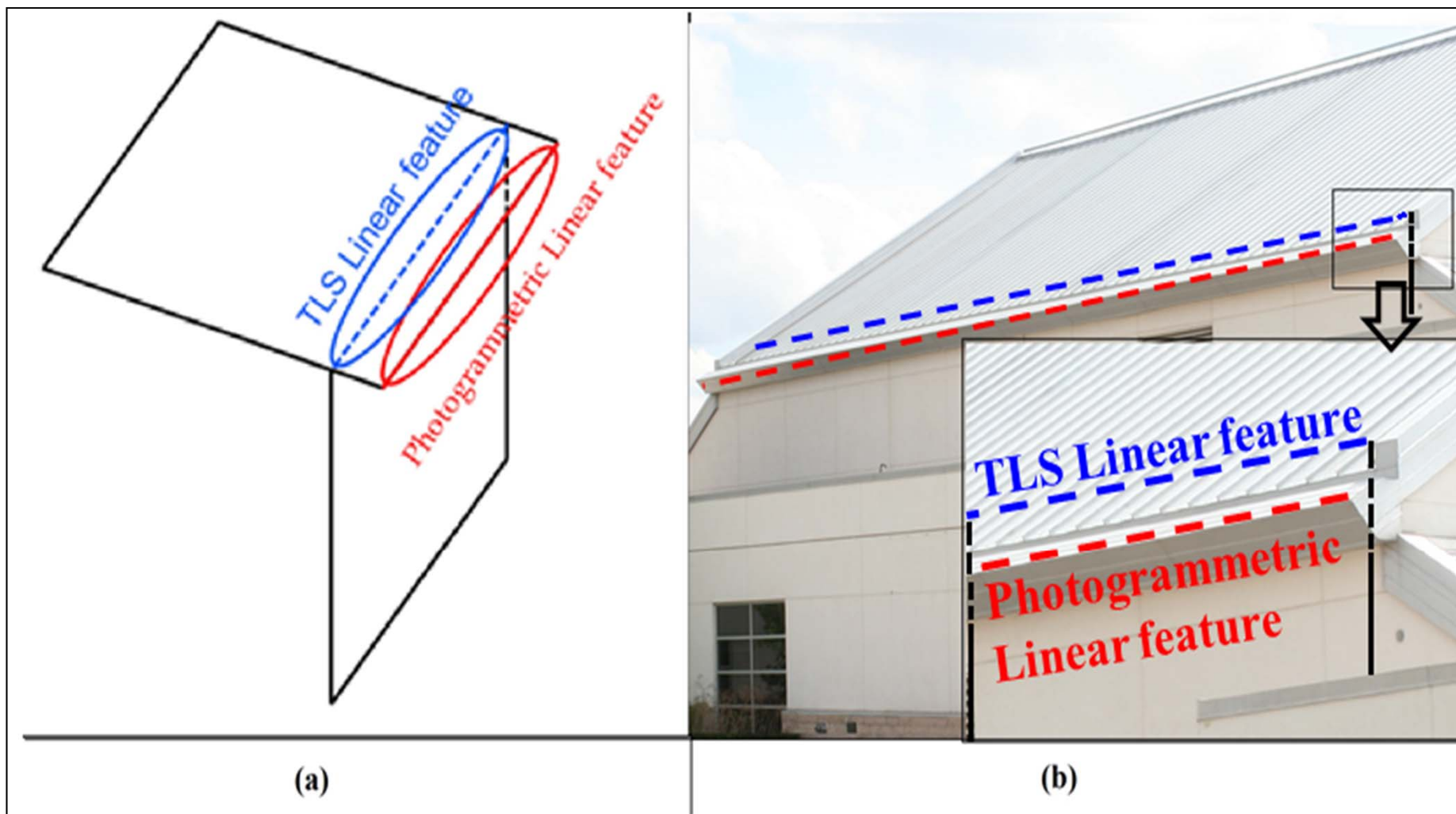
Linear Feature-Based Registration

- **Potential Problem:** Occurs when the derived linear features from neighboring plane intersections might not correspond to physical linear features that could be identified in the imagery.



Linear Feature-Based Registration

- **Potential Problem:**





Comparison with the ICPP

TLS scans	Parameters	the ICPP method	Planar based registration	Linear based registration	the ICPP vs. planar based	the ICPP vs. linear based	Linear vs. planar based
TLS scan2	XT (m)	-23.258	-23.186	-23.217	-0.072	-0.041	0.031
	YT (m)	-14.733	-14.801	-14.792	0.067	0.058	-0.009
	ZT (m)	-0.605	-0.687	-0.667	0.082	0.062	-0.020
	Scale	1	1	1	0	0	0
	$\Omega(^{\circ})$	0.177	0.234	0.869	-0.056	-0.691	-0.635
	$\phi(^{\circ})$	-0.189	-0.429	1.073	0.239	-1.262	-1.502
	$\kappa(^{\circ})$	8.168	8.373	8.421	-0.204	-0.252	-0.048
TLS scan3	XT (m)	69.613	69.677	69.639	-0.063	-0.025	0.038
	YT (m)	92.579	92.511	92.565	0.068	0.014	-0.054
	ZT (m)	1.375	1.335	1.284	0.040	0.091	0.051
	Scale	1	1	1	0	0	0
	$\Omega(^{\circ})$	0.095	0.243	0.681	-0.147	-0.585	-0.438
	$\phi(^{\circ})$	0.194	0.313	0.824	-0.118	-0.629	-0.511
TLS scan4	$\kappa(^{\circ})$	121.388	121.373	121.411	0.015	-0.022	-0.038
	XT (m)	-41.751	-41.693	-41.787	-0.057	0.036	0.094
	YT (m)	91.313	91.37	91.305	-0.056	0.008	0.065
	ZT (m)	-0.259	-0.251	-0.751	-0.008	0.491	0.500
	Scale	1	1	1	0	0	0
	$\Omega(^{\circ})$						0.512
	$\phi(^{\circ})$						0.156
	$\kappa(^{\circ})$						-0.09
PRD	XT (m)						-0.089
	YT (m)						-0.025
	ZT (m)						-0.001
	Scale						0
	$\Omega(^{\circ})$	-	30.584	31.338	-	-	-0.754
	$\phi(^{\circ})$	-	-74.546	-74.372	-	-	-0.174
	$\kappa(^{\circ})$	-	91.168	91.914	-	-	-0.746

The ICPP is possible only after adding more scans to increase the overlap percentage among the scans.

Conclusions & Recommendations



- Commonly used registration methods cannot align TLS scans with minimal overlap area.
- The proposed registration method depends on derived planar and linear features from a photogrammetric model to register TLS scans with minimal overlap.
- Qualitative and quantitative QC procedures proved the feasibility of the proposed approach.
- Planar feature-based registration is quite reliable.
- Linear feature-based registration will have problems when the TLS features are not visible in the image data.
- Current & future work:
 - Automated feature extraction from imagery (Dense Matching Algorithms)
 - Use airborne datasets for the registration of TLS data



References

- Al-Durgham, K., & Habib, A. (2014). Association-Matrix-Based Sample Consensus Approach for Automated Registration of Terrestrial Laser Scans Using Linear Features. *Photogrammetric Engineering & Remote Sensing*, 80(11), 1029-1039.
- Al-Durgham, K., Habib, A., & Mazaheri, M. (2014, March). Solution frequency-based procedure for automated registration of terrestrial laser scans using linear features. In *Proceedings of the ASPRS 2014 Annual Conference, Louisville, Kentucky* (pp. 23-28).
- Al-Durgham, M. M. (2007, September). Alternative methodologies for the quality control of lidar systems. In *Masters Abstracts International* (Vol. 46, No. 03).
- Al-Durgham, M., Datchev, I., & Habib, A. (2011). Analysis of two triangle-based multi-surface registration algorithms of irregular point clouds. *ISPRS-International Archives of the Photogrammetry, Remote Sensing and Spatial Information Sciences*, 3812, 61-66.
- Besl, P. J., & McKay, N. D. (1992, April). Method for registration of 3-D shapes. In *Robotics-DL tentative* (pp. 586-606). International Society for Optics and Photonics.
- Canaz, S., & Habib, A. (2014). Photogrammetric features for the registration of terrestrial laser scans with minimum overlap. *Journal of Geodesy and Geoinformation*, 2(1).
- Chen, Y., & Medioni, G. (1991, April). Object modeling by registration of multiple range images. In *Robotics and Automation, 1991. Proceedings., 1991 IEEE International Conference on* (pp. 2724-2729). IEEE.
- Csanyi, N., & Toth, C. K. (2007). Improvement of lidar data accuracy using lidar-specific ground targets. *Photogrammetric Engineering & Remote Sensing*, 73(4), 385-396.
- Fischler, M. A., & Bolles, R. C. (1981). Random sample consensus: a paradigm for model fitting with applications to image analysis and automated cartography. *Communications of the ACM*, 24(6), 381-395.
- Habib, A., Kersting, A. P., Bang, K. I., & Lee, D. (2010). Alternative methodologies for the internal quality control of parallel LiDAR strips. *Geoscience and Remote Sensing, IEEE Transactions on*, 48(1), 221-236.
- Habib, A. F., & Alruzouq, R. I. (2004). Line-based modified iterated Hough transform for automatic registration of multi-source imagery. *The Photogrammetric Record*, 19(105), 5-21.
- Horn, B. K. (1987). Closed-form solution of absolute orientation using unit quaternions. *JOSA A*, 4(4), 629-642.
- Jaw, J. J., & Chuang, T. Y. (2008). Registration of ground-based LiDAR point clouds by means of 3D line features. *Journal of the Chinese Institute of Engineers*, 31(6), 1031-1045.
- Lari, Z., & Habib, A. (2014). An adaptive approach for the segmentation and extraction of planar and linear/cylindrical features from laser scanning data. *ISPRS Journal of Photogrammetry and Remote Sensing*, 93, 192-212.
- Renaudin, E., Habib, A., & Kersting, A. P. (2011). Feature-based Registration of terrestrial laser scans with minimum overlap using photogrammetric data. *ETRI Journal*, 33(4), 517-527.
- Yao, J., Ruggeri, M. R., Taddei, P., & Sequeira, V. (2010). Automatic scan registration using 3D linear and planar features. *3D Research*, 1(3), 1-18.